DAASM PROJECT-HIGH LATITUDE AIRCRAFT HF PROPAGATION EXPERIMENT

Gary S. Sales, et al

Air Force Cambridge Research Laboratories
Hanscom Air Force Base, Massachusetts

19 May 1975

DISCLAIMER NOTICE

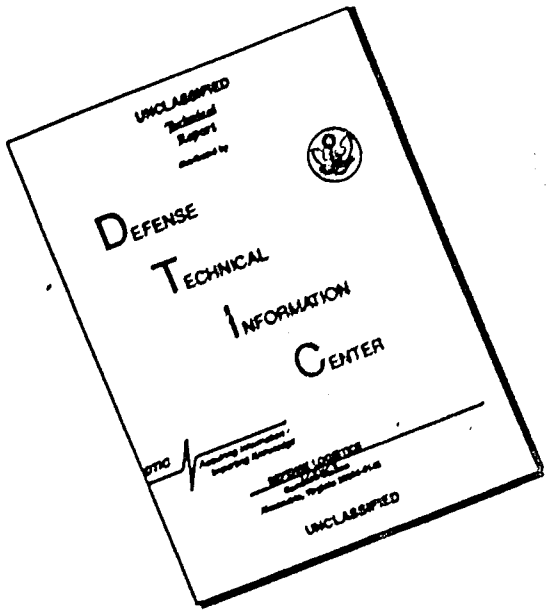

THIS DOCUMENT IS BEST QUALITY AVAILABLE. THE COPY FURNISHED TO DTIC CONTAINED A SIGNIFICANT NUMBER OF PAGES WHICH DO NOT REPRODUCE LEGIBLY.

AFCRL-TR-75-0290
ENVIRONMENTAL RESEARCH PAPERS, NO. 516

DAASM Project—High Latitude Aircraft HF Propagation Experiment

GARY S. SALES
JOHN I. VIDEBERG
RAJAN VARAD

19 May 1975

Approved for public release; distribution unlimited

IONOSPHERIC PHYSICS LABORATORY PROJECT 5631
AIR FORCE CAMBRIDGE RESEARCH LABORATORIES
HANSCOM AFB, MASSACHUSETTS 01731

AIR FORCE SYSTEMS COMMAND, USAF

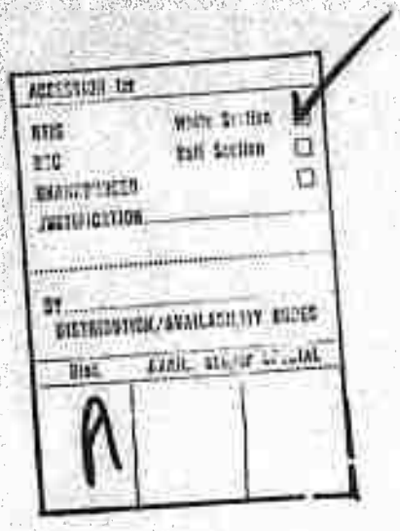

Unclassified

SECURITY CLASSIFICATION OF THIS PAGE (When Data Entered)

REPORT DOCUMENTATION PAGE

READ INSTRUCTIONS BEFORE COMPLETING FORM

1 REPORT NUMBER: AFCRL-TR-75-0290	2 GOVT ACCESSION NO.
3 RECIPIENT'S CATALOG NUMBER	
4 TITLE (and Subtitle): DAASM PROJECT – HIGH LATITUDE AIRCRAFT HF PROPAGATION EXPERIMENT	5 TYPE OF REPORT & PERIOD COVERED: Scientific. Interim.
	6 PERFORMING ORG. REPORT NUMBER: ERP No. 516
7 AUTHOR(s): Gary S. Sales; John L. Videberg; Rajan Varad	8 CONTRACT OR GRANT NUMBER(s)
9 PERFORMING ORGANIZATION NAME AND ADDRESS: Air Force Cambridge Research Laboratories (LH), Hanscom AFB, Massachusetts 01731	10 PROGRAM ELEMENT, PROJECT, TASK AREA & WORK UNIT NUMBERS: 61102F; WU 56311101
11 CONTROLLING OFFICE NAME AND ADDRESS: Air Force Cambridge Research Laboratories (LH), Hanscom AFB, Massachusetts 01731	12 REPORT DATE: 19 May 1975
	13 NUMBER OF PAGES: 103
14 MONITORING AGENCY NAME & ADDRESS (if different from Controlling Office)	15 SECURITY CLASS (of this report): Unclassified
	15a DECLASSIFICATION DOWNGRADING SCHEDULE

16 DISTRIBUTION STATEMENT (of this Report)

Approved for public release; distribution unlimited.

17 DISTRIBUTION STATEMENT (of the abstract entered in Block 20, if different from Report)

18 SUPPLEMENTARY NOTES

*Boston College

19 KEY WORDS (Continue on reverse side if necessary and identify by block number)

Over-the-horizon radar
High latitude ionosphere
HF propagation
Doppler frequency spectra
Arrival angle spectra
Coherence

20 ABSTRACT (Continue on reverse side if necessary and identify by block number)

The purpose of the DAASM project is to investigate the effects and limitations caused by the auroral and polar ionosphere on over-the-horizon HF propagation using a backscatter sounding system.

The technique measures and records the complex amplitude of incoming, forward or backscatter signals, including noise, at each of the 12 elements of a broadside antenna array. The data is subsequently processed using sophisticated software on a CDC-6600 computer at AFCRL. This process, using

DD FORM 1 JAN 73 1473 EDITION OF 1 NOV 65 IS OBSOLETE

Unclassified

SECURITY CLASSIFICATION OF THIS PAGE (When Data Entered)

20. (Cont)

Fourier analysis techniques, provides output in the form of Doppler frequency vs arrival-angle "maps" as well as coherence maps. These maps are used to analyze effects of the irregular high-latitude ionosphere, such as Doppler frequency and arrival-angle spreading of the signal, and the temporal and spacial coherence. Various antenna configurations and spacings, together with adaptive processing techniques, permit optimization of the resolution and signal/noise ratio of the various parameters being analyzed. Use is made of bistatic oblique ionograms and a special polar-model computer prediction program to compliment the analysis.

This report presents selected data and the initial results of the effects on forward propagation using the DAASM system in conjunction with a moving aircraft to provide signal Doppler and arrival-angle information. A KC-135 specially equipped for ionospheric research made six 8-hour flights of up to 3000 km into the Arctic from Goose Bay.

Examples of data selected to illustrate particular propagation effects are presented, such as Doppler frequency spreading, arrival-angle spreading, multiple mode propagation causing deviation from predicted values of both arrival-angles and Doppler frequencies, etc.

Two of the most serious problems indicated by the Goose Bay DAASM experiment, in terms of the operation of OTH radar systems, appear to be the effects of TID's and tilted ionospheres. Investigation of the problem is continuing and further results of the analysis will be presented in a forthcoming report.

Preface

Acknowledgment is extended to Dr. W. Pfister, now at Boston College, for the conception of this effort based on his earlier ionospheric "drift" experiments at AFCRL. Appreciation is extended to William McComish and Robert F. Boudreau of Boston College for their efforts in programming the software for the CDC-6600, and to the members of the Ionospheric Dynamics Branch of AFCRL for their support with the aircraft and some of the data processing. Appreciation is extended to Dr. T. Elkins, Chief, Ionospheric Radio Physics Branch, for his continuing encouragement and assistance in making this endeavor possible. A special word of thanks is extended to Mrs. Linda Gillingham for her efforts in typing the original manuscript.

Contents

Illustrations

Illustrations

Tables

DAASM Project - High Latitude Aircraft HF Propagation Experiment

I. INTRODUCTION

A series of papers[1] described a method of vertical ionospheric "drift" measurements and analysis using complex amplitude measurements at spaced receivers. This method of analysis first Fourier analyzes the received signal at each antenna into its Doppler frequency components, and then for each Fourier component, determines the angle of arrival using the spatial array of antennas. This technique has been adapted into an oblique sounding system using a linear array of antennas and designed to operate either on backscatter signals or signals propagated from a similarly equipped aircraft in a forward-propagation mode. The DAASM system (DAASM is an acronym for Doppler/Arrival Angle Spectral Measurements) has operated at Goose Bay, Labrador (53°20'N, 60°20'W) for just one and one-half years beginning full operation in January 1974.

(Received for publication 19 May 1975)

1. Pfister, W., et al (1968-75) Pulse Sounding with Closely Spaced Receivers as as a Tool for Measuring Atmospheric Motions and Fine Structure in the Ionosphere,
   Vol. I, Environmental Research Paper No. 295, Dec 1968
   Vol. II, Environmental Research Paper No. 295, Dec 1968
   Vol. III, Environmental Research Paper No. 317, Mar 1970
   Vol. IV, Environmental Research Paper No. 329, Aug 1970
   Vol. V, Environmental Research Paper No. 468, Feb 1974
   Vol. VI, Environmental Research Paper No. 470, Mar 1974
   Vol. VII, Environmental Research Paper No. 506, Apr 1975
   Vol. VIII, Environmental Research Paper No. 507, Apr 1975

The purpose of the DAASM program is to investigate the effects of the auroral and polar ionosphere on a backscatter sounding system which at the same time can receive a forward-propagated signal from an airborne transmitter. The aircraft used for these experiments was a KC-135, specially equipped for ionospheric experiments. The questions to be answered concerned the character of the received signals and are focussed on three main areas:

(a) Angle of Arrival – The degree to which the signals from the aircraft is deviated from the known bearing to the aircraft and the amount of angular spreading associated with the particular path.

(b) Doppler Frequency – The extent to which propagation in the auroral regions deviates the expected Doppler frequency associated with the aircraft motion and the amount of frequency spreading that occurs on the signal.

(c) Coherence – The temporal and spatial coherence of these aircraft signals after propagation through the irregular auroral medium.

The basic concept of the DAASM system is to record on digital magnetic tape the signal output of each antenna in the receiving array. This recorded data represents a two-dimensional description of the received wave field, that is, time and a one-dimensional space (linear antenna array). In the most simple approach, a two-dimensional Fourier transform of this data set results in a Doppler frequency vs arrival-angle description of the received signal. These transforms are accomplished at the AFCRL computer facility after the tapes are returned from the Goose Bay site.

The sampled data is limited both in time and space because of the finite duration of the sample (32 sec) and the limited extent of the antenna array (910 m maximum). The resulting Doppler frequency and arrival angle description of the signal is thereby limited in resolution. This is particularly true of the spatial dimension, and advanced processing techniques having been developed to improve the capability of the system in this area.

This report addresses the six aircraft missions carried out during 1974, and an attempt is made to relate the observed character of the received signals to the propagation mode and other geophysical factors which may affect the auroral ionosphere.

2. EXPERIMENT

2.1 DAASM

The DAASM system as configured for the Goose Bay experiments measures the received amplitude and phase of an arriving radio signal as a function of both

time and space. In order to accomplish this, an array of small receiving antennas was erected in a linear configuration broadside to the required receiving direction. In this case the boresight of the array at Goose Bay, that is, the direction normal to the length of the array, was magnetic North, 328° T. In order to provide maximum flexibility in terms of spatial sampling, a complex antenna arrangement was developed[2] using a 20-element array. The DAASM electronic system[3] was designed to use subsets of this array, consisting of either 12 or 6 elements. Each subset has either a uniform spacing or a Minimum Redundancy Array (MRA).[2] The MRA provides all spacings that are multiples of a basic spacing up to some maximum spacing with the minimum number of antennas. In the DAASM system the several antenna sub-array configurations available are briefly described in the following table:

Table 1. DAASM Arrays (Large)

No. of Elements	Min. Spacing	Max. Spacing	Remarks	Configuration Code
12	10 m	110 m	Uniform	5/0
11	10 m	450 m	MRA	5/4

The configuration code above is designated by the symbols T/A, where T selects the frequency mode and sampling sequence and A selects the antenna sequence. As will be described later, the DAASM system was designed to operate with pulsed transmissions at a 400 Hz repetition frequency. The experiments described in this report all involve measurements carried out in conjunction with the transmitter on-board the KC-135 aircraft as a signal source flying to the north of Goose Bay. Because of transmitter average power limitations on the aircraft, pulse repetition frequency was limited to 200 Hz. This necessitated a change in the Goose Bay antenna system. Five additional sub-arrays, each with six elements, were devised. Table 2 describes these sub-arrays. All of the arrays are included in the 20 antennas and are selectable by a single multiposition switch in the DAASM system. Depending on the selected sub-array, the DAASM system samples each antenna sequentially with each transmitted pulse. After completing the sequence of 6 or 12 antennas, the cycle is repeated until 512 samples are acquired on each antenna of the selected array. In fact, the DAASM system operates at any two selected radio frequencies at the same time.

2. Richard, D. W. (1972) Twenty-Element Receive Array for the DAASM Experiment, Instrumentation Paper No. 178.

3. Bibl, K. (1973) Doppler/Angle of Arrival Spectral Measurement System, AFCRL-TR-73-0759.

time and space. In order to accomplish this, an array of small receiving antennas was erected in a linear configuration broadside to the required receiving direction. In this case the boresight of the array at Goose Bay, that is, the direction normal to the length of the array, was magnetic North, 328° T. In order to provide maximum flexibility in terms of spatial sampling, a complex antenna arrangement was developed[2] using a 20-element array. The DAASM electronic system[3] was designed to use subsets of this array, consisting of either 12 or 6 elements. Each subset has either a uniform spacing or a Minimum Redundancy Array (MRA).[2] The MRA provides all spacings that are multiples of a basic spacing up to some maximum spacing with the minimum number of antennas. In the DAASM system the several antenna sub-array configurations available are briefly described in the following table:

Table 1. DAASM Arrays (Large)

No. of Elements	Min. Spacing	Max. Spacing	Remarks	Configuration Code
12	10 m	110 m	Uniform	5/0
11	10 m	450 m	MRA	5/4

The configuration code above is designated by the symbols T/A, where T selects the frequency mode and sampling sequence and A selects the antenna sequence. As will be described later, the DAASM system was designed to operate with pulsed transmissions at a 400 Hz repetition frequency. The experiments described in this report all involve measurements carried out in conjunction with the transmitter on-board the KC-135 aircraft as a signal source flying to the north of Goose Bay. Because of transmitter average power limitations on the aircraft, pulse repetition frequency was limited to 200 Hz. This necessitated a change in the Goose Bay antenna system. Five additional sub-arrays, each with six elements, were devised. Table 2 describes these sub-arrays. All of the arrays are included in the 20 antennas and are selectable by a single multiposition switch in the DAASM system. Depending on the selected sub-array, the DAASM system samples each antenna sequentially with each transmitted pulse. After completing the sequence of 6 or 12 antennas, the cycle is repeated until 512 samples are acquired on each antenna of the selected array. In fact, the DAASM system operates at any two selected radio frequencies at the same time.

2. Richard, D. W. (1972) Twenty-Element Receive Array for the DAASM Experiment, Instrumentation Paper No. 178.

3. Bibl, K. (1973) Doppler/Angle of Arrival Spectral Measurement System, AFCRL-TR-73-0759.

Table 2. Additional Sub-Arrays

No. of Elements	Min. Spacing	Max. Spacing	Remarks	Configuration Code
6	10 m	50 m	Uniform	7/0
6	20 m	100 m	Uniform	7/2
6	20 m	320 m	MRA (Approx)	7/4
6	30 m	720 m	MRA (Approx)	7/6
6	70 m	910 m	MRA (Approx)	7/7

The actual procedure is to cycle through the array the first time using the first frequency, then a second time through the array using the second frequency. On the third sampling sequence through the array, the first frequency is used again and this cycling is repeated until the 512 time samples at each antenna and at each frequency have been recorded.

This technique results in a sampling rate of approximately 16 Hz per antenna, per frequency, and a 32 sec time sample when the system prf is 200 Hz.

The signals are recorded synchronously on digital magnetic tape from four sampling gates delayed in time from the transmitter pulse by a selectable amount. The output of the four gates is digitized with seven bits and then recorded. Each sample is recorded in quadrature at the 100 kHz IF. For the experiments described here, the delayed gates are set at the time of the arriving signals from the aircraft which is equipped with a similar DAASM system and operates synchronously with Goose Bay.

The spatial (antenna array) and temporal samples form the two-dimensional array which is used in the data analysis to generate the two-dimensional DAASM maps as described in detail in the next section.

The experiment described in this report consists of six aircraft missions covering the period of December 1973 to July 1974. Each flight was approximately 8 hours in duration, and several different flight patterns were executed flying out to distances of 3000 km to the north of Goose Bay. The details of these plans will follow in Section 2.3. Whenever obliquely propagated signals from the aircraft were available, the delayed sampling gates were made to coincide with the received signal and the data digitized and recorded. Two frequencies were selected for each half hour of the flight before take-off using the best propagation predictions available. In general, each predicted frequency was used for at least 1 hour. With the availability of real-time oblique ionograms (Section 2.2) between aircraft and Goose Bay, the selection of operating frequency was often made during the flight.

2.2 Oblique Ionograms

In November 1973, it was decided to generate oblique stepped frequency ionograms between the KC-135 aircraft and the Goose Bay Ionospheric Observatory during the same time that the routine backscatter ionogram was being made at Goose Bay. Both the Goose Bay and the aircraft sounding systems begin the stepped frequency mode simultaneously and each records an oblique ionogram. The frequency range is normally 6 to 16 MHz in 100 kHz steps and the ionogram takes approximately 1 min (Figure 1). These ionograms, although instituted primarily for the purpose of studying the propagation in the polar regions, have played a major role in the DAASM experiment. First they have made possible the real-time selection of the two operating frequencies. By agreement with the operating personnel of both the ground station and the aircraft, and after inspection

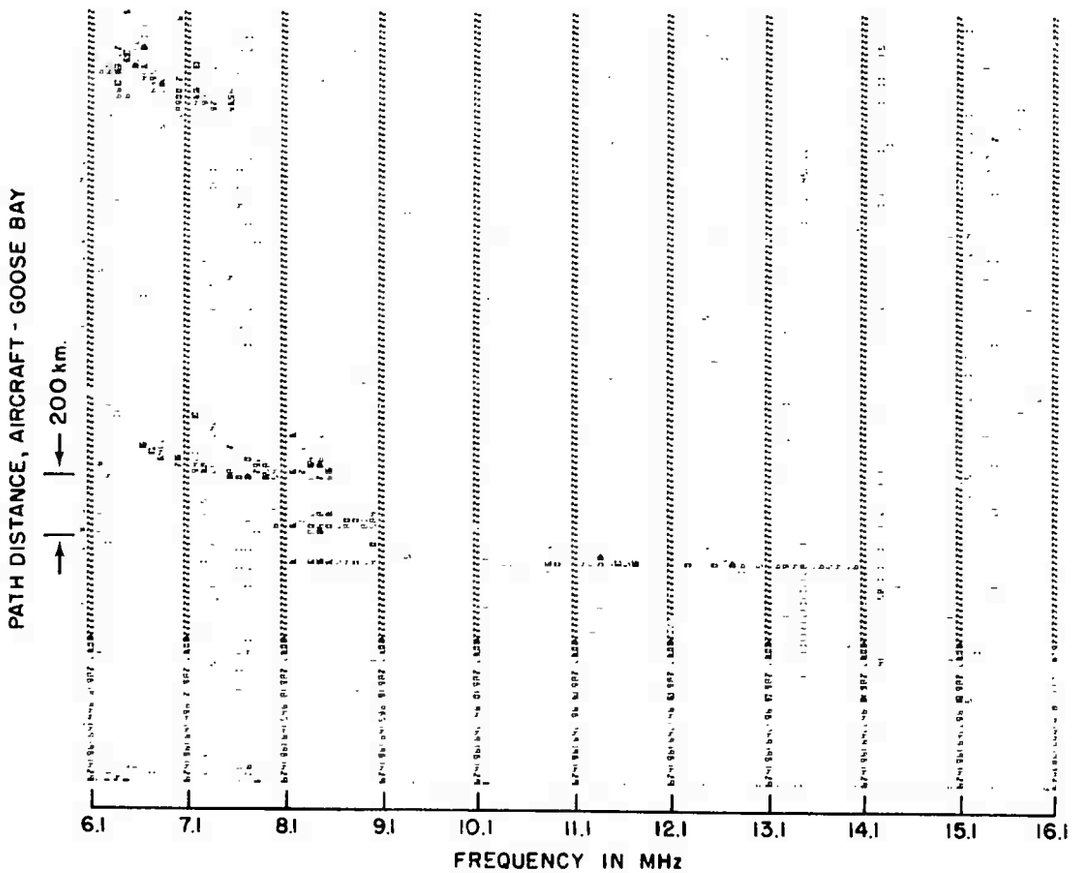

Figure 1. Oblique Ionogram, Goose Bay, Flight 4-196, 15 Jul 1974: 1641 UT: 1240 km

of the oblique ionogram, certain specified changes are allowed at one end of the path and the operator at the other end attempts to follow these changes. With the two-way oblique ionograms, this real-time method has worked exceedingly well and has resulted in frequency usage closer to the optimum than is possible using predictive methods.[4]

The second benefit derived from the oblique ionogram has been in the post analysis, specifically the possibility of making mode identifications. An important part of the DAASM program is to relate the observed spectral character of the fixed frequency maps to the propagation mode. It is through understanding this relationship that techniques for improving OTH radar performance can be developed.

The oblique ionograms are made using the existing Digisonde 128[5] systems located at Goose Bay and in the AFCRL KC-135 aircraft. The data is recorded on digital magnetic tape as well as displayed on site in real time in the manner used for all "Digisonde" data.

2.3 Flight Plans

For each of the six flights used for this report, a flight plan was developed for use by the aircraft navigator. The actual flight paths deviated only slightly from the planned path, and in the subsequent description only the actual paths are presented. The chosen paths were often a compromise between competing objectives. Certain compromises in flight path were sometimes made to permit auroral oval monitoring by other scientists involved in the airborne measurements program.

Each of the six flight paths are presented in three different manners. The first display for each flight shows the actual geographic location of the aircraft as a function of time on a geomagnetic projection, while the second display shows range and bearing of the aircraft from Goose Bay. The third display shows the path of the aircraft in corrected geomagnetic time vs latitude. The auroral oval for Q = 3 remains fixed in this coordinate system. This allows the user to see the physical relationship between the aircraft, Goose Bay and the oval during the flight. These aircraft track maps are useful when interpreting the observed propagation modes and DAASM maps.

---

4. Barghausen, A. F., et al (1969) Predicting Long Term Operational Parameters of High Frequency Sky-Wave Telecommunications Systems, ESSA Tech. Report ERL 110-ITS-78.

5. Bibl, K., et al (1970) Digital Interpreting Goniometric Ionospheric Sounder, AFCRL-71-0002.

The six flights used in this report are detailed in the following table:

Table 3. DAASM Flights

DAASM No.	Date	Take-Off (UT)	Landing (UT)
DM 4-058	27 Feb 1974	1900	0342
DM 4-060	1 Mar 1974	2355	0829
DM 4-141	21 May 1974	1743	0220
DM 4-142	22 May 1974	2032	0457
DM 4-193	12 Jul 1974	1440	2250
DM 4-196	15 Jul 1974	1440	2236

3. ANALYTIC TECHNIQUES

3.1 DAASM

As stated in the introduction, the purpose of the DAASM project is to provide a description of the character of radio signals arriving from a point source through a relatively disturbed ionospheric medium. In order to provide such a description the approach chosen is to devise a signal power density estimate as a function of two variables. Doppler frequency, ω, and wave number, k, associated with arrival angle.

The power as a function of these two variables results from the two-dimensional transforms of the recorded amplitude data in space and time, that is, x and t. The DAASM system at Goose Bay utilizes a one-dimensional linear azimuthal arrival angle. The data is ambiguous with respect to the elevation angle of the source or sources.

Three methods of estimating the power density function are described. The three methods arose from the various antenna configurations available with the DAASM system. The third method is the only one used for all the data presented here, even though it is relatively time consuming on the computer because it involves matrix inversion.

As a general introduction to the analytic techniques used here, a short description of the basic approach is given.

If the time samples are understood to constitute one dimension and the spatial samples to be the second dimension, then the two-dimensional Fourier transforms yields the Doppler frequency/wavenumber power density (FWPD) spectrum.

Thus, if $A_j(\omega)$ and $A_m(\omega)$ denote the discrete complex Fourier spectral line at Doppler frequency, ω at antennas j and m respectively, then the cross spectrum between the antennas is given by:

$$S_{jm}(\omega) = A_j(\omega) \cdot A^*_m(\omega) .$$

In general, a smoothed version of cross-spectral estimates $S_{jm}(\omega)$ is always used. The estimated FWPD spectrum is defined by

$$P(\omega, \vec{k}) = \sum_{j=1}^{N} \sum_{m=1}^{N} W_j W_m \hat{S}_{jm}(\omega) \cdot \exp i \vec{k} \cdot (\vec{r}_j - \vec{r}_m) \qquad (1)$$

where N is the total number of antennas, $\vec{r}_n$'s are the vector distances from some arbitrary origin, k is the wavenumber vector, and the W's are suitable weights imposed on the i^{th} antenna.

In a report,[1] different methods of spectral analysis to extract Doppler frequency, phase and coherence information are described in detail. It was found that the frequency-averaging technique provided a very efficient and reliable means of cross-spectral estimation, and only the frequency-averaging technique of estimating the cross-spectra is used in all of the data involved here. Once the cross-spectra have been estimated, the spatial component of the FWPD spectrum can be estimated by several methods. The three methods of wavenumber analysis can be delineated in terms of the choice of the weights W_i and are: (1) The Fast Fourier Frequency-Wavenumber Analysis or the Conventional Analysis, which is most useful for an initial diagnostic scan in the frequency-wavenumber (ω- k) space. Wavenumber sidelobe characteristics can be varied by proper choice of weights for the different cross-spectral terms; however, the resolution is relatively poor. (2) The minimum redundancy version of the conventional method is only applicable to the data from a strict minimum redundancy configuration of the antennas. (3) The adaptive method using the maximum likelihood principle offers high resolution in spatial characteristics and is applicable to any arbitrary antenna configuration. Unlike the other two methods, this method assigns adaptive weights to the different cross-spectral terms depending on the azimuthal look-angle and the spatial characteristics of interference and noise.

The part of the analysis and computation common to all three methods is the determination of a suitable cross-spectral estimate between any given pair of antennas.

The recorded data, 512 points per subcase for each antenna, consists of two sets of 256 equally-spaced complex-valued time samples displaced from each other by a ratio $\beta = \frac{6}{25}$. Each 256 sample set could be used for processing; however, it is practical to treat only the middle 128 samples in each set in order to

1. Pfister, W., et al (1975) Pulse Sounding with Closely Spaced Receivers as a Tool for Measuring Atmospheric Motions and Fine Structure in the Ionosphere, Vol. VII, Environmental Research Paper No. 506, April 1975.

allow for adjustment of range gates and frequency before processing the data. Thus, the sets consisting of 128 samples in each subcase are immediately transformed into the frequency domain via a Fast Fourier Transform. The resulting 128 complex-valued discrete Fourier spectrum spans a basic Doppler frequency range of 8 Hz. It is possible to either combine or interlace the resulting two sets of Fourier spectra. If the Fourier spectra are aligned, the signal-to-noise ratio can be improved but the basic Doppler frequency range is still 8 Hz. If the two sets are interlaced, the Doppler frequency range can be doubled to 16 Hz without any improvement in the signal-to-noise ratio.

In the case of signals transmitted by the aircraft, the basic range of 8 Hz is sufficient. Backscatter signals often occupy a band wider than 8 Hz, in which case interlacing proves to be very useful. In any case, the combined or interlaced Fourier spectra form the starting point for further data processing.

Three types of output have been designed. These consist of (1) power spectra, (2) coherence spectra, and (3) maps of Doppler frequency vs arrival angle called DAASM maps.

3.1.1 POWER SPECTRA

Power spectra are calculated for each antenna by taking the product of each Fourier spectral line with its own complex conjugate. Of course, the Fourier spectra are normalized in each channel so that the total power in each channel equals unity. That is, if g'_m represents the unnormalized m^{th} frequency line, then the normalized Fourier spectrum is simply

$$g_m = \frac{g'_m}{\sqrt{\sum_{i=1}^{N} g'_i \cdot g'^{*}_i}} .$$

The power spectra are smoothed by the frequency-averaging technique[1] over seven frequencies concurrently with the operation of evaluating the product of the Fourier spectra. This feature enables the cross-spectra to be estimated in an identical way merely by inserting the Fourier spectra of the appropriate pair of antennas. The power spectra and the cross-spectra are different only in a matter of the antennas involved.

The power spectra thus obtained are plotted on a standard format of logarithmically-scaled numbers ranging from 0 to 15 which corresponds to a linear scale from 0 to 99. The exact equation defining the scales is

1. Pfister, W., et al (1975) Pulse Sounding with Closely Spaced Receivers as a Tool for Measuring Atmospheric Motions and Fine Structure in the Ionosphere, Vol. VII, Environmental Research Paper No. 506, April 1975.

$$P_{log} = 2 + 7 \log_{10} P_{lin} \qquad 1 \leq P_{lin} < 100$$

$$= 2 \times P_{lin} \qquad P_{lin} \leq 1$$

where P_{log} is the printed output integer and P_{lin} is the value of the normalized power for the i^{th} frequency designed to have a maximum of 100.

$$P_{lin} = \frac{P_i}{\sum_{i=1}^{256} P_i} \cdot 256 .$$

The power spectral outputs provide the basis for selection of data segments suitable for the more complex and time consuming $P(\omega, k)$ analysis. The data consists of subcases where each subcase has four different range gates and two carrier frequencies. Therefore, for the six antenna configurations there will be 48 channels of power spectra for each subcase.

3.1.2 COHERENCE

Coherence spectra between the m^{th} and the n^{th} channels (antenna) is defined by the equation:

$$\left| COH(\omega)_{mn} \right| = \frac{|\hat{S}_{mn}(\omega)|}{\sqrt{\hat{S}_{mm}(\omega) \cdot \hat{S}_{nn}(\omega)}}$$

where $\hat{S}_{mn}(\omega)$ is the smoothed cross spectrum at Doppler frequency ω between m^{th} and n^{th} channels and $\hat{S}_{mm}(\omega)$ would be the power spectrum of the m^{th} channel. It is clear that the coherence is a number which lies between 0 and 1. This linear range is converted to an inverse hyperbolic tangent scale and multiplied by a suitable scale factor to provide the printed output numbers for the data in Section 4. The following table shows the relationship between coherence value and output numbers. The coherence spectra are plotted for each available distance between the various pairs of antennas in order of increasing distance. Since the coherence is only available at specified distances, the plots are backfilled at intermediate distances with the same value. It was found that the raw coherence thus plotted appeared sometimes to be a discontinuous function of distance instead of a monotonically decreasing function. Therefore, three successive subcases have been averaged for each distance at each Doppler frequency to provide a much smoother picture and thus improve the statistical confidence limits which depend on the sample size. A least-square linear fit is plotted for a sample of these data in Figure 2.

Table 4. Coherence Table

Coherence	Printed Number
≤ 0.30	0
0.31	1
0.56	2
0.74	3
0.86	4
0.92	5
0.96	6
0.98	7
> 0.99	8 through 15

The coherence spectra are primarily useful in determining the maximum useful aperture as a function of operating frequency and the signal propagation mode.

3.1.3 DAASM MAPS

DAASM maps consist of plots of power density vs Doppler frequency and wavenumber which, in turn, is simply related to the azimuthal angle of arrival.

3.1.3.1 Bartlett Estimate

A particularly efficient algorithm to calculate the $(\omega - k)$ spectra is achieved if the weights in Eq. (1) are chosen to correspond to a triangular taper function and will be referred to as Fast Frequency-Wavenumber analysis or the generalized Bartlett estimate.

In such a case, the individual cross-spectral terms need not be separately calculated. The separate Fourier spectra from each antenna output can be used directly, and frequency smoothing can be applied in the final step. The details of the algorithm are as follows:

Let $|A_j(\omega)| \exp i \phi_j(\omega)$ represent the Fourier spectral line at frequency ω from the j^{th} antenna. Then the cross-spectrum between the j^{th} and m^{th} antennas is

$$S_{jm}(\omega) = |A_j(\omega)| \; |A_m(\omega)| \exp i (\phi_j - \phi_m)$$

and the $(\omega - k)$ spectrum

$$P(\omega, \vec{k}) = \sum_{j=1}^{N} \sum_{m=1}^{N} S_{jm}(\omega) \exp -\left\{ i\vec{k} \cdot (r_j - r_m) \right\} \qquad (2)$$

where $\vec{k}$ is the wavenumber.

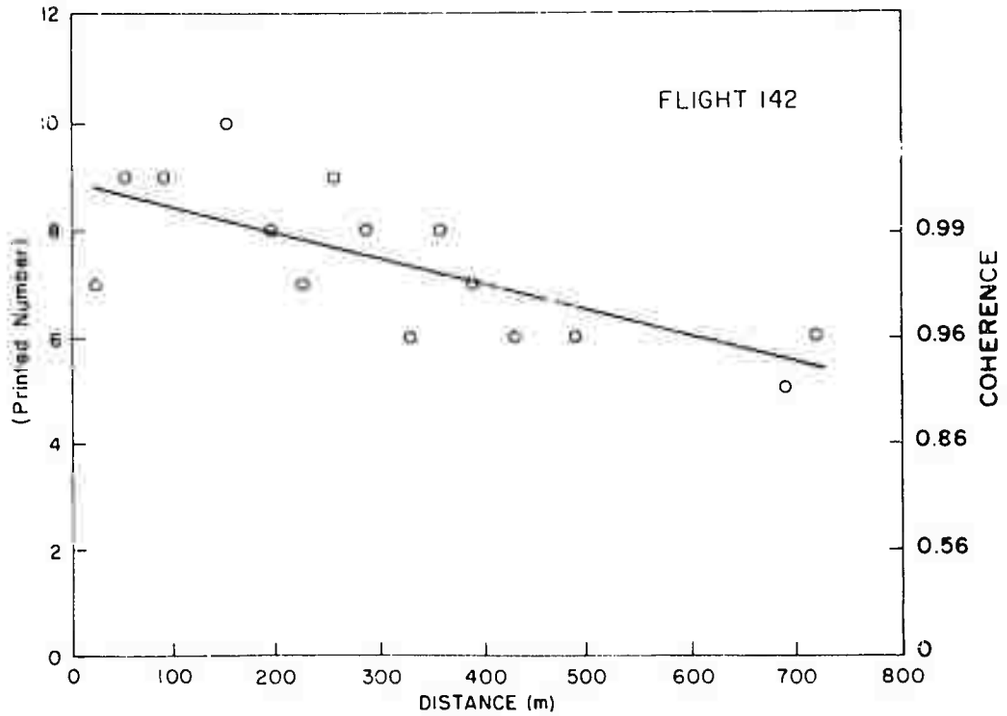

(a) Frequency 11.22 MHz, Flight 4-142, 2253 UT

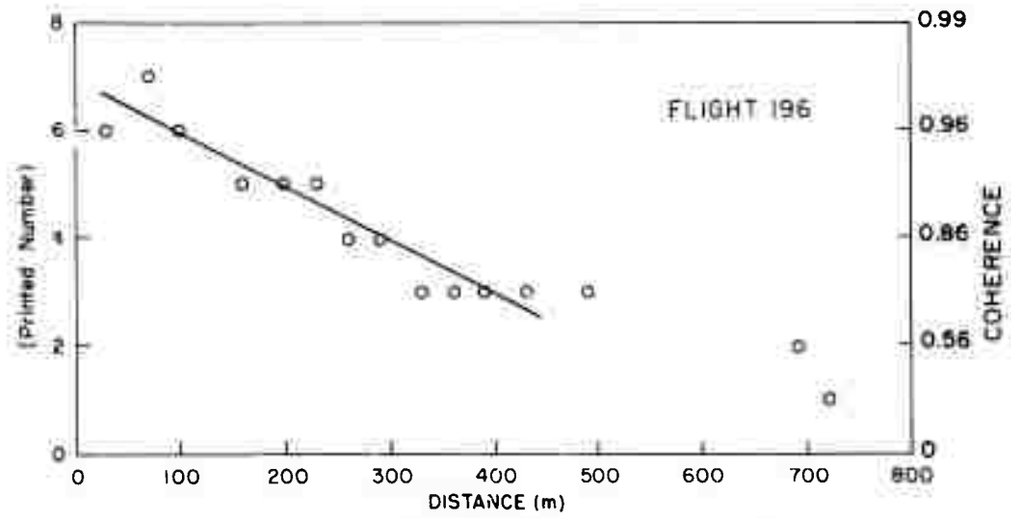

(b) Frequency 8.22 MHz, Flight 4-196, 1940 UT

Figure 2. Coherence vs Distance, Typical Plot

Eq. (2) can be written alternately as

$$P(\omega, \vec{k}) = \sum_{j=1}^{N} |A_j(\omega)| \exp\left\{ i \left| \phi_j(\omega) - \vec{k} \cdot \vec{r}_j \right| \right\} \times$$

$$\sum_{m=1}^{N} |A_m(\omega)| \exp\left\{ - i \left| \phi_m(\omega) - \vec{k} \cdot \vec{r}_m \right| \right\} . \qquad (3)$$

The subscripts j and m can be replaced by a single subscript n m-j, and the double summation can be replaced by a single summation. Thus,

$$P(\omega, \vec{k}) = \left| \left\{ \sum_{n=1}^{N} A_n(\omega) \exp i \left| \phi_n(\omega) - \vec{k} \cdot \vec{r}_n \right| \right\} \right|^2 . \qquad (4)$$

Eq. (4) can be computed much faster than Eq. (3).

$P(\omega, \vec{k})$ is calculated at as many points as desired in $\vec{k}$, say with increments $\Delta\vec{k}$. Each successive point in k can be computed from the previously computed point by simple complex multiplication because exp i (k + Δk) = exp ik · exp iΔk. This step is common to all three approaches of (ω-k) spectral calculations and saves considerable computer memory and time.

Since frequency smoothing is independent of the operations of k, a set of weights W(ω) is calculated using P(ω, o) for each ω, and each P(ω, k) is multiplied by the appropriate W(ω) to yield P(ω, k), the frequency smoothed estimate. The relation between the wavenumber k and the direction of arrival ∅ measured from boresight for the case of a linear array is given by

$$k = |k| = \frac{2\pi f}{c} \sin \phi$$

where k is now a scalar, f the operating carrier frequency, and c the velocity of light.

3.1.3.2 Hanning Estimate (Minimum Redundancy Version)

The minimum redundancy array version can be treated as a special case of the general equation for the (ω-k) spectra given by Eq. (1). It is assumed, of course, that a certain number of consecutive multiples of the basic antenna spacing are available by suitably placing the different antennas. Distances beyond the largest consecutive multiple are considered as having zero weight; that is, their contribution to the (ω-k) spectra is zero. The non-zero weights decrease as a cosine squared function with distance. In addition, the self-spectral term is assigned a weight of 0.5, so that the expression for the (ω-k) spectrum can be written as

$$P(\omega,\vec{k}) = \frac{1}{2} S_o + \sum_{\ell=1}^{L} W_\ell S_\ell \exp i(k \cdot d_\ell) \qquad (5)$$

where S_o corresponds to the self term and S_ℓ is the cross-spectral term corresponding to the pair of antennas separated by a distance d_ℓ. L is the largest successive multiple of the basic spacing and W_ℓ is the weight given by the cosine-squared function. It is well known that the cosine-squared weights result in good sidelobe suppression. It can be shown[6] that for 6 antennas only 13 consecutive multiples are possible, and for 11 antennas the corresponding number is 45. A similar configuration for more than 11 antennas is not known at the present time. Each spacing occurs only once, and hence the name "minimum redundancy" for the array. Only those cross-spectral terms corresponding to the multiples of the basic spacing need be calculated. Thus, for 11 antennas, 45 of 66 possible terms are available. The applied weights are almost optimal for the configuration and there is excellent sidelobe suppression. If the carrier frequency is chosen such that the basic spacing is a half-wave length or smaller, then there will be no grating lobes.

3.1.3.3 Maximum Likelihood Estimate

The third approach to (ω-k) spectral estimation employs an adaptive scheme to generate the set of weights in the filter given by Eq. (1) Instead of using a fixed set of weights for all k, the adaptive scheme allows for the set of weights to be varied depending on the particular k as well as the character of the signal, that is, interference and noise. In other words, the set of weights is dictated by the data sample available, subject to the constraints that a unit plane wave signal travelling with a given wavenumber $k = k_o$ (arriving from the direction towards which the antenna beam is pointed), is passed undisturbed through the spatial filter, but everything else for which $k = k_o$ (arriving from other directions) is rejected in an optimal manner. Thus, the true spectrum is reproduced with high resolution and not smeared, which normally occurs as a result of the convolution between the true spectrum and the particular array pattern. This choice of constraints results in a convenient mathematical formulation. It is only necessary to calculate the inverse of the matrix of cross-spectral terms for each Doppler frequency of interest in order to furnish the optimal set of weights automatically adapted to each k for a given data sample. The computational procedure is set forth in the following steps.

The normalized input Fourier spectra from the various antennas is converted to cross-spectral estimates $S_{jm}(\omega)$ by any one of several spectral estimation procedures, in this case by frequency averaging and smoothing with seven frequencies.

6. Moffet, A.T. (1968) IEEE Transactions on Antennas and Propagation AP-16 (No. 2):172.

Subscripts j and m refer to the antennas in question. Next, an N×N matrix of cross-spectral estimates [S(ω)] is organized at each ω, where N is the total number of antennas. Not all N×N terms need be evaluated since $S_{jm}(\omega) = S^*_{mj}(\omega)$, where the asterisk denotes complex conjugation. The sum of the diagonal elements in the matrix is stored as a measure of total power at any given Doppler frequency and used later for renormalization. The matrix itself is normalized by replacing each element $S_{jm}(\omega) \times S_{jm}\omega)/[S_{jj}(\omega)\, S_{mm}(\omega)]^{1/2}$, a step which ensures sensor equalization. The normalized cross-spectral matrix for Doppler frequency ω is then inverted. The elements of the inverted matrix are used in the equation for (ω-k) spectra

$$P(\omega, \vec{k}) = \left| \sum_{m=1}^{N} \sum_{n=1}^{N} [S_{jm}]^{-1} \exp i \vec{k} \cdot (\vec{r}_j - \vec{r}_m) \right|^{-1} . \qquad (6)$$

It is seen that the weights W_i and the cross-spectral elements [Eq. (1)] together are replaced by the corresponding inverted matrix elements and the reciprocal is taken to yield the high-resolution (ω-k) power density estimate. The increments over k are calculated in a chain sequence from the various values in the same manner as indicated before. The final step is to restore relative power levels at the different Doppler frequencies. First, the values of P(ω, k) are summed over all k and the normalized values of P(ω, k) are obtained by simply dividing by this sum. Next, the normalized P(ω, k) are multiplied by the sum of the diagonal elements of the original cross-spectral matrix which have been stored as indicated before. Thus, the renormalized P(ω, k) are obtained with an appropriate scale factor and are recorded on magnetic tape for later printouts (see Section 4.2.3).

3.2 Oblique Ionograms

During the six flights, the oblique ionograms have been scaled for both mode availability and frequency. The oblique ionograms are taken, one every 5 min, which represents a considerable effort. The results are used to provide the identification necessary to relate the DAASM maps with propagation mode Another aid to mode identification is the Polar Model ITS-78 program.[7] The polar model program has been modified for use with aircraft to Goose Bay propagation paths, that is, where one end of the propagation path is continuously changing. A synthesized ionogram is calculated from this program and compared with the measured one.

The calculated and measured oblique ionograms together provide a reasonably reliable method of mode identification.

7. Elkins, T. J. (1973) An Empirical Model of the Polar Ionosphere, Survey in Geophysics, No. 267.

4. RESULTS

4.1 General

The results of the aircraft measurements will be presented in sequential sections with each flight as a complete package. The detailed analysis of the DAASM data will be presented in a subsequent report, and here only data will be presented to illustrate the character of the aircraft signals propagated over auroral paths. Within each flight section, the different types of display will be indicated. Figures 3(a), (b), (c) through 8(a), (b), (c) for Flights 4-058, 4-060, 4-141, 4-142, 4-193, and 4-196 are concerned with the aircraft track and propagation paths.

A limited quantity of data is presented here, varying from eight maps for Flight 4-196 to two maps for Flight 4-141. These maps are given in Figures 9(a) and (b) through 14(a) and (b). The maps were selected to illustrate certain general

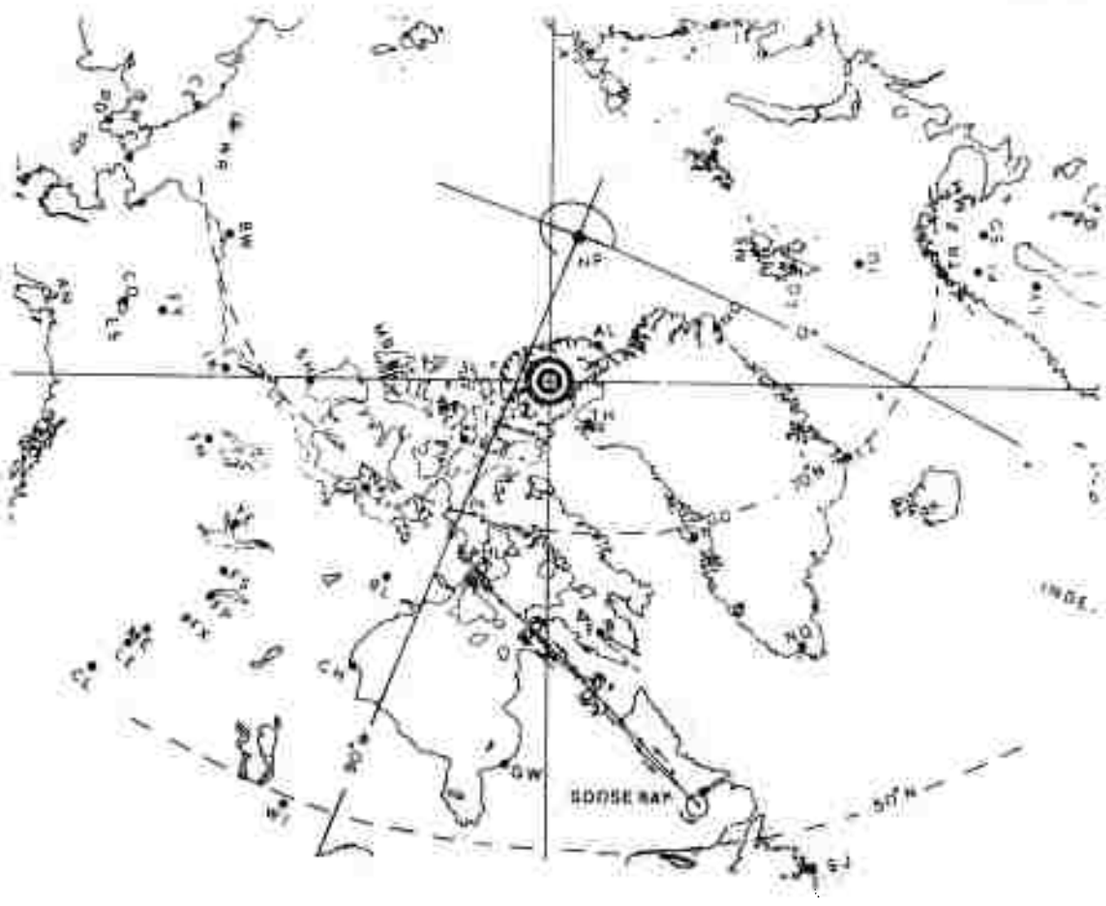

(a) Aircraft Path in Geographic Coordinates on a Polar Geomagnetic Projection

Figure 3. DAASM Flight 4-058, 27 Feb 1974

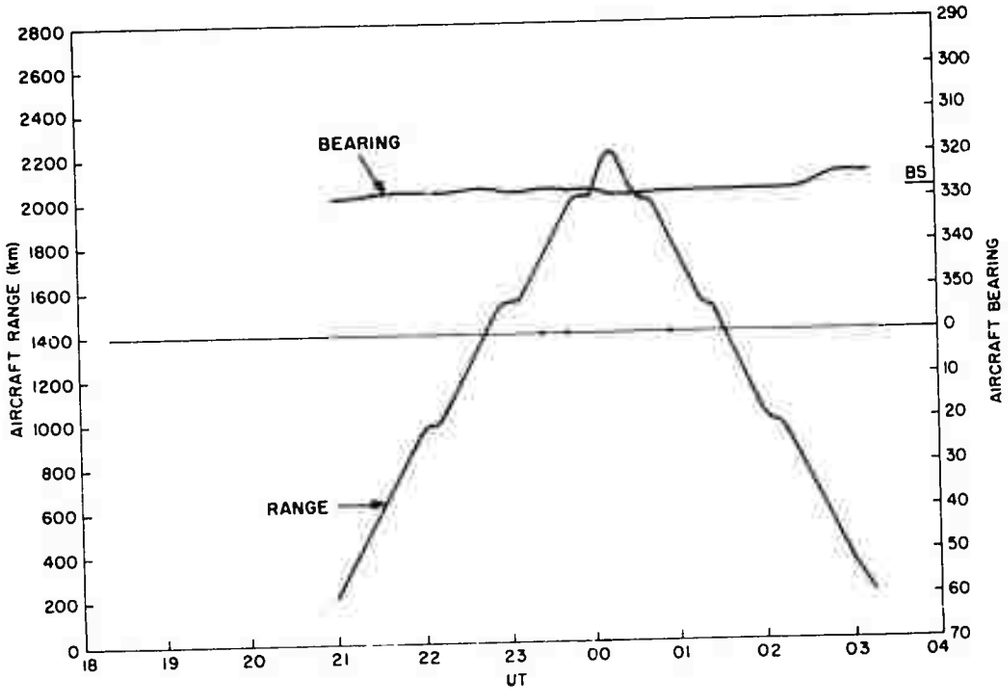

(b) Range and Bearing vs Time of Aircraft from Goose Bay

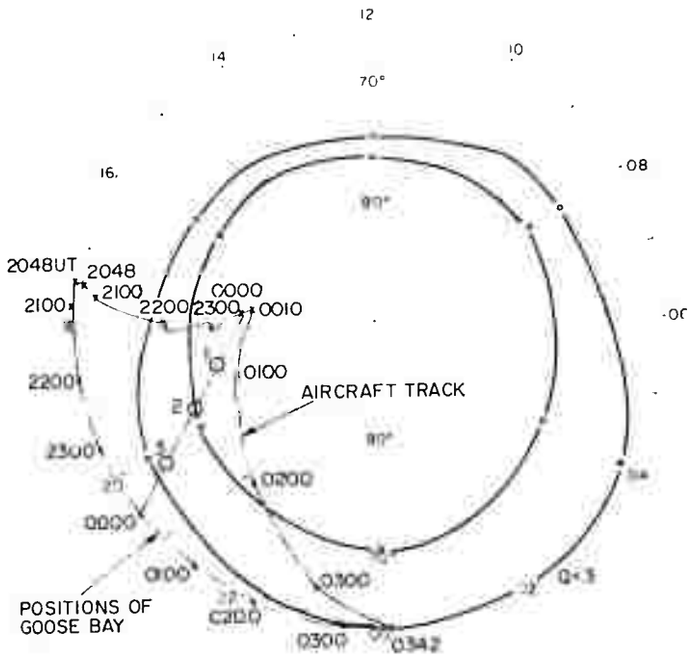

(c) Aircraft Tracks Relative to Auroral Oval (Q = 3), in Geomagnetic Local Time and Latitude

Figure 3. DAASM Flight 4-058, 27 Feb 1974

features of the observed behavior and special events. For each time selected, the maps are included for both Doppler/Arrival Angle and Doppler Frequency/Coherence Distance. This results in a rather complete description of the received signals. The details of the format for this map data will be given in Sections 4.2.3 and 4.2.4. For each flight, the maps will begin with Figure 9(a) for Doppler/Arrival Angle and Figure 9(b) for Doppler/Coherence Distance maps. Each figure will consist of all the maps for that flight identified by time and arranged sequentially.

The map data for each flight is supplemented by the geographical and auroral oval plots of the aircraft track. The auroral oval aircraft track shows the relative position of the aircraft, Goose Bay, and the auroral oval at all times during the flight.

4.2 Data Format

4.2.1 AIRCRAFT TRACK – GEOGRAPHICAL COORDINATES

Using the KC-135 aircraft navigator log, the position of the aircraft at each observation time is plotted in geographic coordinates in Figures 3(a) through 8(a) for each flight on a polar projection of the Earth. Along the track are indicated the hourly positions. In order to make some of the more complicated flight paths clear and for use in analysis of the DAASM maps, Figure 2(b) is a plot of range and bearing of the aircraft measured from Goose Bay as a function of time.

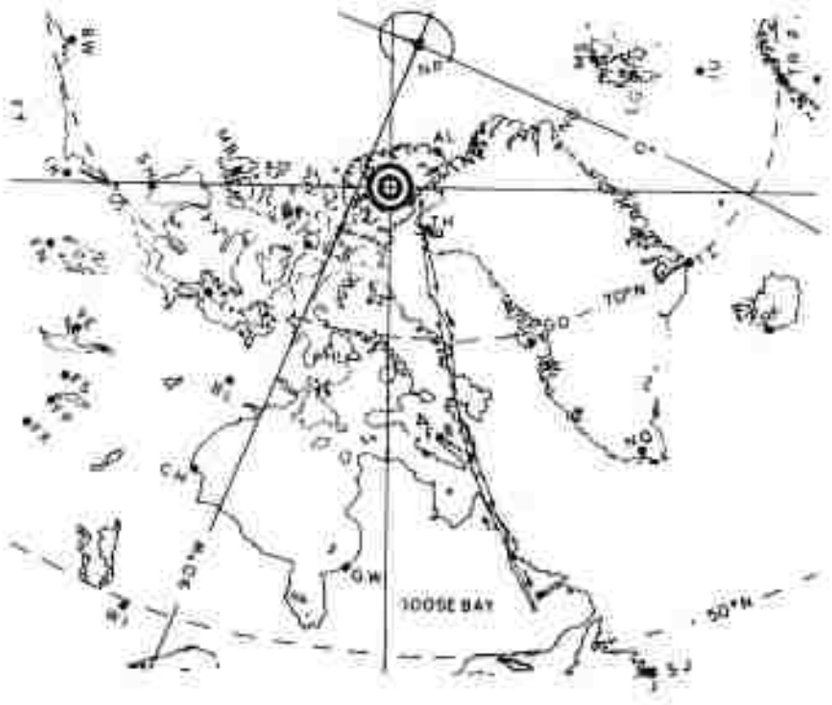

(a) Aircraft Path in Geographic Coordinates on a Polar Geomagnetic Projection

Figure 4. DAASM Flight 4-060, 1 Mar 1974

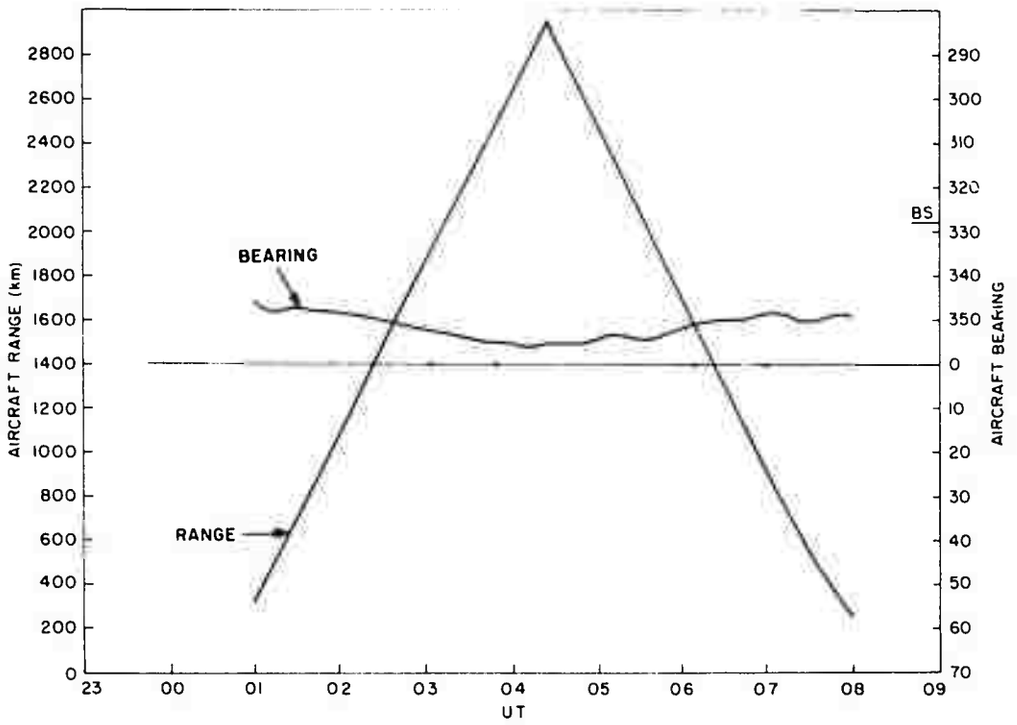

(b) Range and Bearing vs Time of Aircraft from Goose Bay

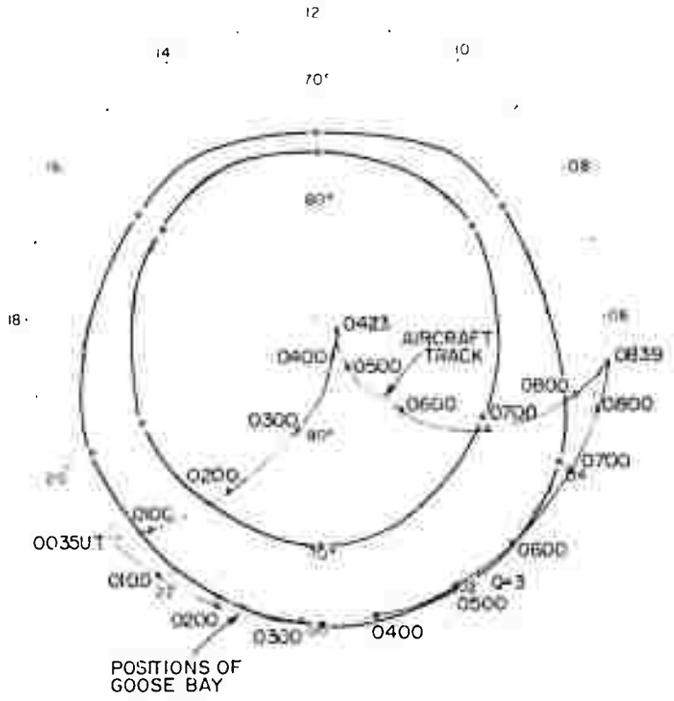

(c) Aircraft Tracks Relative to Auroral Oval (Q = 3), in Geomagnetic Local Time and Latitude

Figure 4. DAASM Flight 4-060, 1 Mar 1974

4.2.2 AIRCRAFT TRACK – AURORAL OVAL COORDINATES

In order to see the relationship between the aircraft position and the auroral oval as a function time during the flight, a second plot of aircraft position in geomagnetic latitude against corrected geomagnetic time, in polar form, is shown in Figures 3(c) through 8(c). In this coordinate system, the auroral oval remains fixed while the receiving site at Goose Bay circles at constant geomagnetic latitude, 53.3°N, and is shown at hourly positions. In Figure 3(c), the one-hop and two-hop reflection points are indicated for the aircraft to Goose Bay at 0000 UT. The points labelled 1 and 3 are the two-hop reflection points, and the point labelled 2 is the one-hop reflection point. It is obvious from Figure 3(c) that the one-hop reflection point lies within the oval near the poleward edge while for the two-hop mode, one reflection point lies in the polar cap and the second reflection lies within the oval. This information will be useful for one interpretation of the DAASM maps.

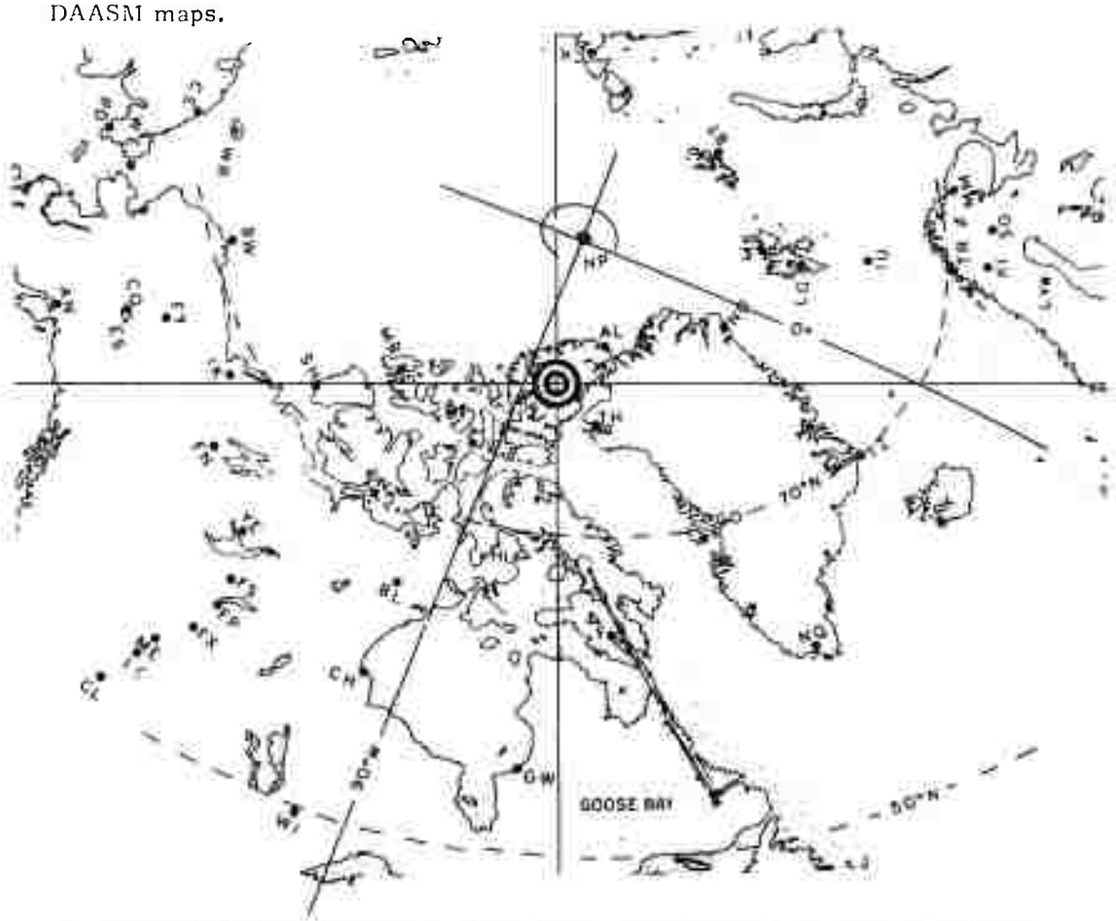

(a) Aircraft Path in Geographic Coordinates on a Polar Geomagnetic Projection

Figure 5. DAASM Flight 4-141, 21 May 1974

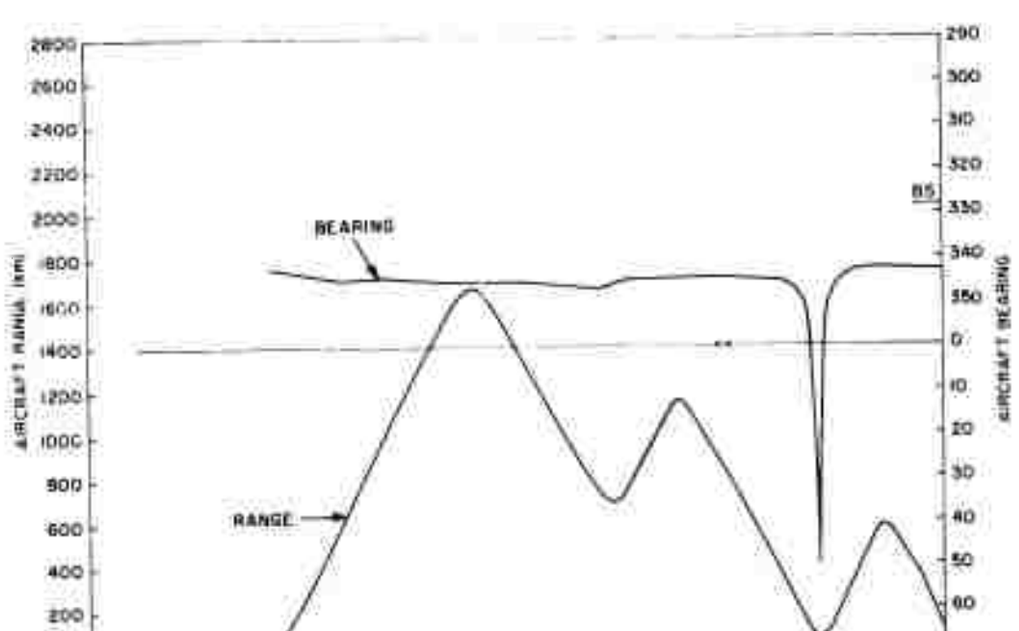

(b) Range and Bearing vs Time of Aircraft from Goose Bay

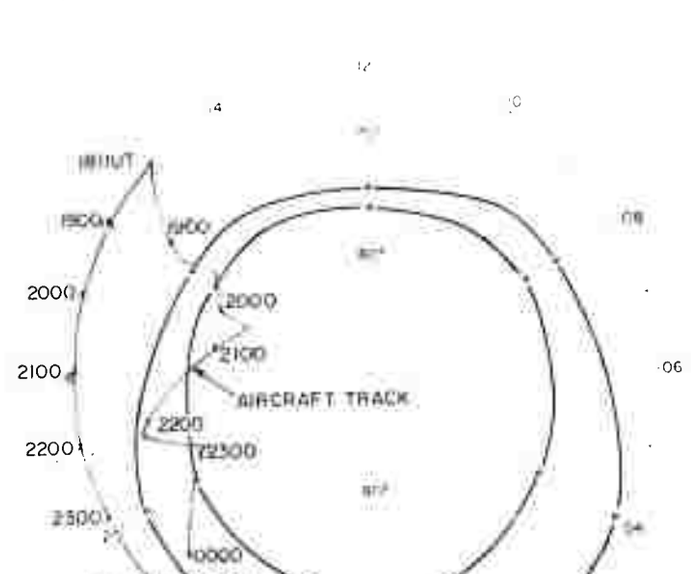

(c) Aircraft Tracks Relative to Auroral Oval (Q = 3), in Geomagnetic Local Time and Latitude

Figure 5. DAASM Flight 4-141, 21 May 1974

4.2.3 DAASM Maps

At any selected time and range, a DAASM map is generated according to the technique described in Section 3.1.3.3. These maps, for each of the two selected operating radio frequencies, represent the Doppler frequency vs arrival-angle spectrum of the aircraft signal. The two operating frequencies are displayed one above the other, and the abscissa is the Doppler frequency in 1 Hz steps about a chosen center frequency indicated in the legend attached to each map. The total Doppler frequency range is always 8 Hz for the maps included in this report. The ordinate scale represents the arrival angle, linear in wave number, measured from boresight (0°) to ± 90° at the end of each map. The arrival-angle scale is repeated twice; once for each radio frequency. The first frequency listed corresponds to the lower map.

Using a special printing system,[5] the presented maps have a dynamic range of approximately 22 dB with the difference between adjacent numbers equal to

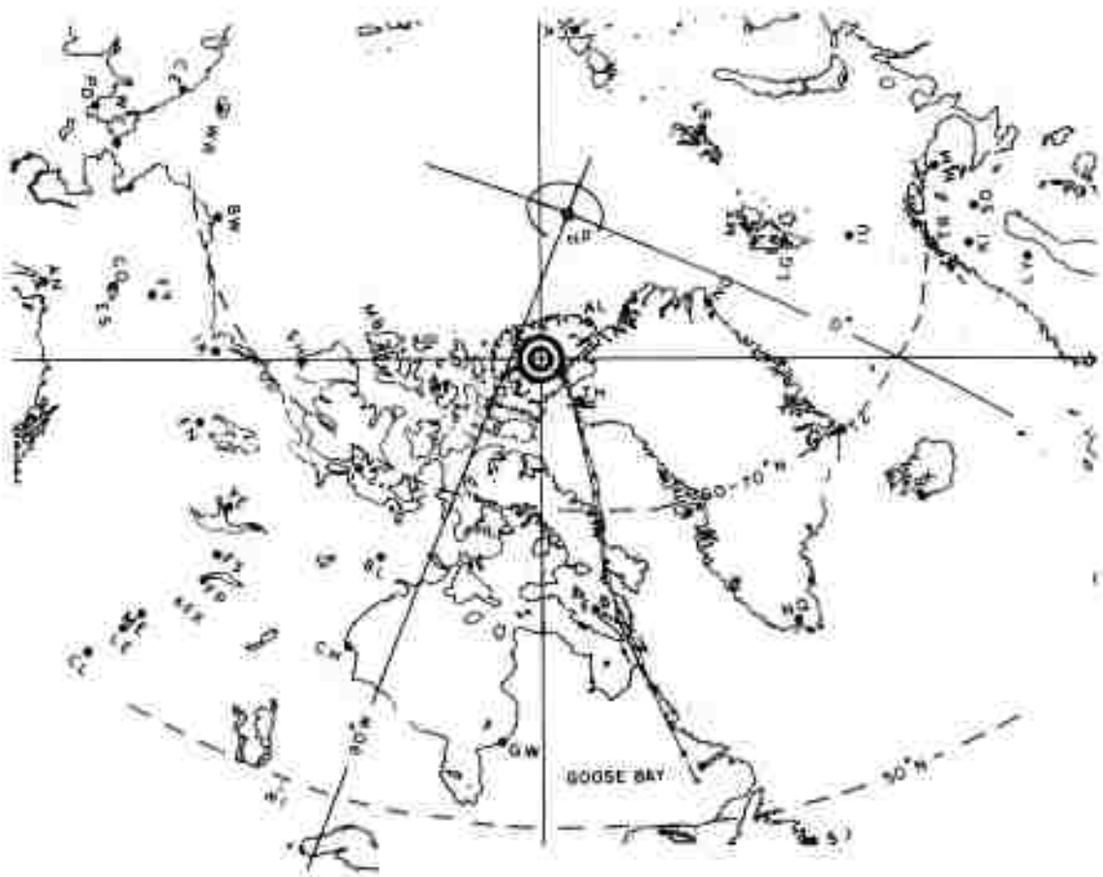

(a) Aircraft Path in Geographic Coordinates on a Polar Geomagnetic Projection

Figure 6. DAASM Flight 4-142, 22 May 1974

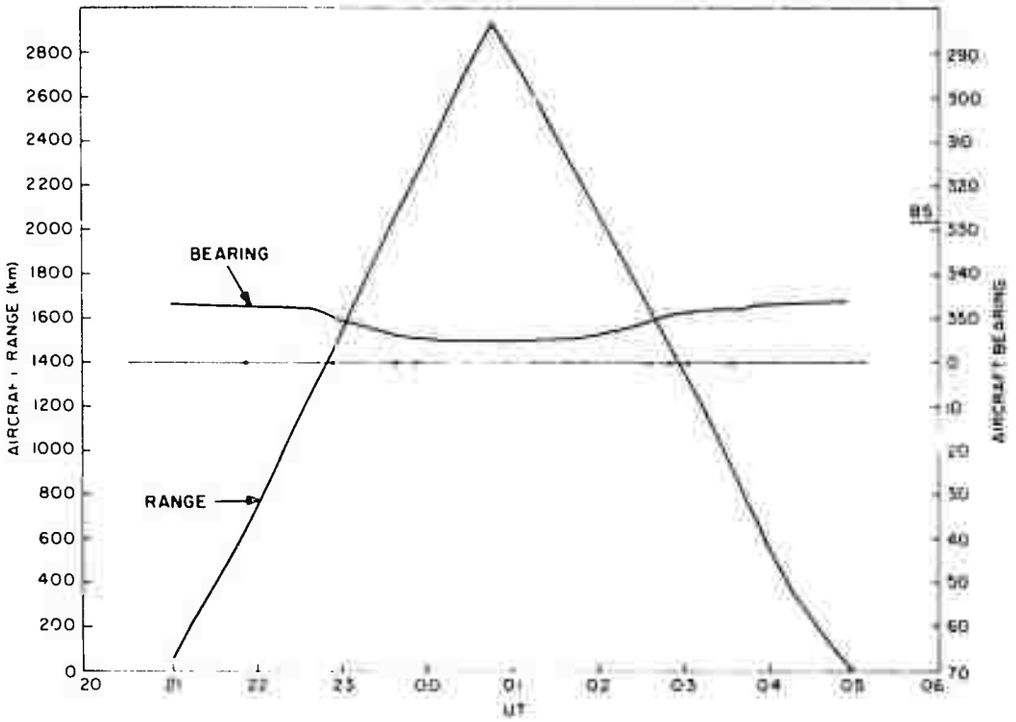

(b) Range and Bearing vs Time of Aircraft from Goose Bay

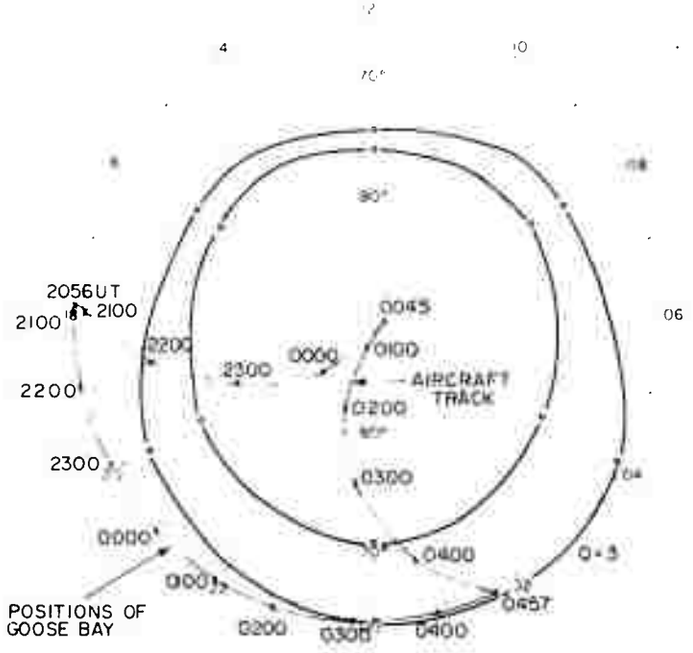

(c) Aircraft Tracks Relative to Auroral Oval (Q = 3), in Geomagnetic Local Time and Latitude

Figure 6. DAASM Flight 4-142, 22 May 1974

1.5 dB. The numbering system is designed so that the larger numbers (numbers range from 0 to 15) appear more dense, giving a visual appearance of increasing blackness near the peaks of the signal. For example, Figure 9(a) (UT 2343) shows the DAASM map for aircraft signals at 8.2 and 6.6 MHz over a distance of 1960 km. The DAASM map in this case was generated using a rather small array with an aperture of 50 m (see Section 2.1). For frequency 1, 8.2 MHz, the received power is very close to boresight, 0°, and at a Doppler frequency of -5.4 Hz. The raw Fourier spectra were smoothed over seven frequencies,[1] and the small antenna aperture results in a minimum width of the displayed signal of the order shown. For other maps where the large antenna arrays were used, narrower angular

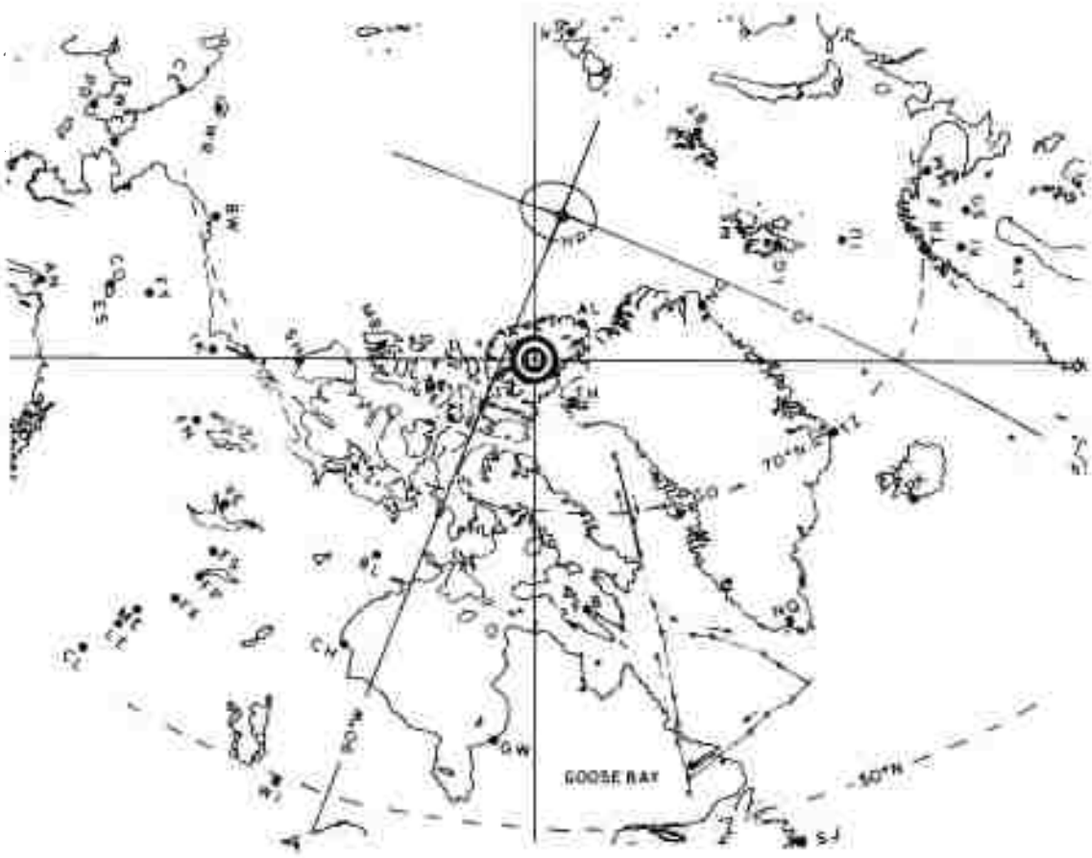

(a) Aircraft Path in Geographic Coordinates on a Polar Geomagnetic Projection

Figure 7. DAASM Flight 4-193, 12 Jul 1974

1. Pfister, W., et al (1975) Pulse Sounding with Closely Spaced Receivers as a Tool for Measuring Atmospheric Motions and Fine Structure in the Ionosphere, Vol. VII, Enivornmental Research Paper No. 506, April 1975.

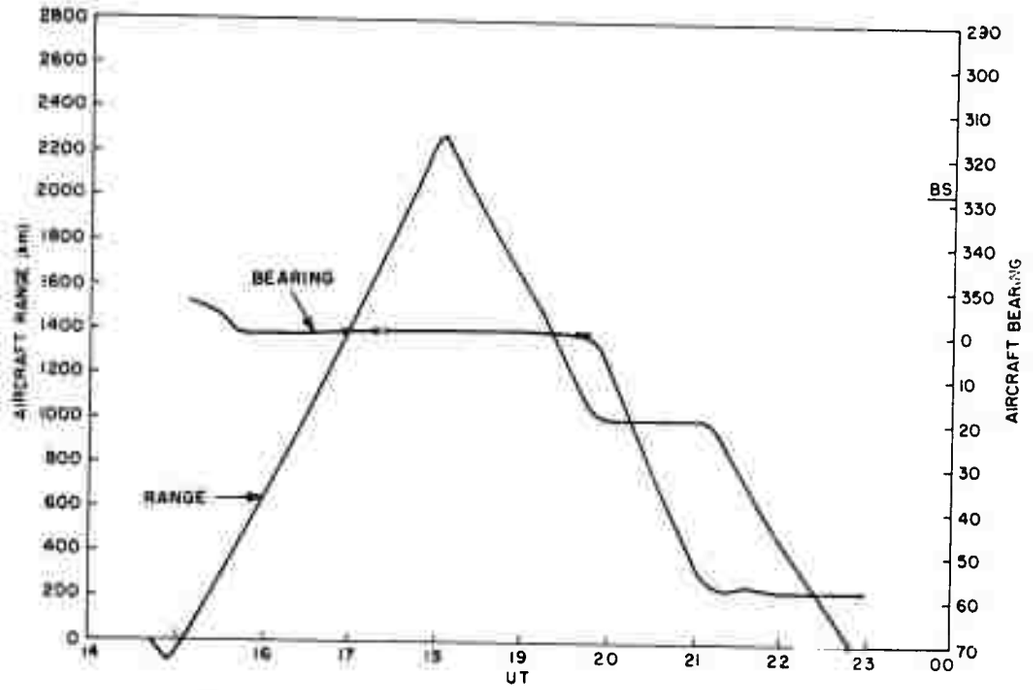

(b) Range and Bearing vs Time of Aircraft from Goose Bay

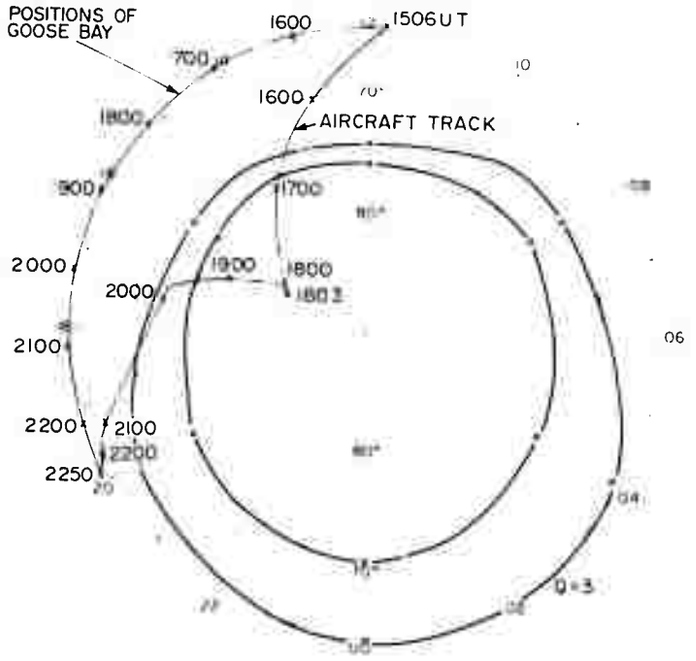

(c) Aircraft Tracks Relative to Auroral Oval (Q = 3), in Geomagnetic Local Time and Latitude

Figure 7. DAASM Flight 4-193, 12 Jul 1974

spectra are often observed. Caution must be exercised in interpreting the observed angular spreading until the specific antenna array is taken into account. The bulk of the data in this report was taken using the 7/6 configuration with an aperture of 720 m allowing relatively high angular resolution.

Examples of narrow angular spectra using the 7/6 array are shown in Figure 13(a) (UT 1940). Here the angular width is as small as any observed for signals propagated in the Arctic ionosphere. The Doppler frequency spreading is also minimal, consistent with the Doppler frequency smoothing. The relatively high amplitude at other arrival angles for the same Doppler frequency as the aircraft signal results from the sidelobes generated by the "Maximum Likelihood" processing (Section 3.1.3.3). In this case, the sidelobes are some 15 dB below the peak. This is acceptable considering the relatively few antennas (six) used in these samples. The sidelobe level suppression depends critically on the number

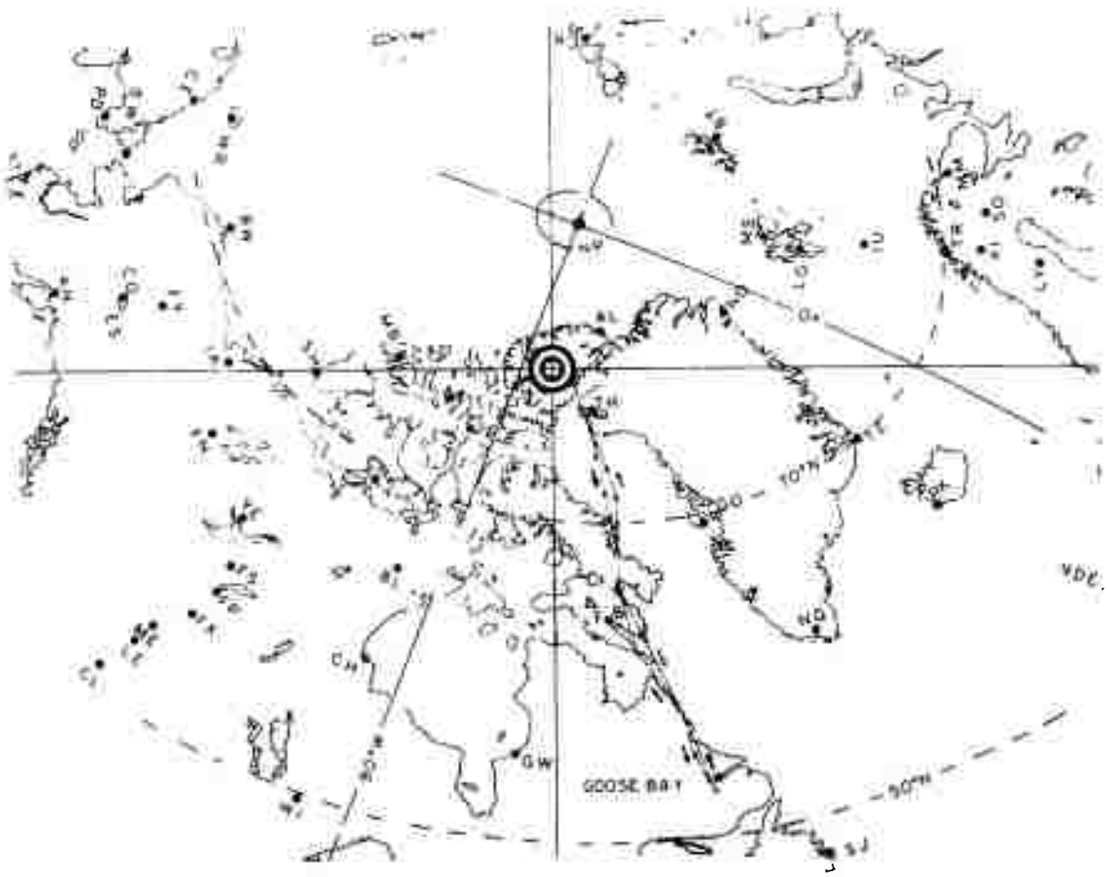

(a) Aircraft Path in Geographic Coordinates on a Polar Geomagnetic Projection

Figure 8. DAASM Flight 4-196, 15 Jul 1974

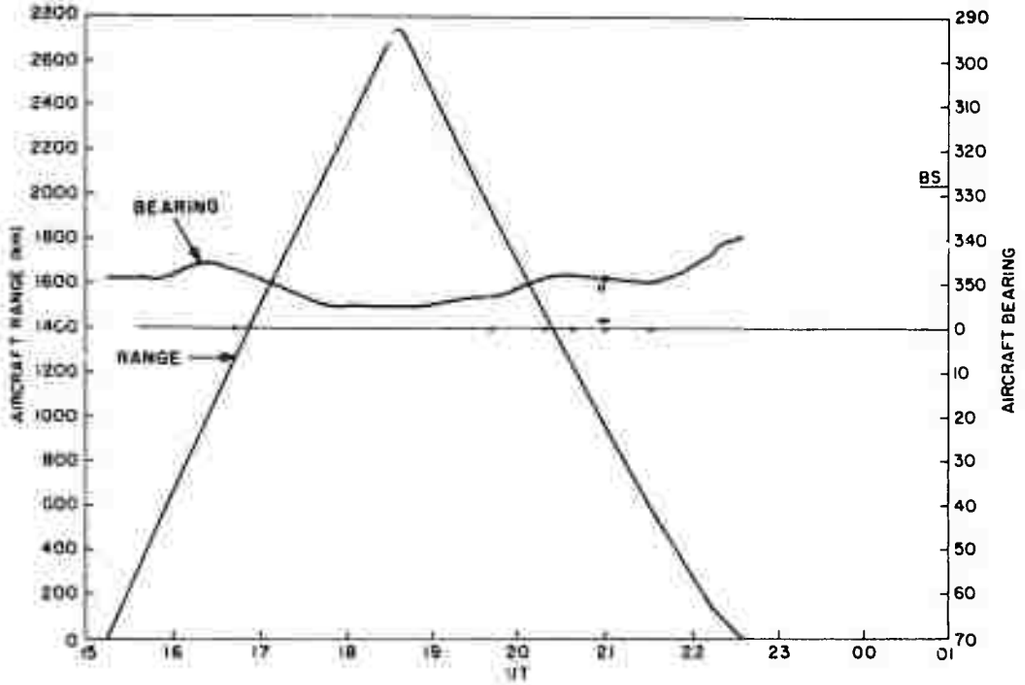

(b) Range and Bearing vs Time of Aircraft from Goose Bay

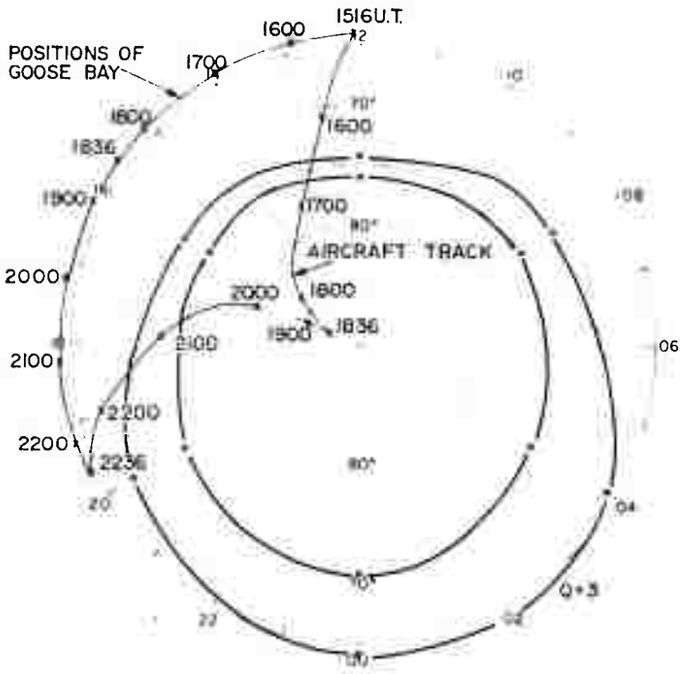

(c) Aircraft Tracks Relative to Auroral Oval (Q = 3), in Geomagnetic Local Time and Latitude

Figure 8. DAASM Flight 4-196, 15 Jul 1974

of antennas used in the analysis. All data processed for this report used six antenna arrays. The resulting high sidelobe level often makes it difficult to identify the aircraft signal; however, the MLM always results in the largest power (highest number) at the correct signal.

4.2.4 COHERENCE MAPS

The coherence between pairs of antennas within the array is defined as the magnitude of the cross-spectra (Section 3.1.2). For each Doppler frequency line in the spectra the coherence is calculated for all the pairs of antennas, that is, all spacings available in the selected antenna array. The coherence map (Figures 9(b) through 14(b) displays the coherence level plotted for each Doppler frequency vs distance. Each distance line in the coherence map represents 10 meters spacing up to a maximum of 960 meters. The maximum distance and the available intermediate distances depends again on the antenna configuration chosen.

For example, the commonly used 7/6 antenna array uses six antennas with physical spacings of 30, 60, 100, 200, and 330 meters giving 15 possible spacings of 30, 60, 100, 160, 200, 230, 260, 290, 330, 360, 390, 430, 490, 690, and 720 meters. All of these spacings are used for coherency calculations and for plotting purposes. The coherence for distances less than 30 meters is set equal to COH (30 m) and the coherence for distances of 40 and 50 meters is set equal to COH (60 m). This back-filling continues up to the largest available distance; in this case 720 meters. Between 720 meters and 960 meters, the end of the graph, no data are available. For the filled arrays, configuration 5/0, 7/0, and 7/2, the largest spacing is in general less than 100 meters and the coherence data of little value, though these coherence maps are included for completeness.

Two typical examples are discussed here for general information. The first example chosen illustrates high coherence across the entire large array and the second coherence which becomes small after only a short distance across the array. The actual computer-printed data is shown in Figures 12(b) (UT 2253) and 14(b) (UT 1940). The upper half of Figure 12(b) (UT 2253) shows a strong line at approximately -8 Hz Doppler frequency where the coherence remains relatively high above the background noise level out to the maximum distance of 720 meters. The lower half of Figure 14(b) (UT 1940) shows a strong line at +5 Hz with a rapidly decreasing coherence as the antenna spacing increases. The coherence is a relatively noisy statistical parameter[8,1] resulting in fluctuations which make the

---

8. Jenkins, G. M., and Watts, D.G. (1968) Spectral Analysis and Its Applications, Holden-Day, pp 374-411.

1. Pfister, W., et al (1975) Pulse Sounding with Closely Spaced Receivers as a Tool for Measuring Atmospheric Motions and Fine Structure in the Ionosphere, Vol. VII, Environmental Research Paper No. 506.

simple concept of monotonically decreasing coherence with distance appear to be violated. Figure 2 shows the least square linear fit to the above illustrated data. For Flight 4-142 at 2253 UT, an antenna separation of approximately 1450 meters would be required for the coherence to decrease to a value of 0.56, while for Flight 4-196 at 1940 UT, the distance required for the coherence to decrease to 0.56 is approximately 500 meters. As will be shown in subsequent reports, this difference in behavior can be related to the propagation mode; that is, the E-modes having high spatial coherence and F-modes relatively shorter coherence distances.

4.3 Aircraft Data

The data consists of compilation of samples of data selected from six aircraft missions (Figures 3 through 14).

5. CONCLUSIONS

The nucleus of this report comprises compilation of samples of data taken from six aircraft missions each lasting approximately 8 hours. This selection process is meant to illustrate several features that are common to the propagation of radio signals from a small source, basically point-to-point propagation in the auroral ionosphere. At this point, it is necessary to recognize the fact that these aircraft signals are often spread both in Doppler frequency and azimuthal arrival angle. Spreading sometimes occurs in only one of these two dimensions. For example, spreading occurs in Doppler frequency and not in arrival angle as can be seen in Figure 14(a) at 2038 UT. There are times when multiple modes are set up which have different Doppler frequencies and arrival angles than that expected from the known aircraft speed and direction. A good example of many modes set up simultaneously is shown in Figure 13a at 1719 UT. Here several modes are established at the same time, very likely due to the passage of a travelling ionospheric disturbance. Another very common feature is reflection from a tilted ionosphere which alters the arrival angle by several degrees.

The two most serious problems encountered in the DAASM experiment at Goose Bay, in terms of the operation of an over-the-horizon radar system appears to be TID's and tilted ionospheres. How much of the occurrence of these features can be ascribed to propagation across the auroral oval needs to be investigated. For this purpose similar measurements at mid-latitude should be undertaken.

The relationship between the observations cataloged here and ionospheric conditions and propagation modes will be presented in a subsequent report.

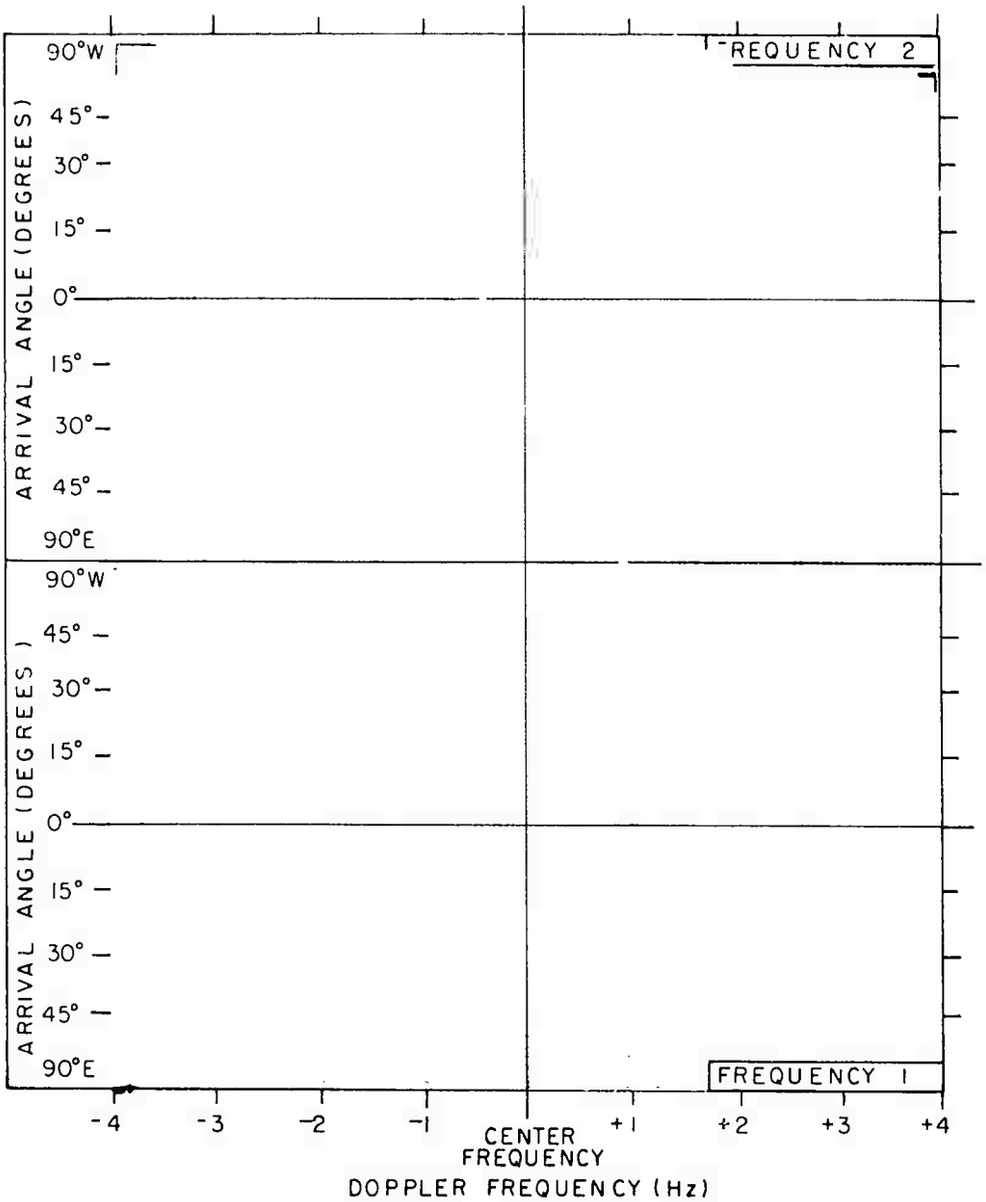

DATE ---------- 2-27-74 (058)
TIME (UT) ---------- 2325
FREQ 1 (MHz) ---------- 8.22
FREQ 2 (MHz) ---------- 10.2
RANGE (Km) ---------- 1710
AZIMUTH (deg.) ---------- 328T
ANT. CONFIGURATION - 7/1
CENTER FREQ (Hz) ---------- -6

a. DAASM Map

Figure 9. Flight 4-058, 27 Feb 1974, UT 2325

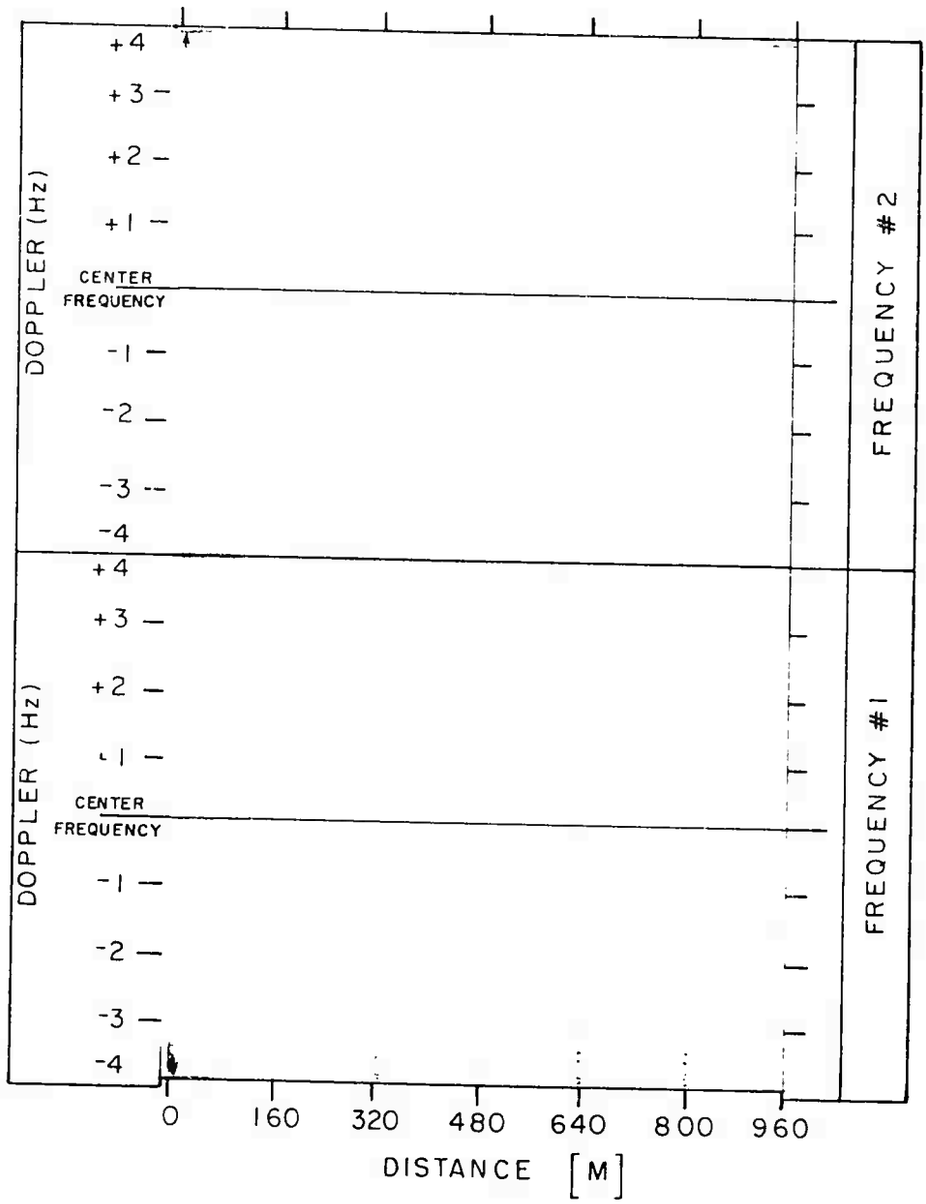

b. Coherence

Figure 9. Flight 4-058, 27 Feb 1974, UT 2325

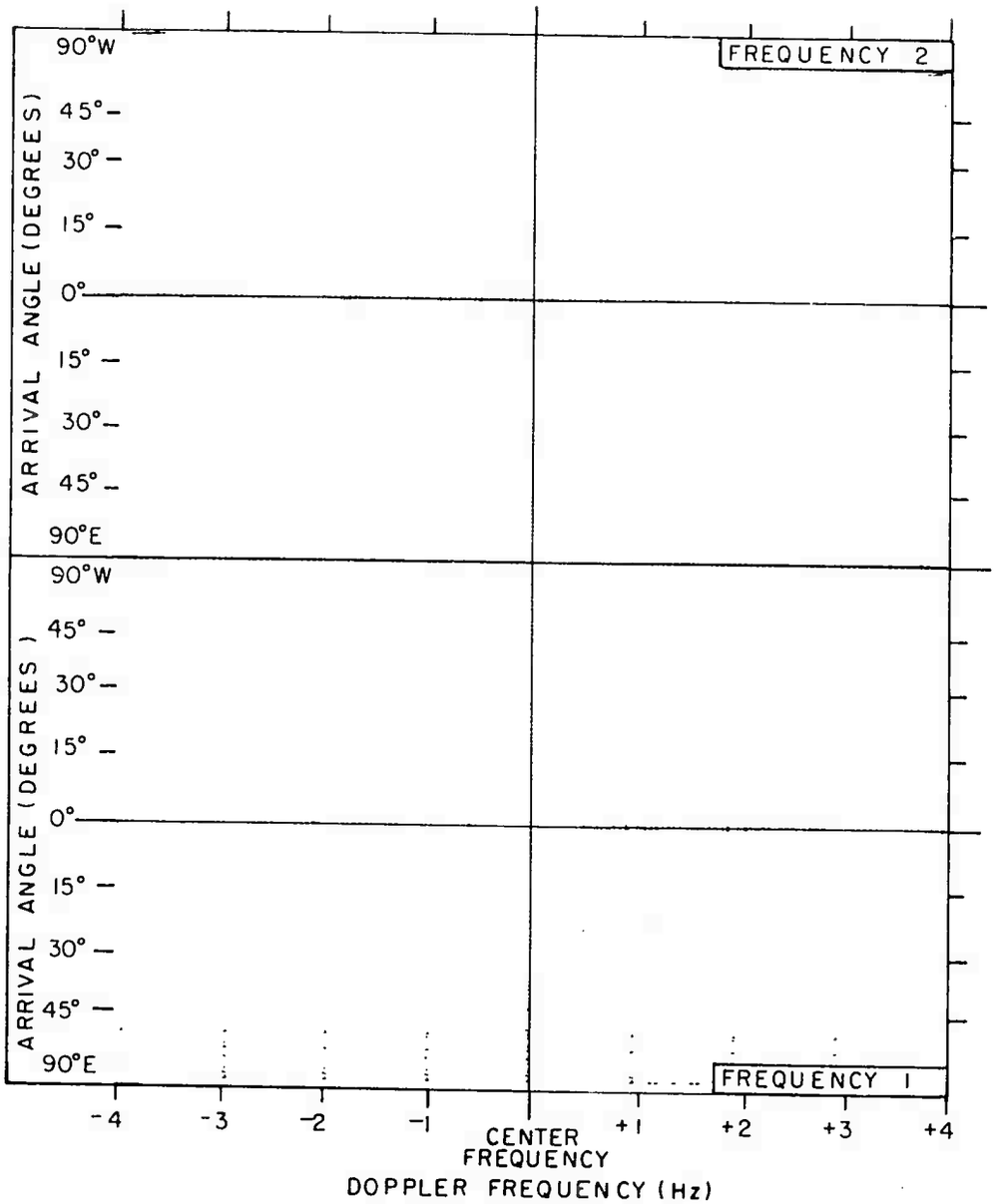

DATE ---------- 2-27-74 (058)
TIME (UT) ---------- 2343
FREQ 1 (MHz) ---------- 8.22
FREQ 2 (MHz) ---------- 11.22
RANGE (Km) ---------- 1960
AZIMUTH (deg.) ---------- 328T
ANT. CONFIGURATION - 7/0
CENTER FREQ (Hz) ------ -6

a. DAASM Map

Figure 9. Flight 4-058, 27 Feb 1974, UT 2343

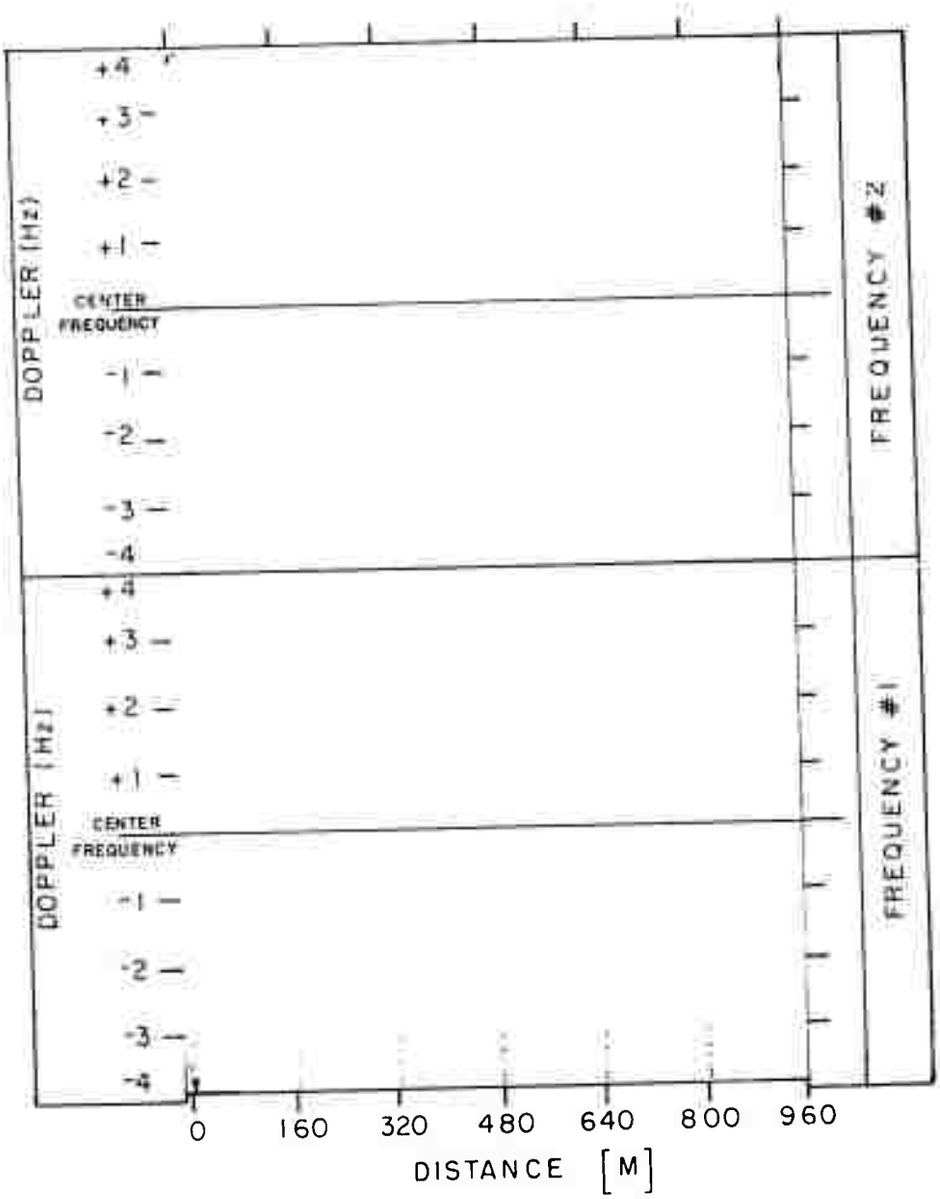

b. Coherence

Figure 9. Flight 4-058, 27 Feb 1974, UT 2343

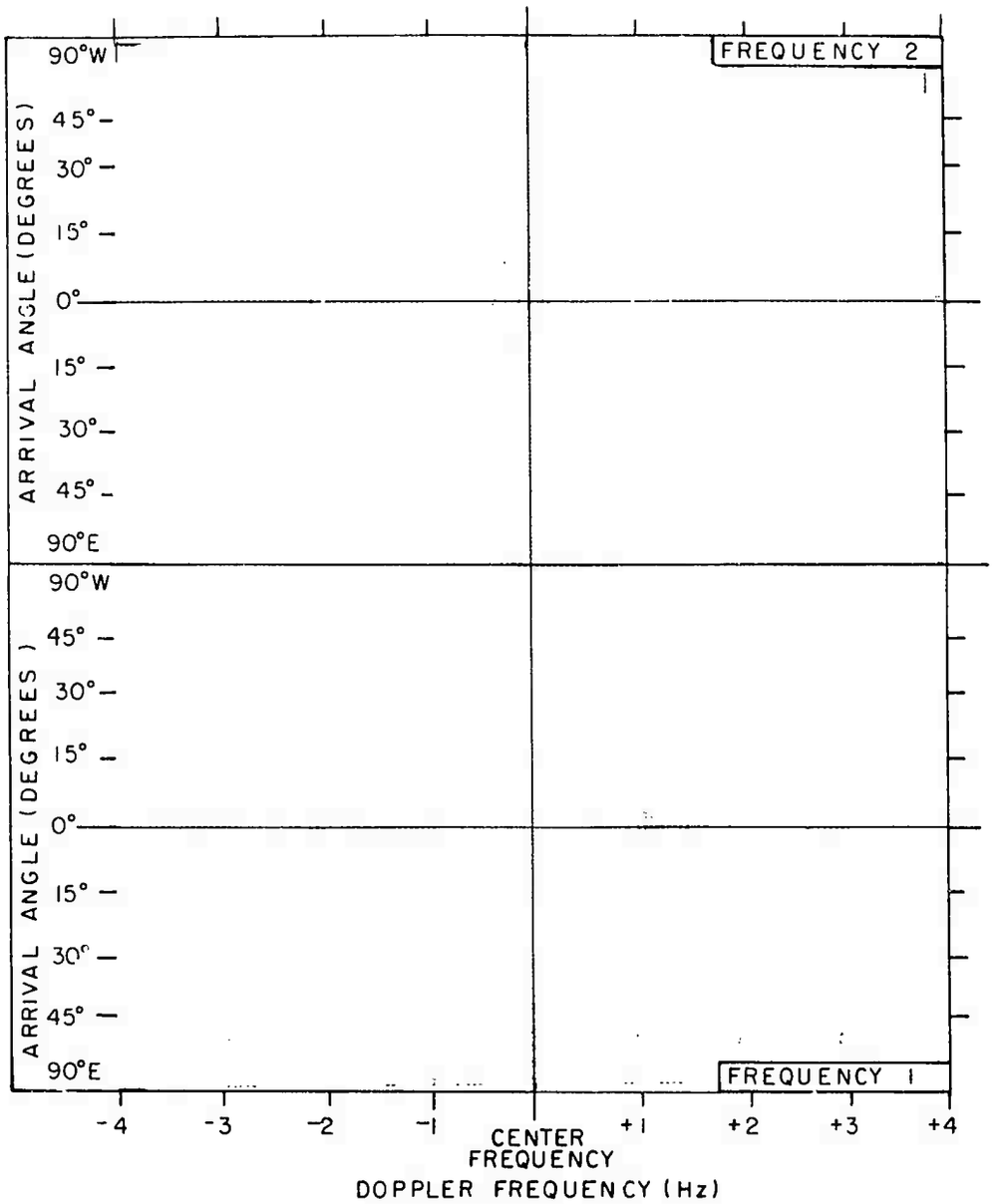

a. DAASM Map

DATE ---------- 2-27-74 (058)
TIME (UT) ---------- 0058
FREQ 1 (MHz) ---------- 8.22
FREQ 2 (MHz) ---------- 662
RANGE (Km) ---------- 1830
AZIMUTH (deg.) ---------- 328T
ANT. CONFIGURATION - 7/2
CENTER FREQ (Hz) ---------- +6

Figure 9. Flight 4-058, 27 Feb 1974, UT 0058

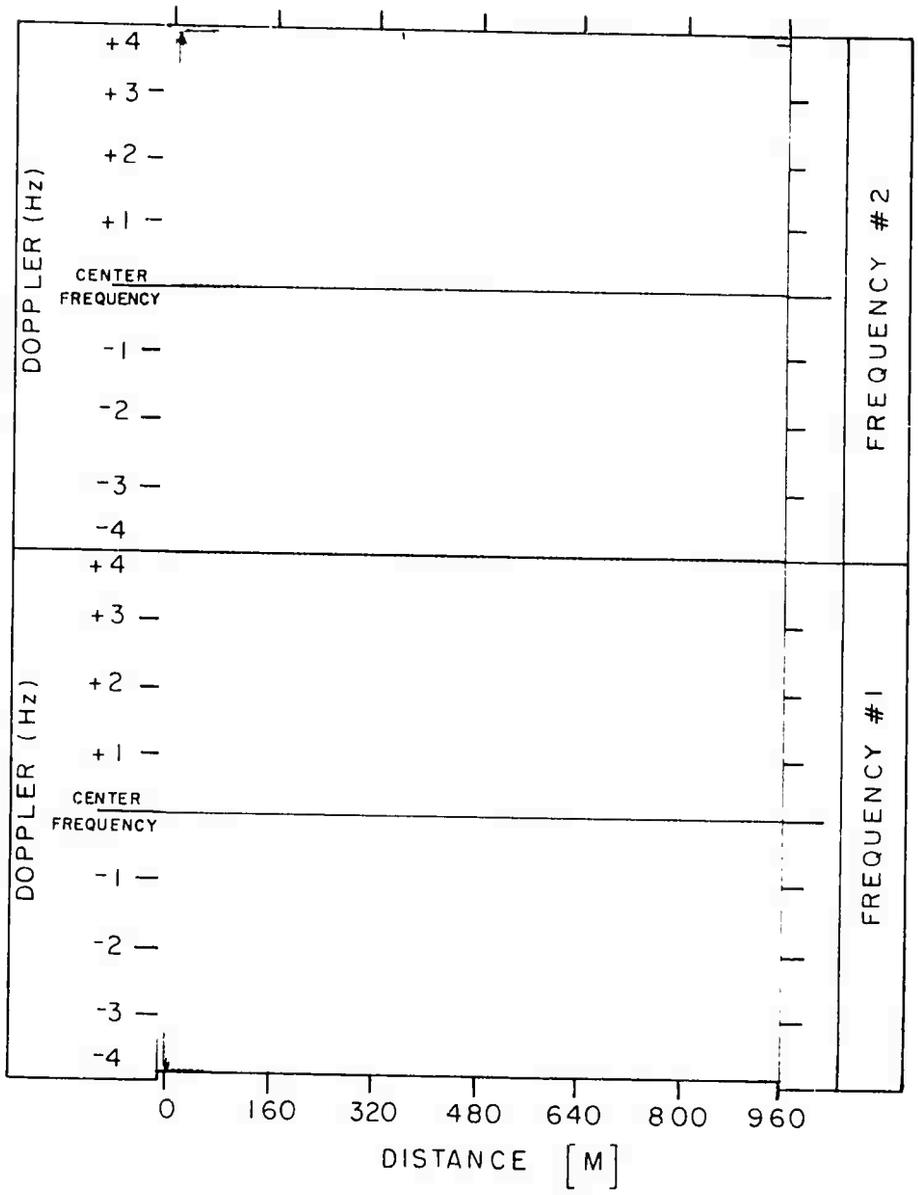

b. Coherence

Figure 9. Flight 4-058, 27 Feb 1974, UT 0058

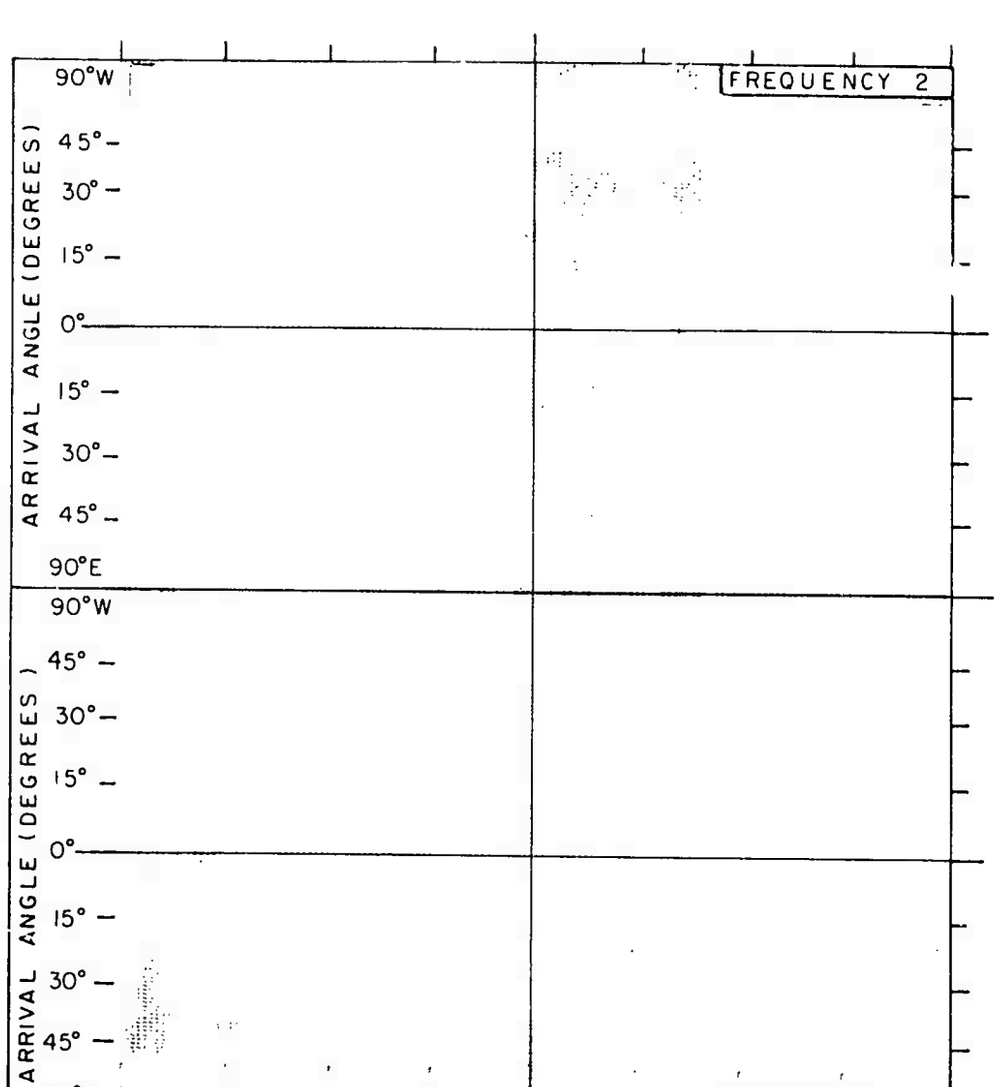

DATE ---------- 3-1-74 (060)
TIME (UT) ---------- 0303
FREQ 1 (MHz) ---------- 13.22
FREQ 2 (MHz) ---------- 11.22
RANGE (Km) ---------- 1900
AZIMUTH (deg.) ---------- 352T
ANT. CONFIGURATION - 7/2
CENTER FREQ (Hz) ---------- -8

a. DAASM Map

Figure 10. Flight 4-060, 1 Mar 1974, UT 0303

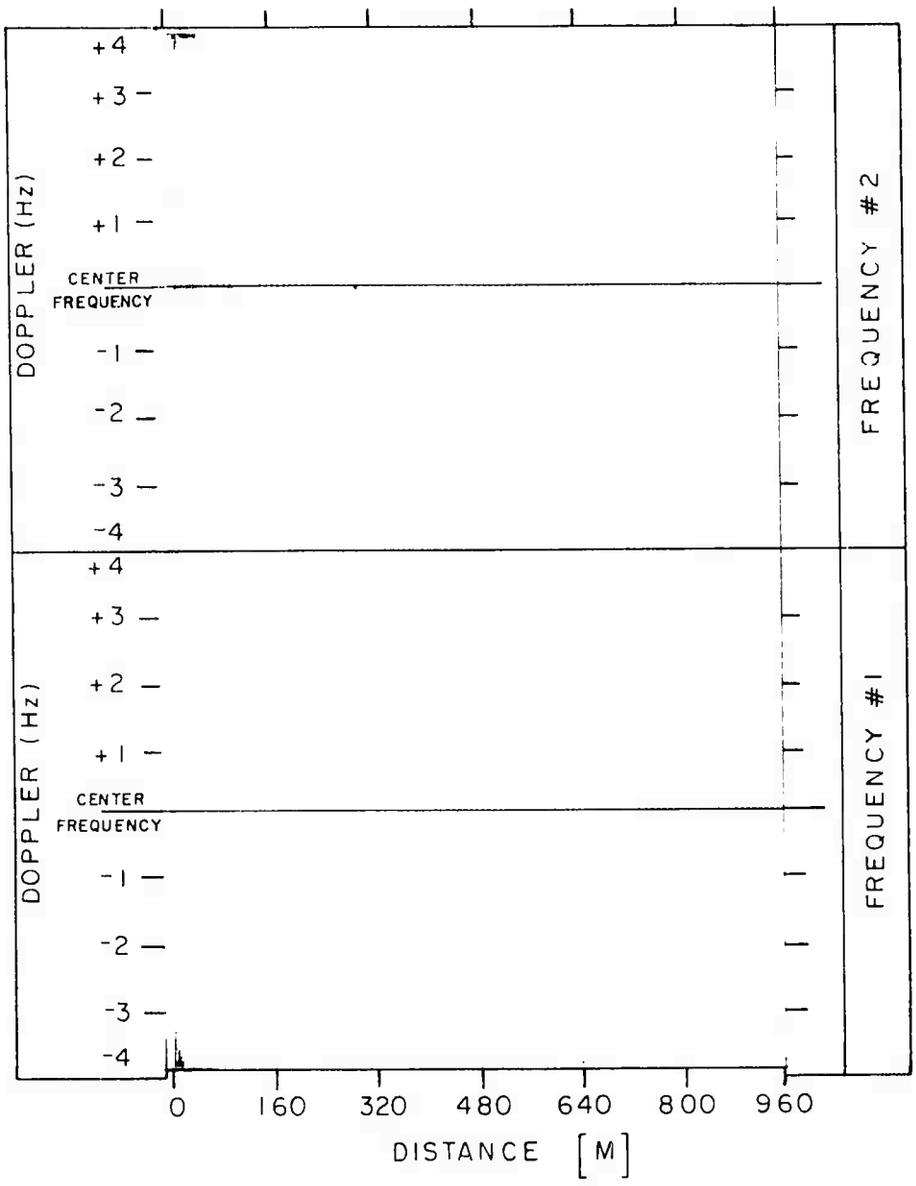

b.Coherence

Figure 10. Flight 4-060, 1 Mar 1974, UT 0303

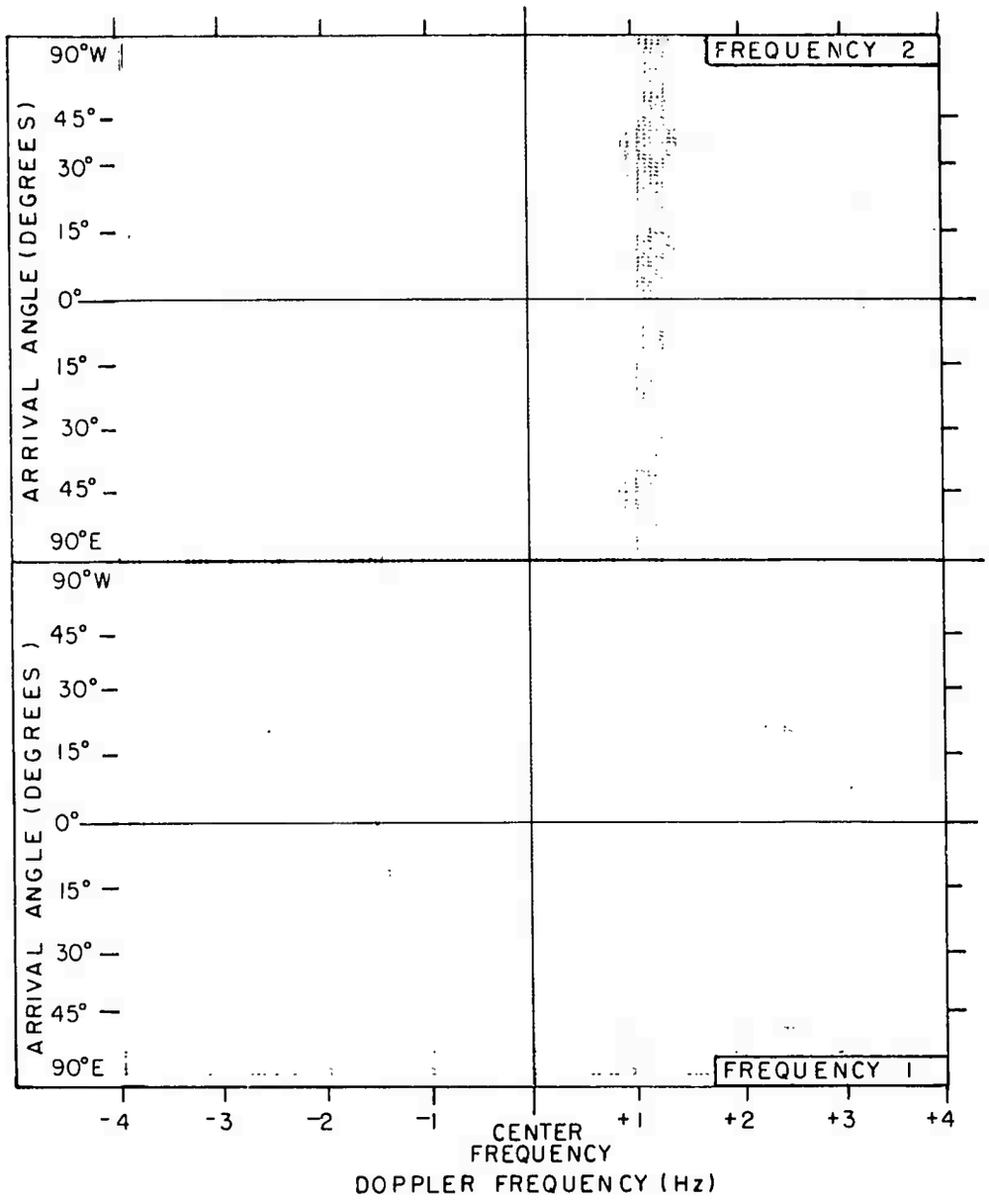

a. DAASM Map

DATE	3-1-74 (060)
TIME (UT)	0348
FREQ 1 (MHz)	13.22
FREQ 2 (MHz)	11.22
RANGE (Km)	2480
AZIMUTH (deg.)	355T
ANT. CONFIGURATION	7/2
CENTER FREQ (Hz)	-8

Figure 10. Flight 4-060, 1 Mar 1974, UT 0348

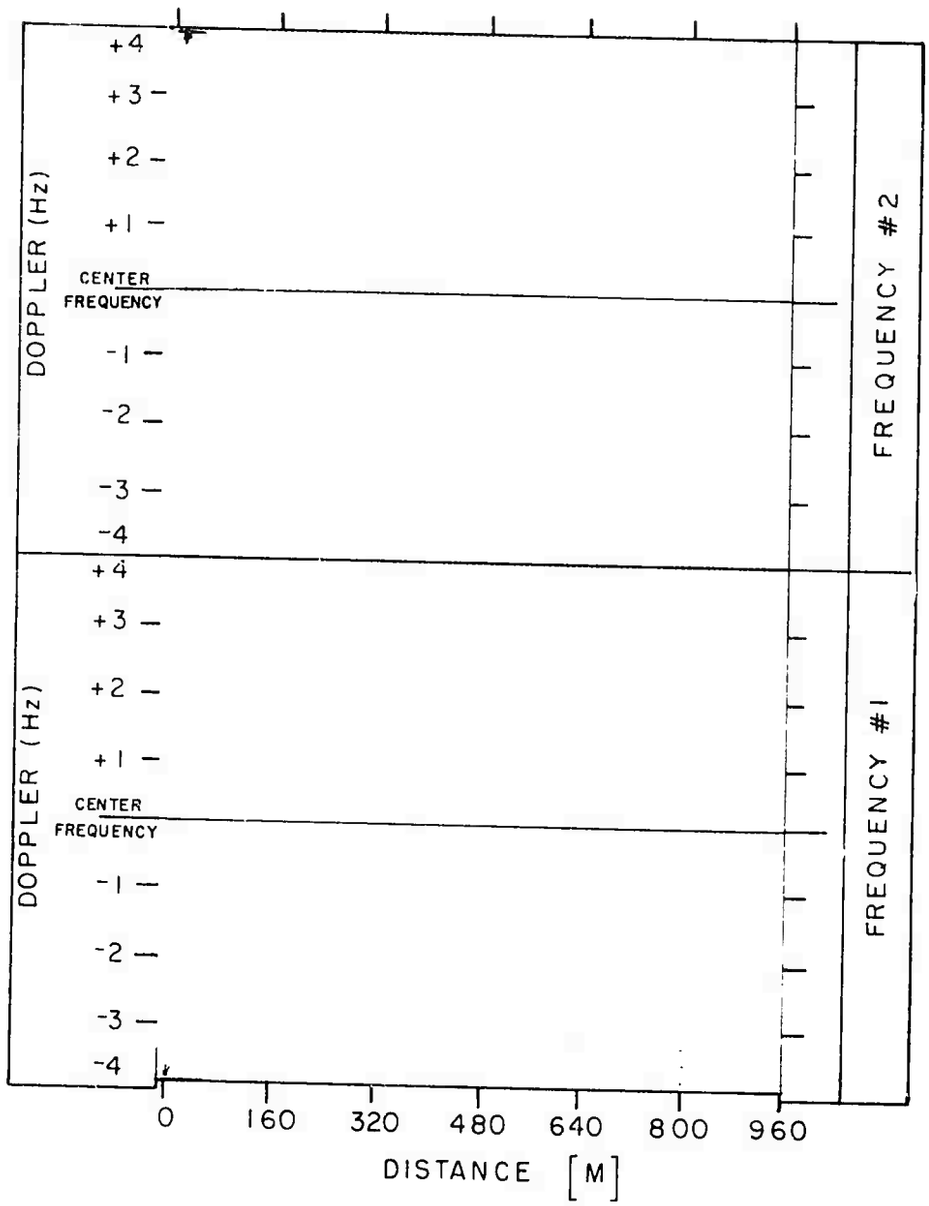

b.Coherence

Figure 10. Flight 4-060, 1 Mar 1974, UT 0348

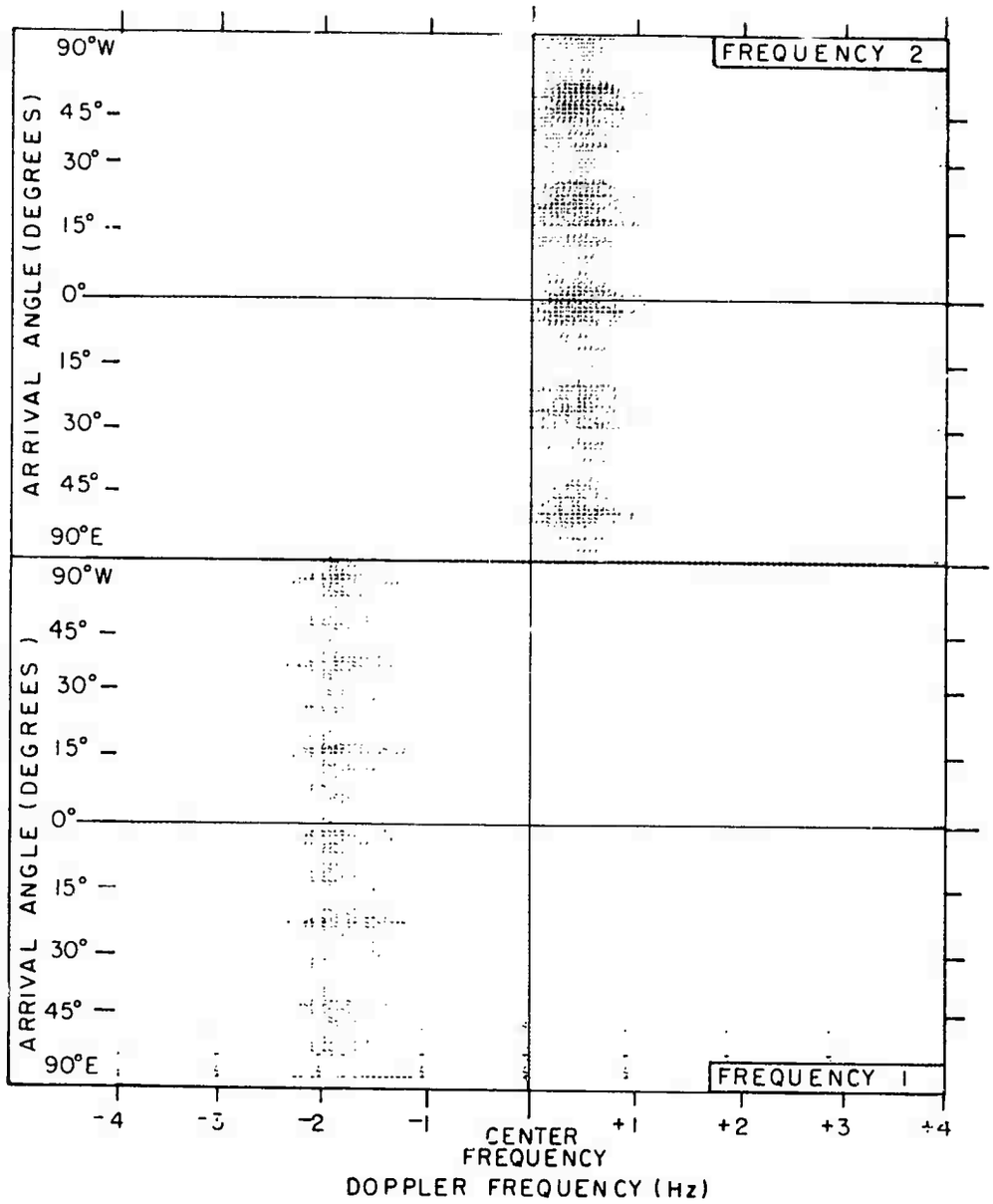

a. DAASM Map

DATE ---------- 3-1-74 (060)
TIME (UT) ---------- 0610
FREQ 1 (MHz) ---------- 13.22
FREQ 2 (MHz) ---------- 11.22
RANGE (Km) ---------- 1590
AZIMUTH (deg.) ---------- 351T
ANT. CONFIGURATION - 7/7
CENTER FREQ (Hz) ---------- +9

Figure 10. Flight 4-060, 1 Mar 1974, UT 0610

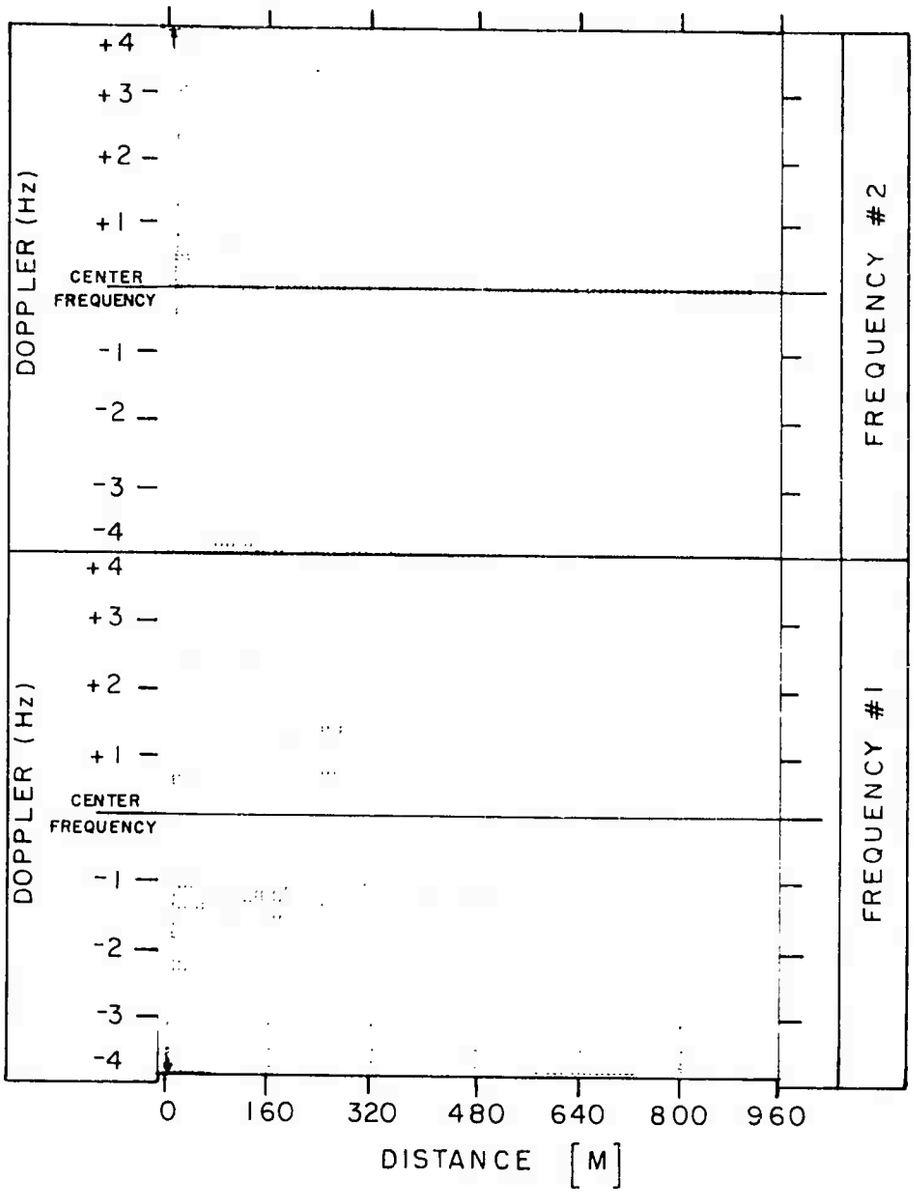

b.Coherence

Figure 10. Flight 4-060, 1 Mar 1974, UT 0610

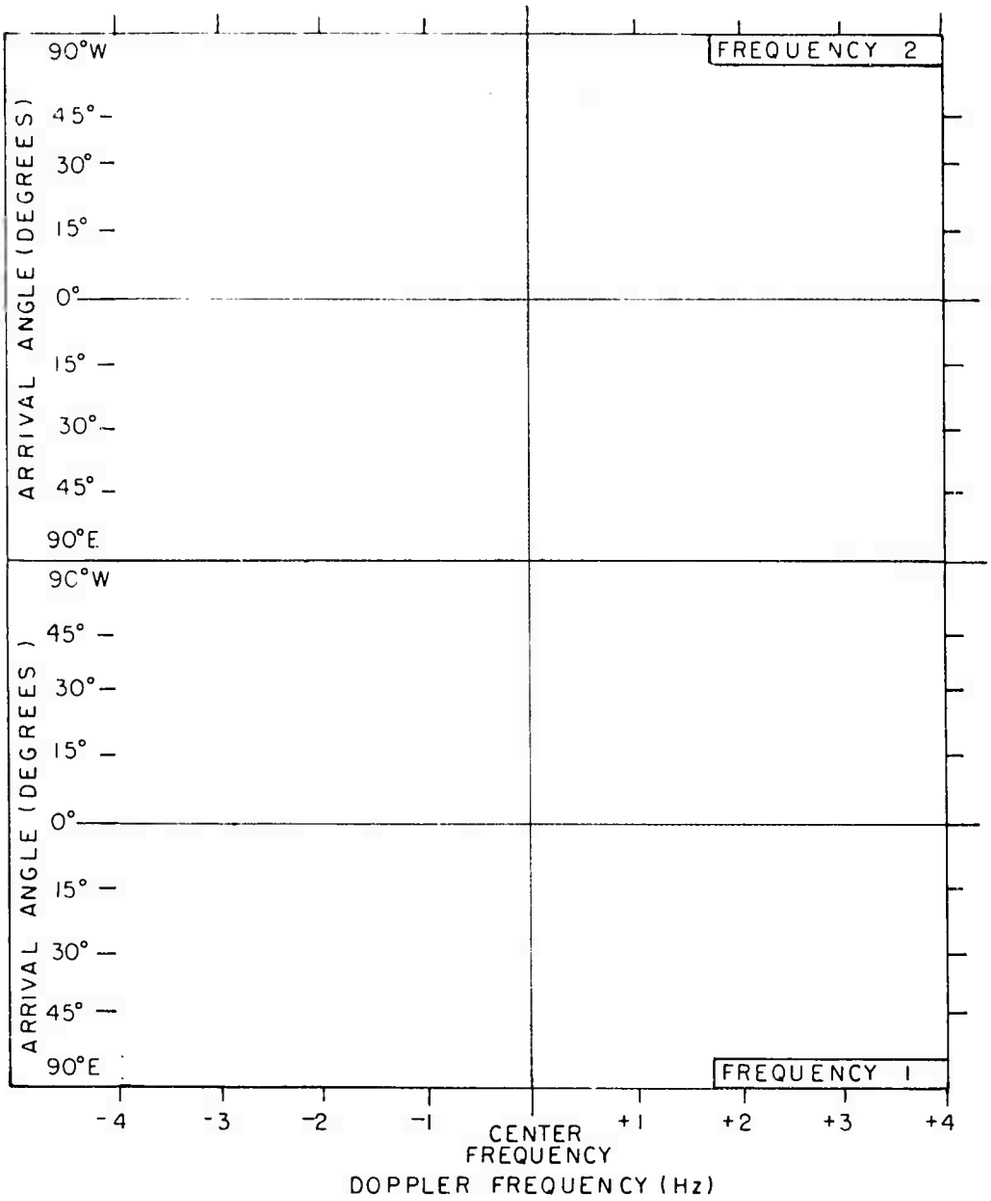

a. DAASM Map

DATE	3-1-74 (060)
TIME (UT)	0701
FREQ 1 (MHz)	13.22
FREQ 2 (MHz)	11.22
RANGE (Km)	930
AZIMUTH (deg.)	349T
ANT. CONFIGURATION	7/7
CENTER FREQ (Hz)	+9

Figure 10. Flight 4-060, 1 Mar 1974, UT 0701

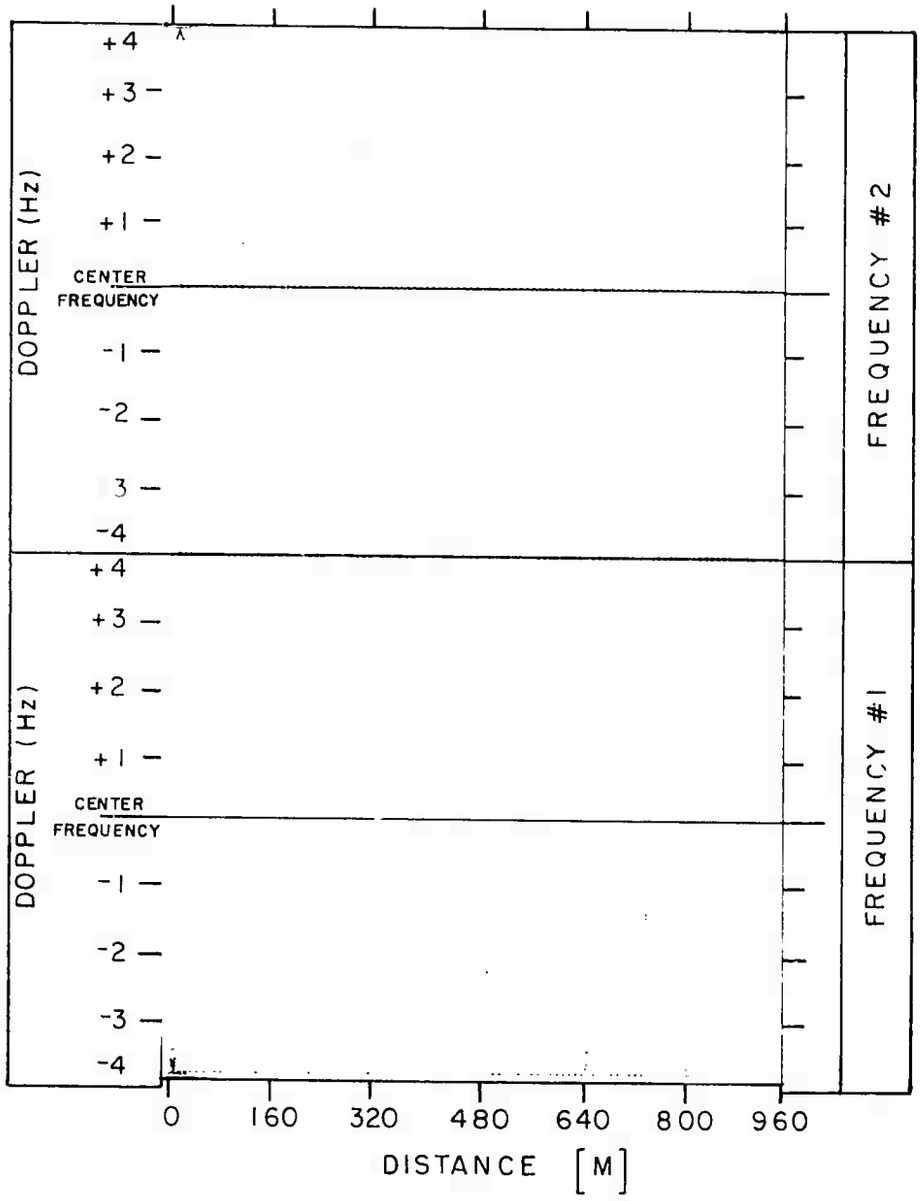

b. Coherence

Figure 10. Flight 4-060, 1 Mar 1974, UT 0701

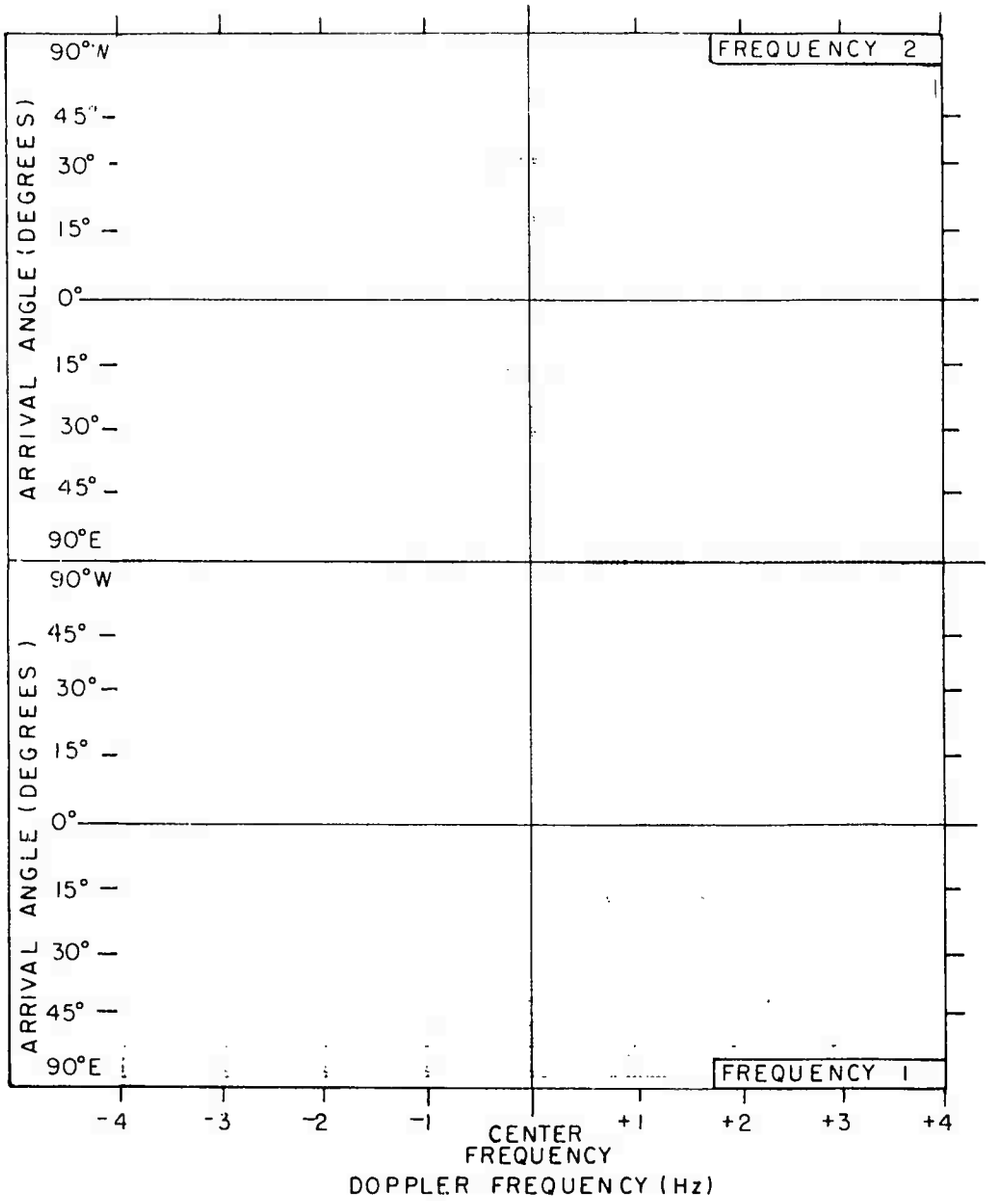

a. DAASM Map

DATE	5-21-74 (141)
TIME (UT)	2325
FREQ 1 (MHz)	8.22
FREQ 2 (MHz)	6.62
RANGE (Km)	910
AZIMUTH (deg.)	344T
ANT. CONFIGURATION	7/6
CENTER FREQ (Hz)	+4

Figure 11. Flight 4-141, 21 May 1974, UT 2325

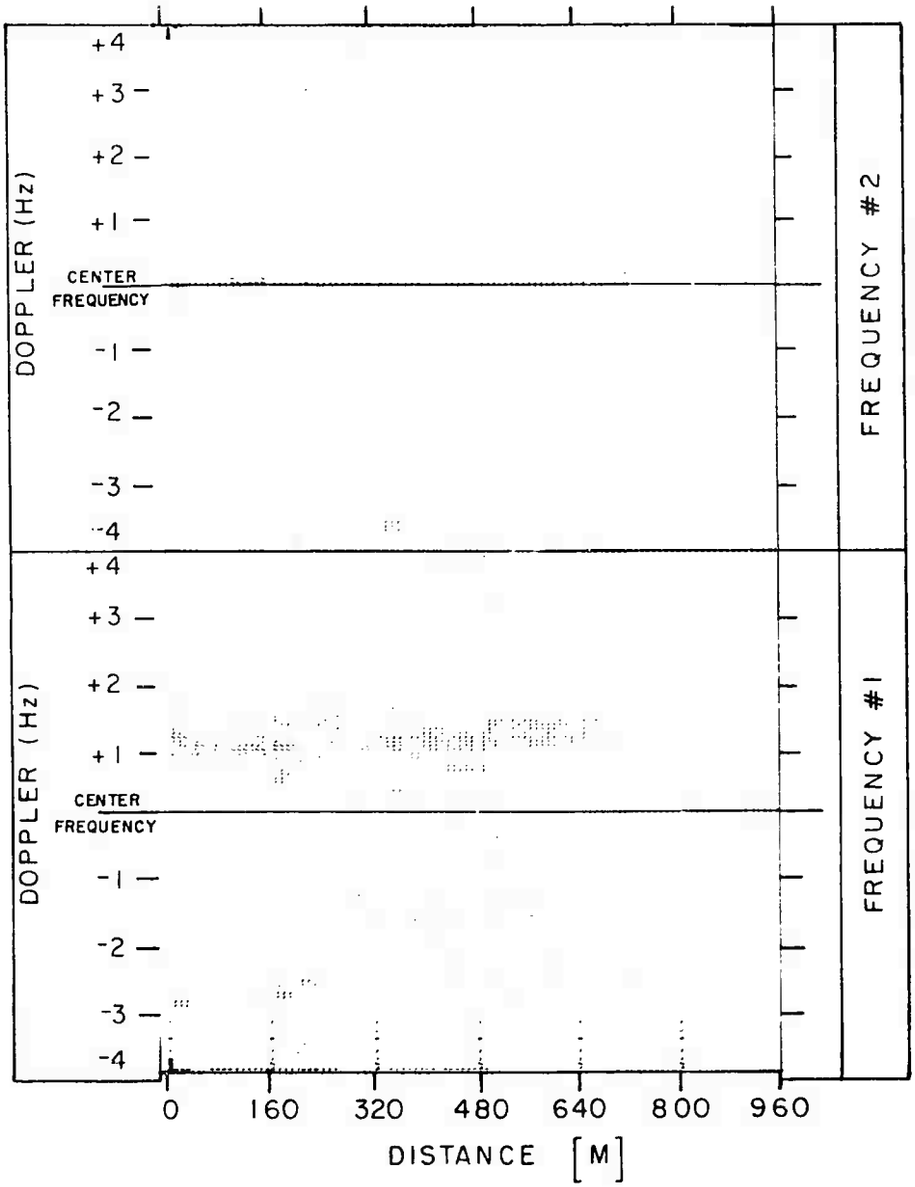

b. Coherence

Figure 11. Flight 4-141, 21 May 1974, UT 2325

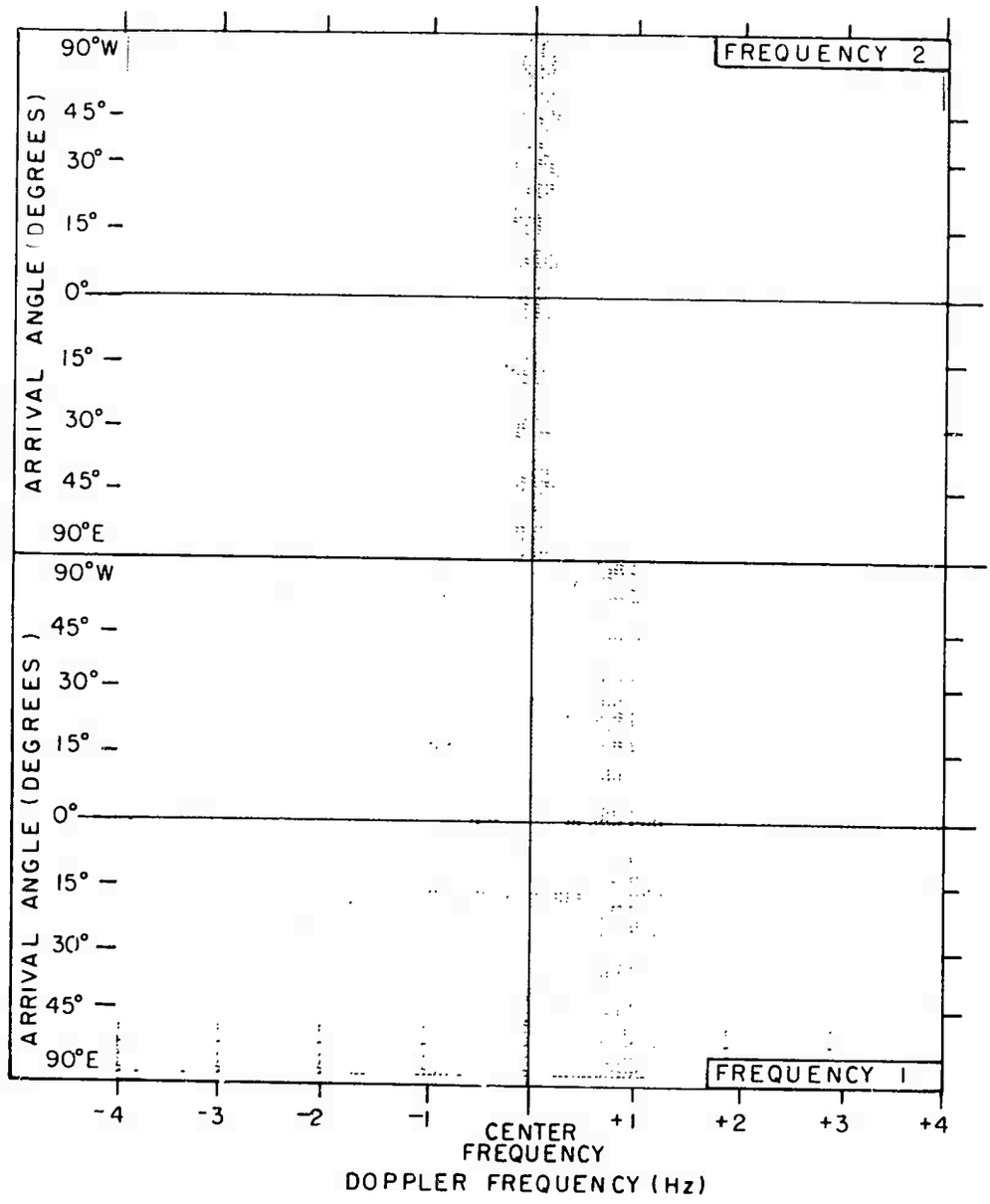

a. DAASM Map

DATE	5-21-74 (141)
TIME (UT)	2332
FREQ 1 (MHz)	8.22
FREQ 2 (MHz)	6.62
RANGE (Km)	810
AZIMUTH (deg.)	344T
ANT. CONFIGURATION	7/6
CENTER FREQ (Hz)	+4

Figure 11. Flight 4-141, 21 May 1974, UT 2332

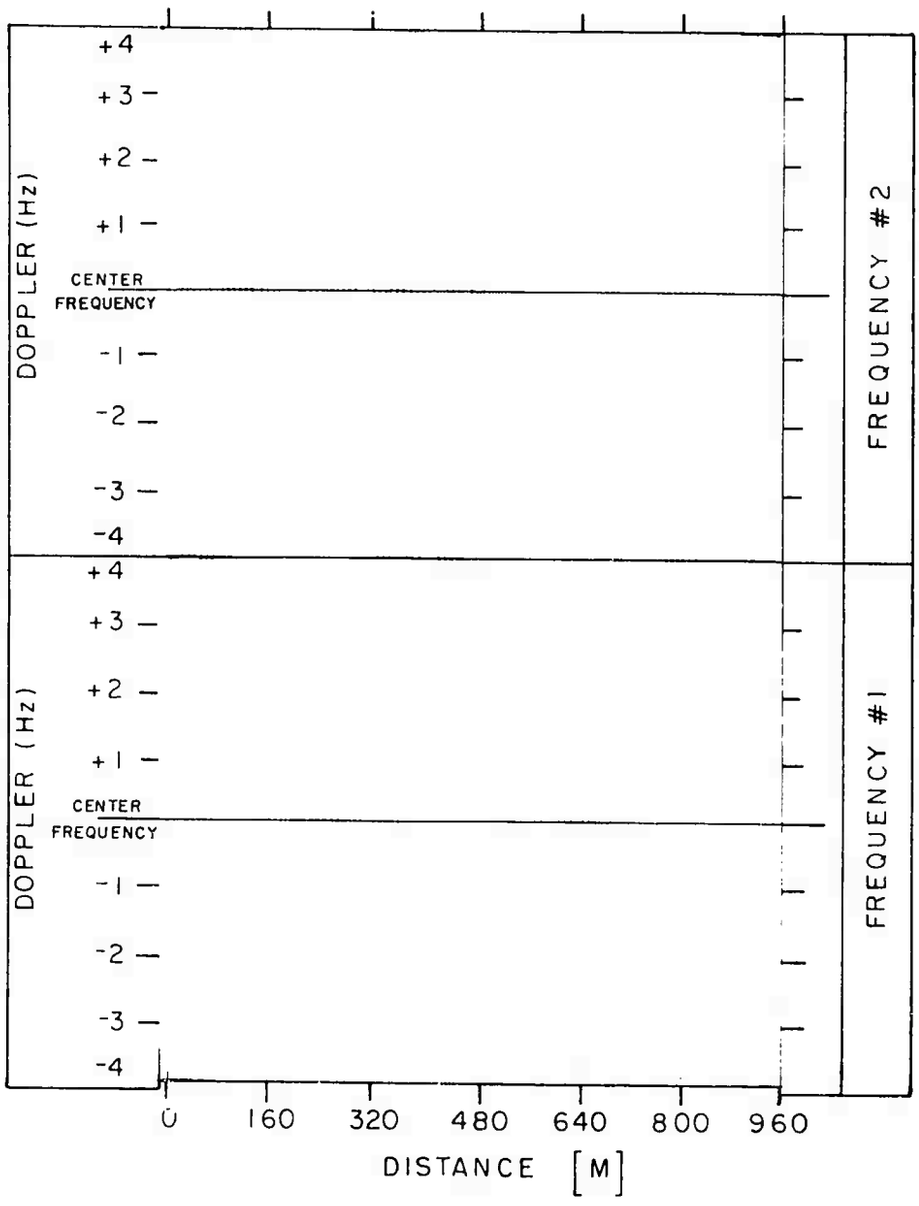

b. Coherence

Figure 11. Flight 4-141, 21 May 1974, UT 2332

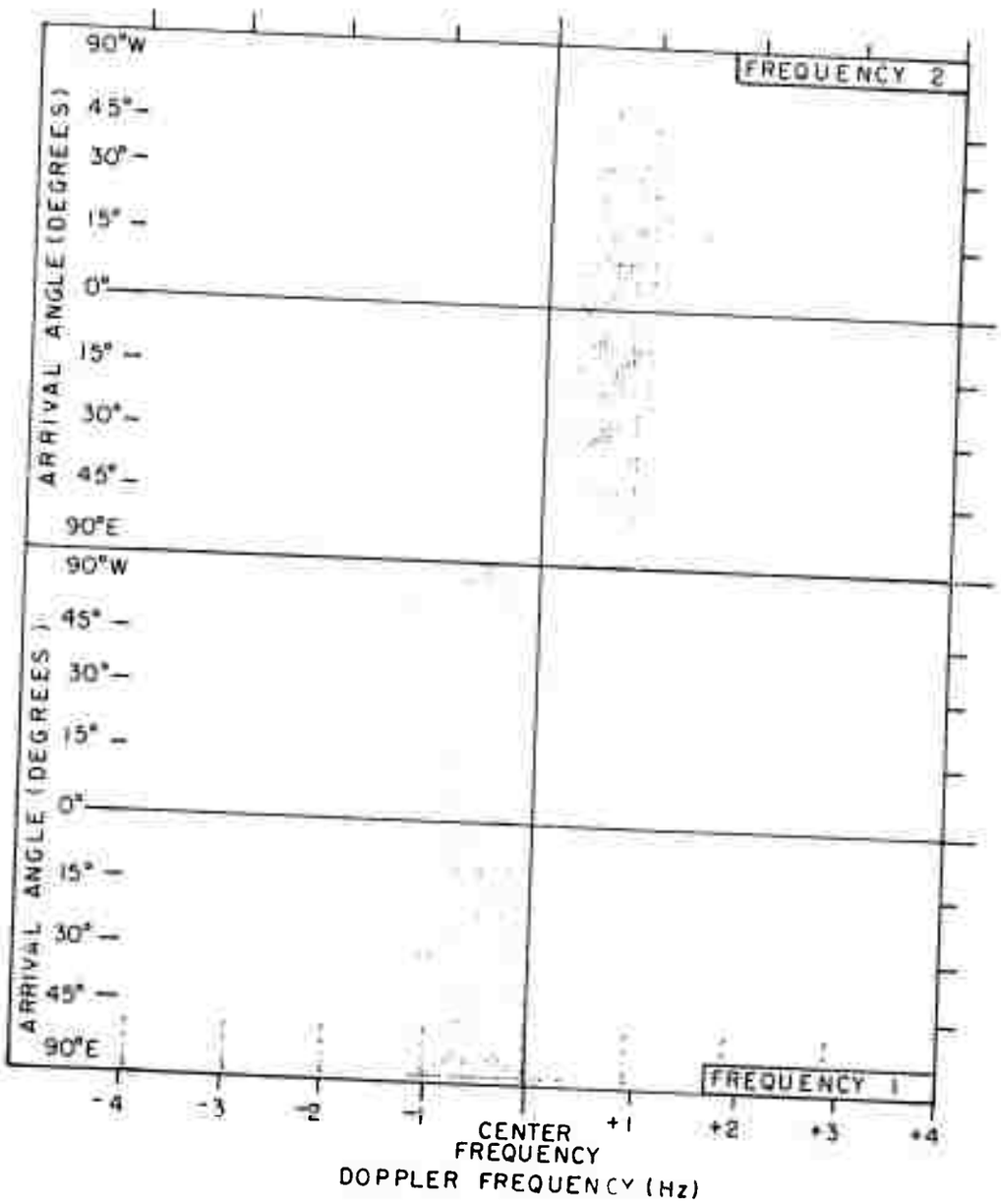

a. DAASM Map

DATE	5-22-74 (142)
TIME (UT)	2153
FREQ 1 (MHz)	8.22
FREQ 2 (MHz)	6.62
RANGE (Km)	680
AZIMUTH (deg.)	347T
ANT. CONFIGURATION	7/6
CENTER FREQ (Hz)	-5

Figure 12. Flight 4-142, 22 May 1974, UT 2153

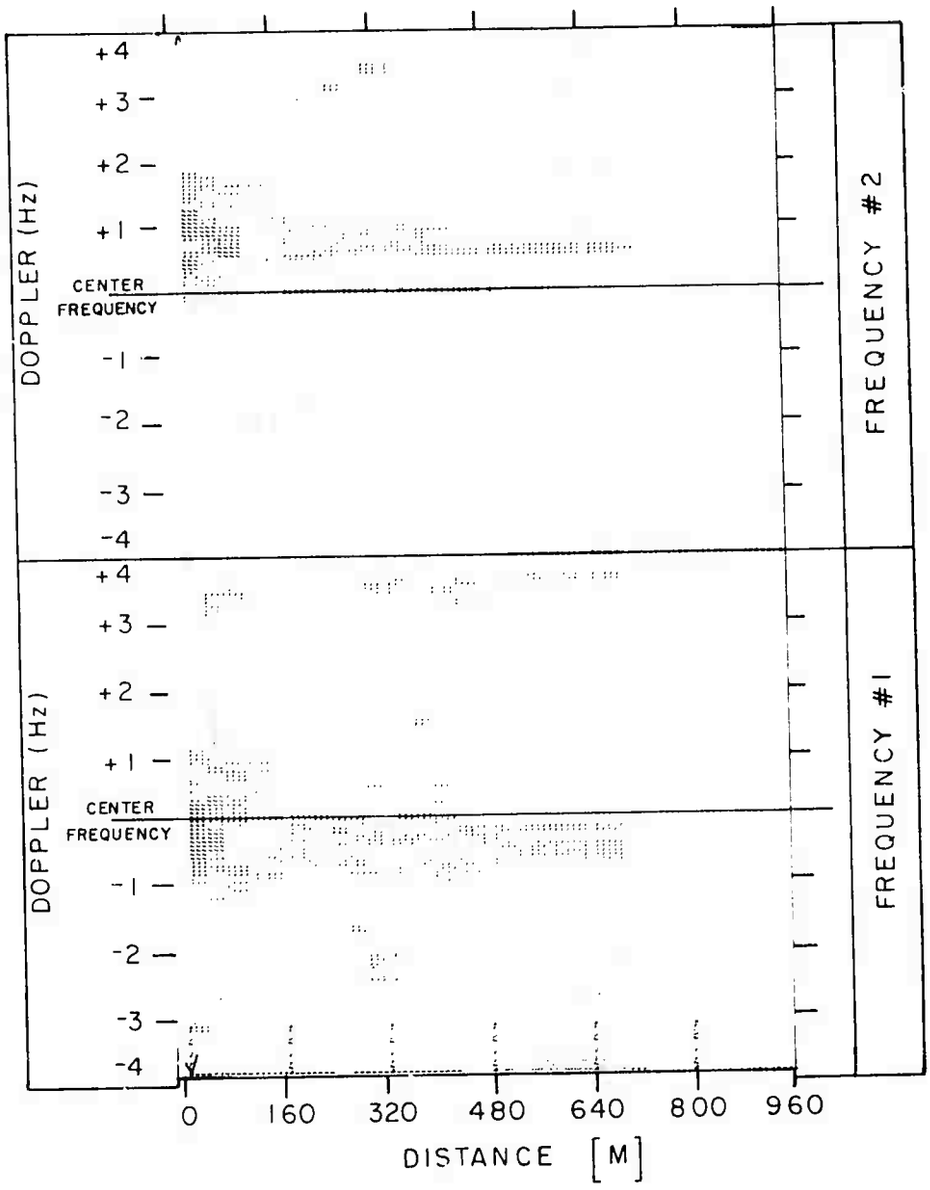

b. Coherence

Figure 12. Flight 4-142, 22 May 1974, UT 2153

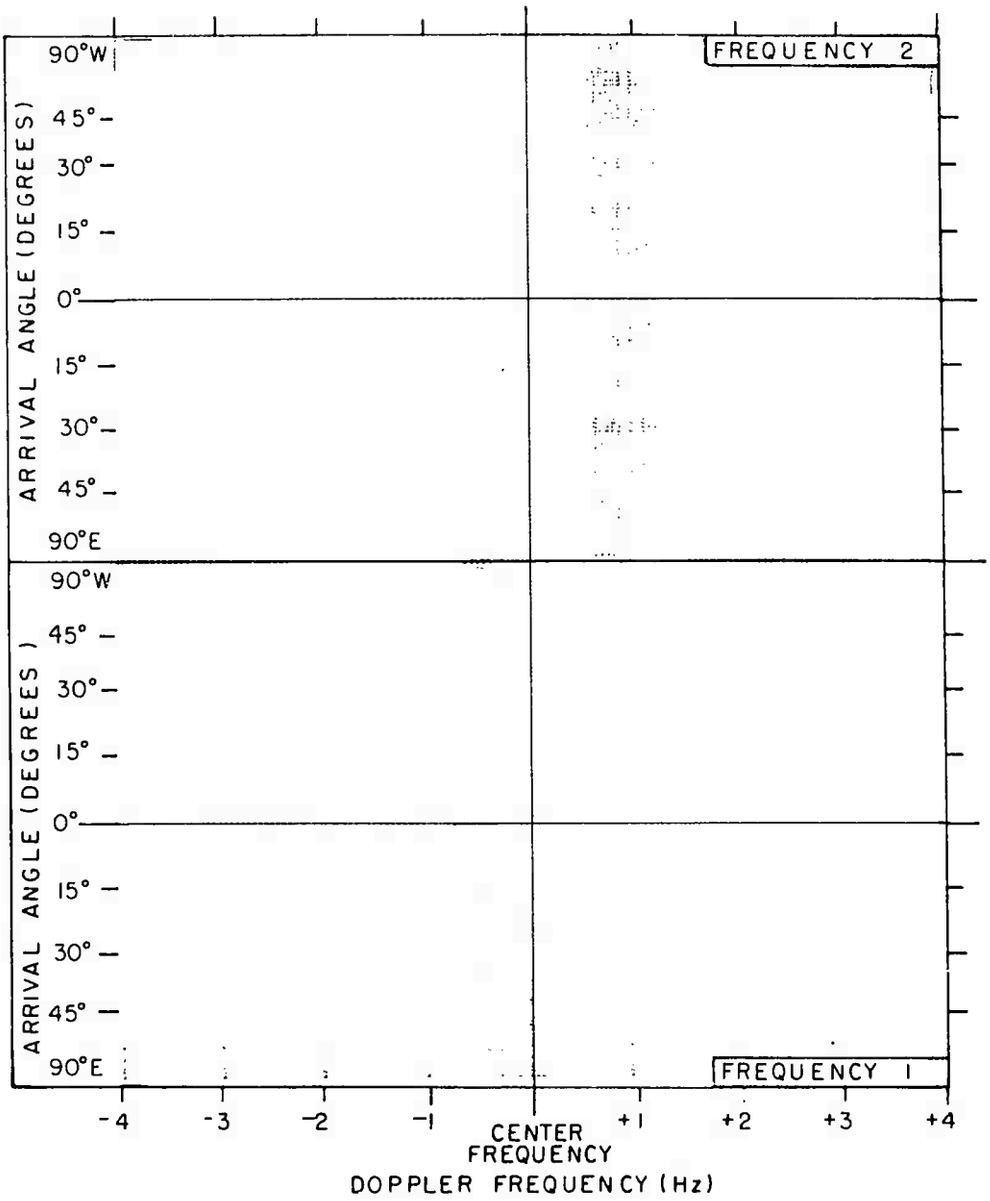

DATE ---------- 5-22-74 (142)
TIME (UT) ---------- 2253
FREQ 1 (MHz) ---------- 13.22
FREQ 2 (MHz) ---------- 11.22
RANGE (Km) ---------- 1440
AZIMUTH (deg.) ---------- 349T
ANT. CONFIGURATION - 7/6
CENTER FREQ (Hz) ------ -9

a. DAASM Map

Figure 12. Flight 4-142, 22 May 1974, UT 2253

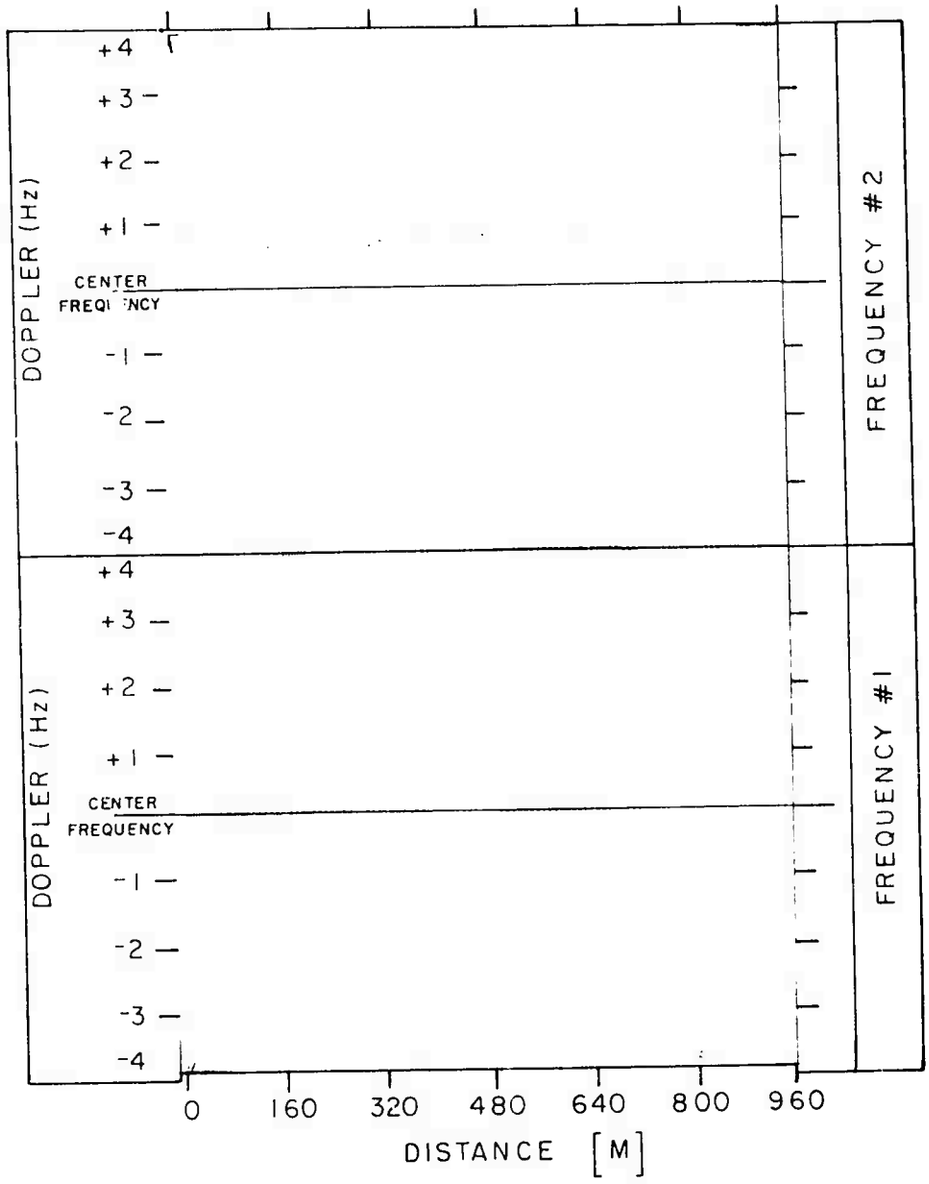

b. Coherence

Figure 12. Flight 4-142, 22 May 1974, UT 2253

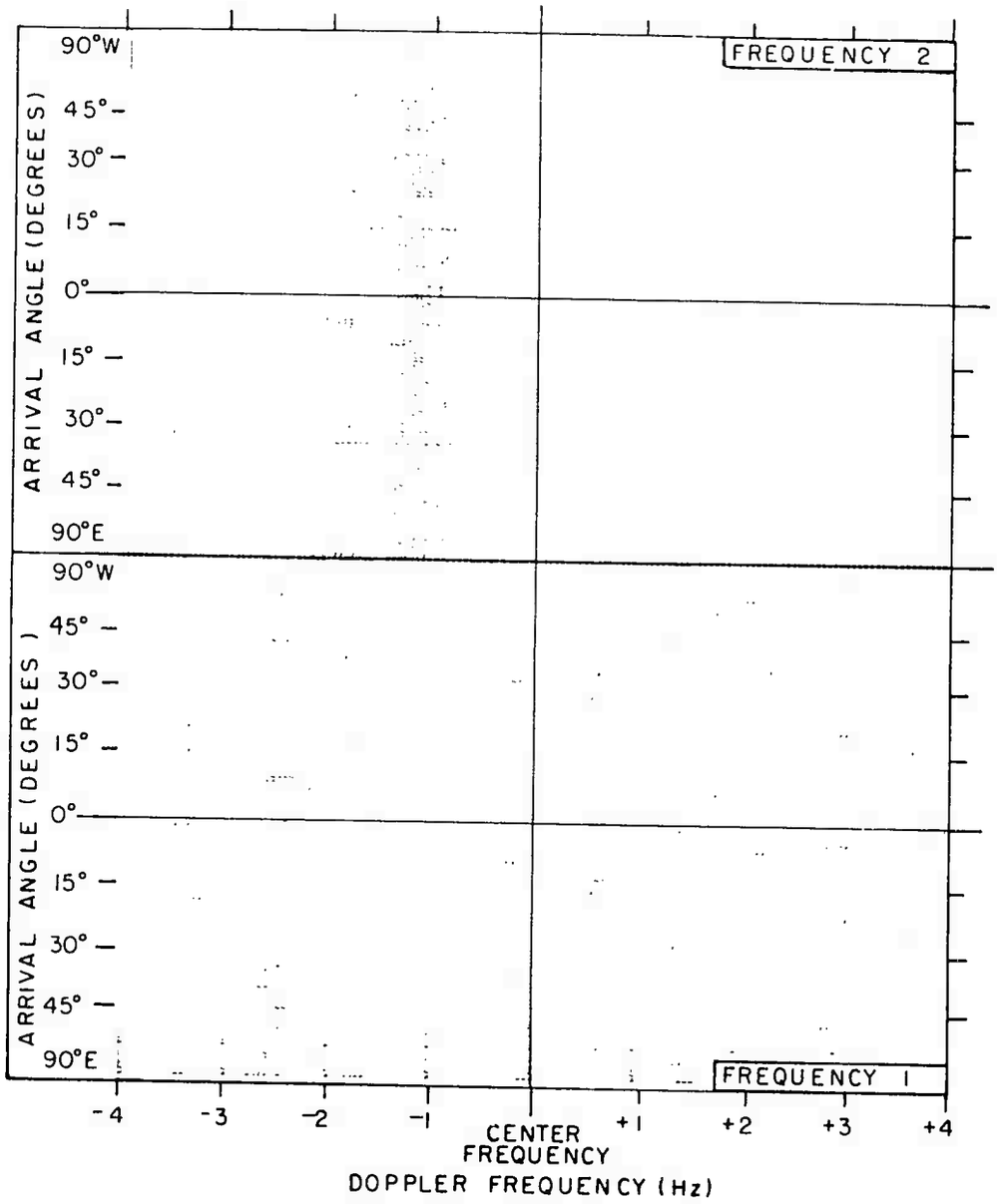

a. DAASM Map

DATE ---------- 5-22-74 (142)
TIME (UT) ---------- 2342
FREQ 1 (MHz) ---------- 13.22
FREQ 2 (MHz) ---------- 11.22
RANGE (Km) ---------- 2070
AZIMUTH (deg.) ---------- 354T
ANT. CONFIGURATION - 7/6
CENTER FREQ (Hz) ---------- -7

Figure 12. Flight 4-142, 22 May 1974, UT 2342

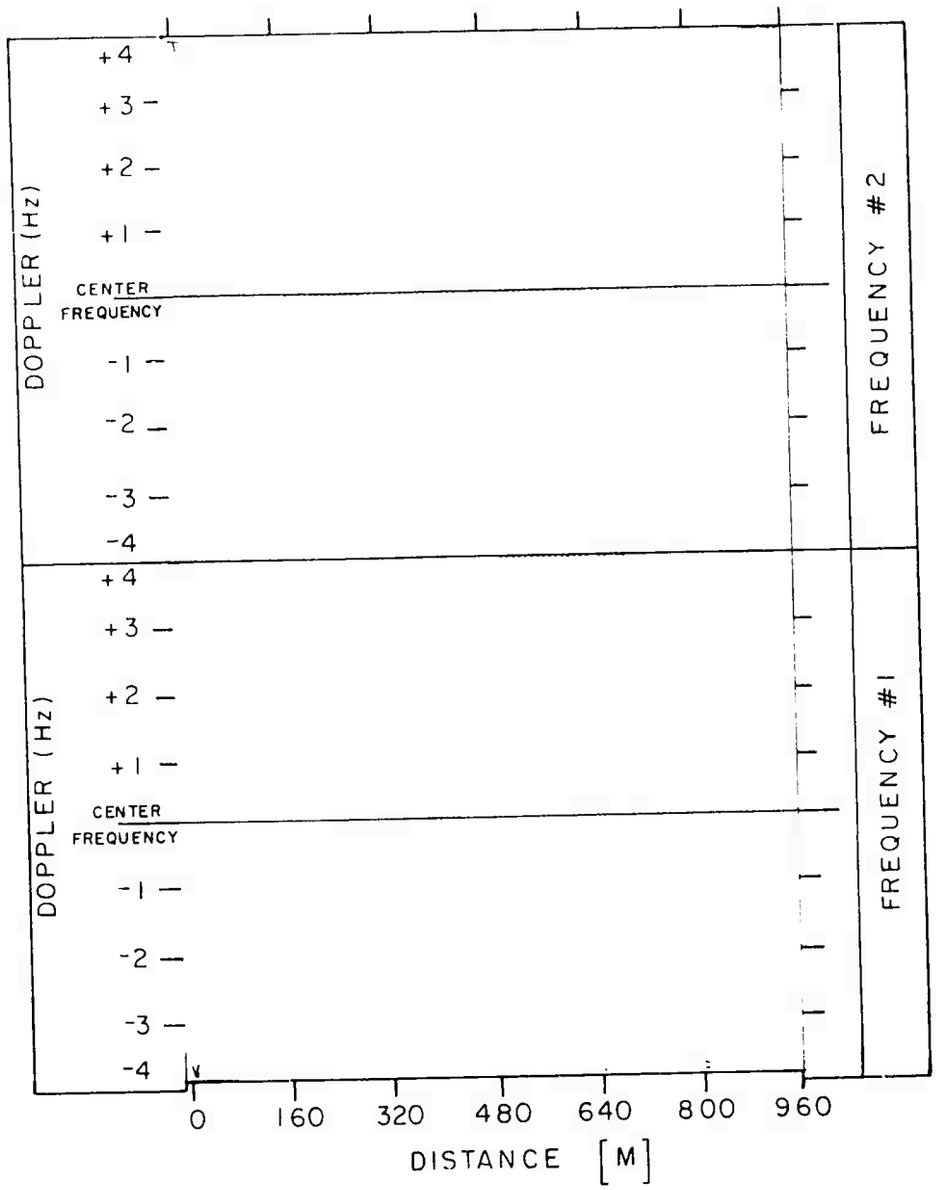

b.Coherence

Figure 12. Flight 4-142, 22 May 1974, UT 2342

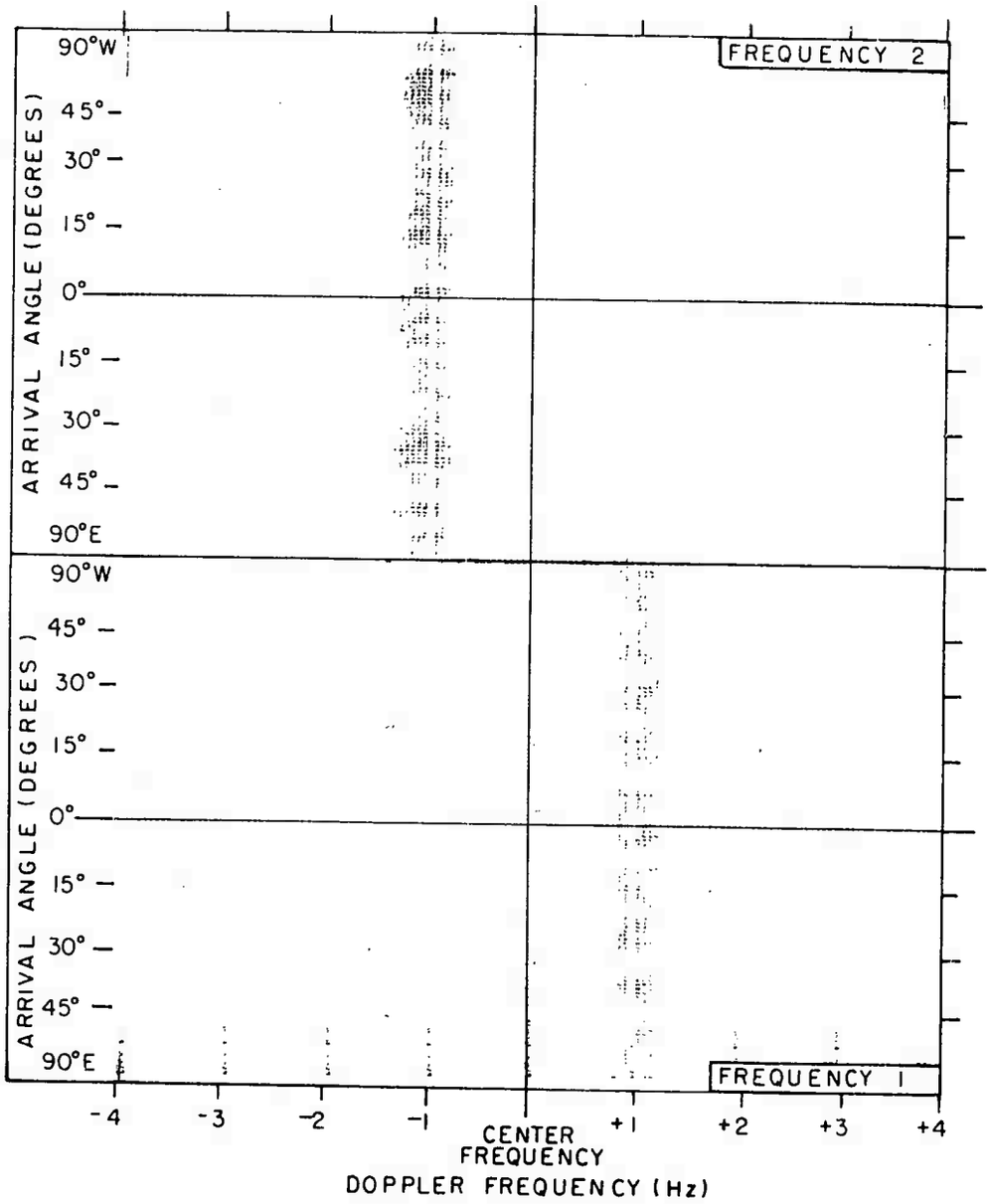

DATE ---------- 5-22-74 (142)
TIME (UT) ---------- 2355
FREQ 1 (MHz) ---------- 8.22
FREQ 2 (MHz) ---------- 11.22
RANGE (Km) ---------- 2270
AZIMUTH (deg.) ---------- 354T
ANT. CONFIGURATION - 7/6
CENTER FREQ (Hz) ---------- -7

a. DAASM Map

Figure 12. Flight 4-142, 22 May 1974, UT 2355

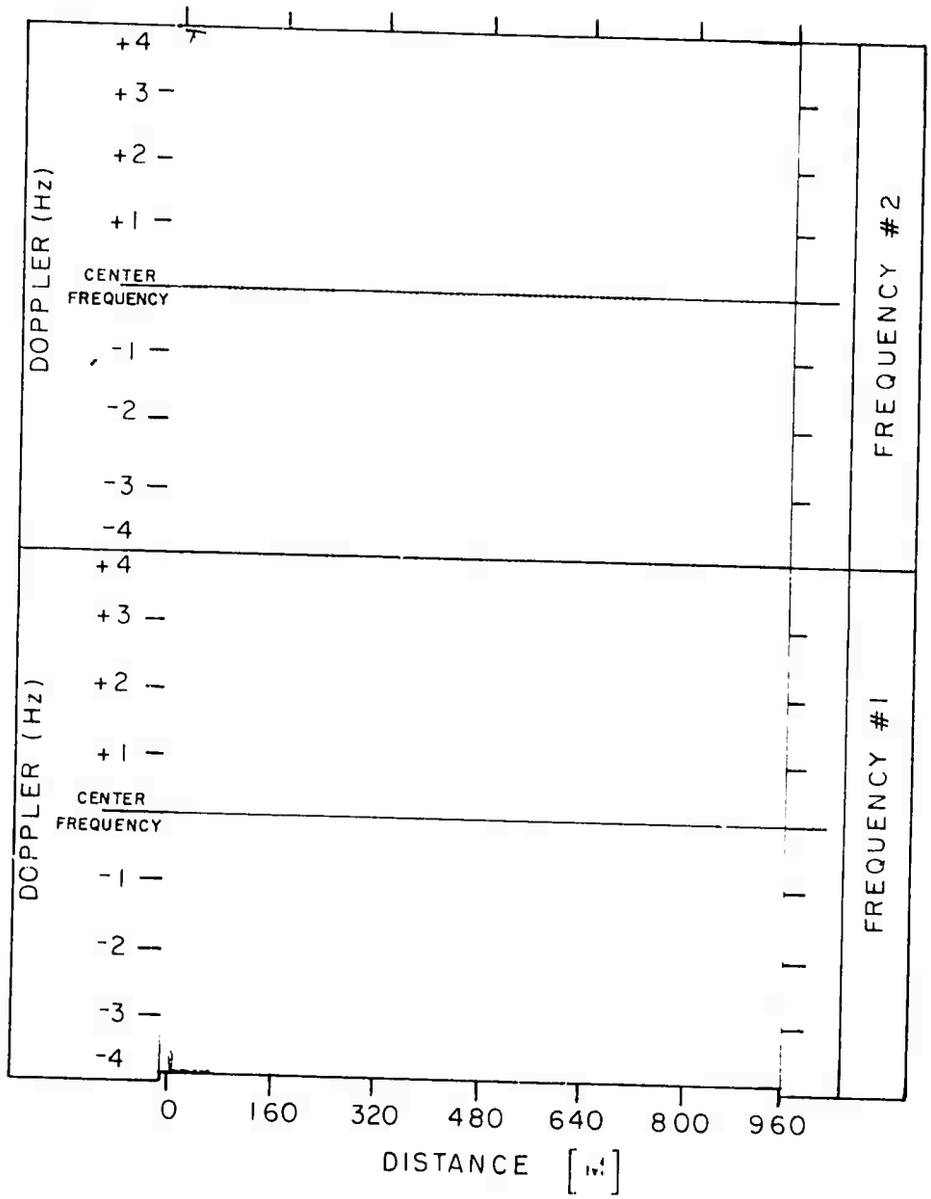

b.Coherence

Figure 12. Flight 4-142, 22 May 1974, UT 2355

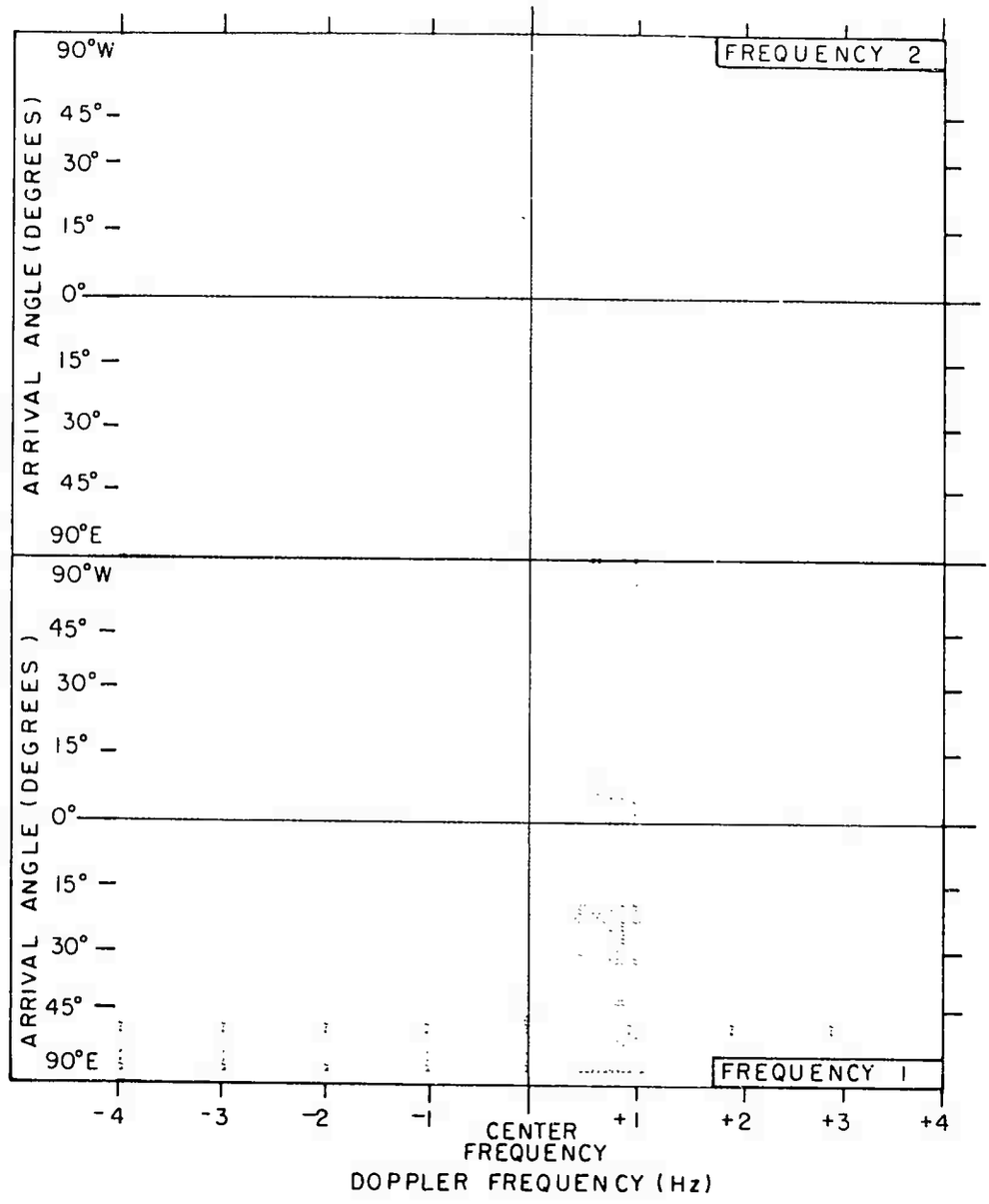

a. DAASM Map

DATE	5-22-74 (142)
TIME (UT)	0238
FREQ 1 (MHz)	8.22
FREQ 2 (MHz)	6.62
RANGE (Km)	1630
AZIMUTH (deg.)	350T
ANT. CONFIGURATION	7/6
CENTER FREQ (Hz)	+5

Figure 12. Flight 4-142, 22 May 1974, UT 0238

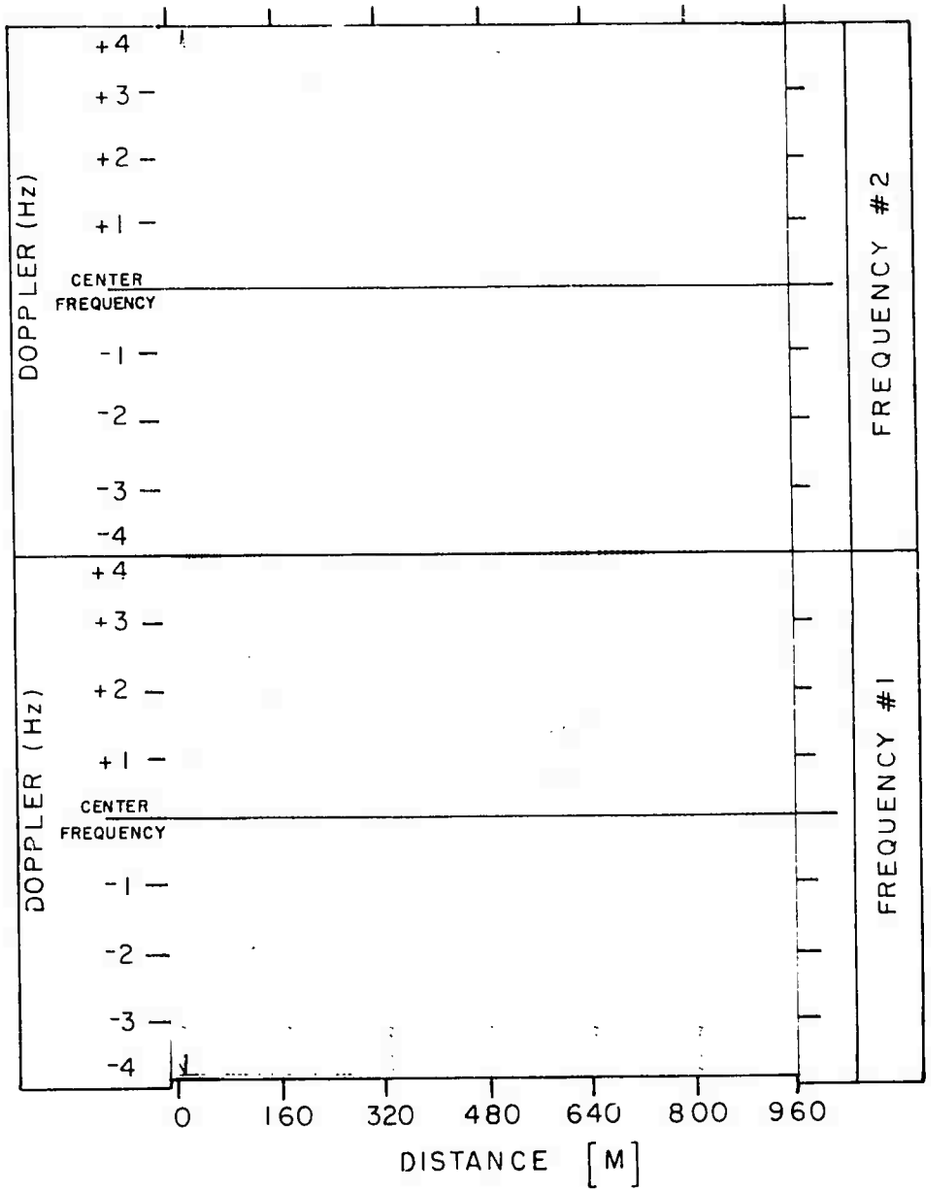

b.Coherence

Figure 12. Flight 4-142, 22 May 1974, UT 0238

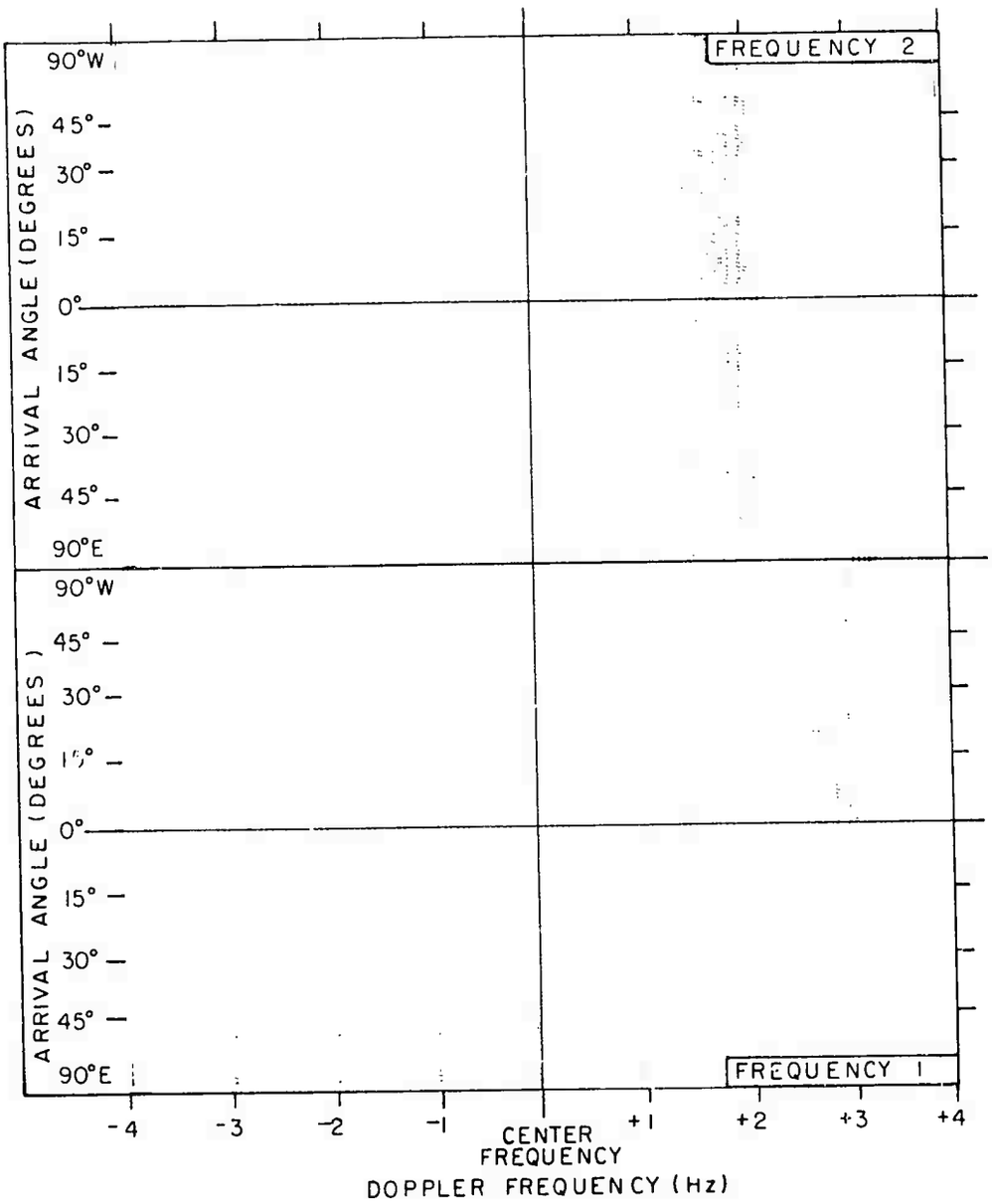

a. DAASM Map

DATE	5-22-74 (142)
TIME (UT)	0251
FREQ 1 (MHz)	8.22
FREQ 2 (MHz)	6.62
RANGE (Km)	1460
AZIMUTH (deg.)	349T
ANT. CONFIGURATION	7/6
CENTER FREQ (Hz)	+3

Figure 12. Flight 4-142, 22 May 1974, UT 0251

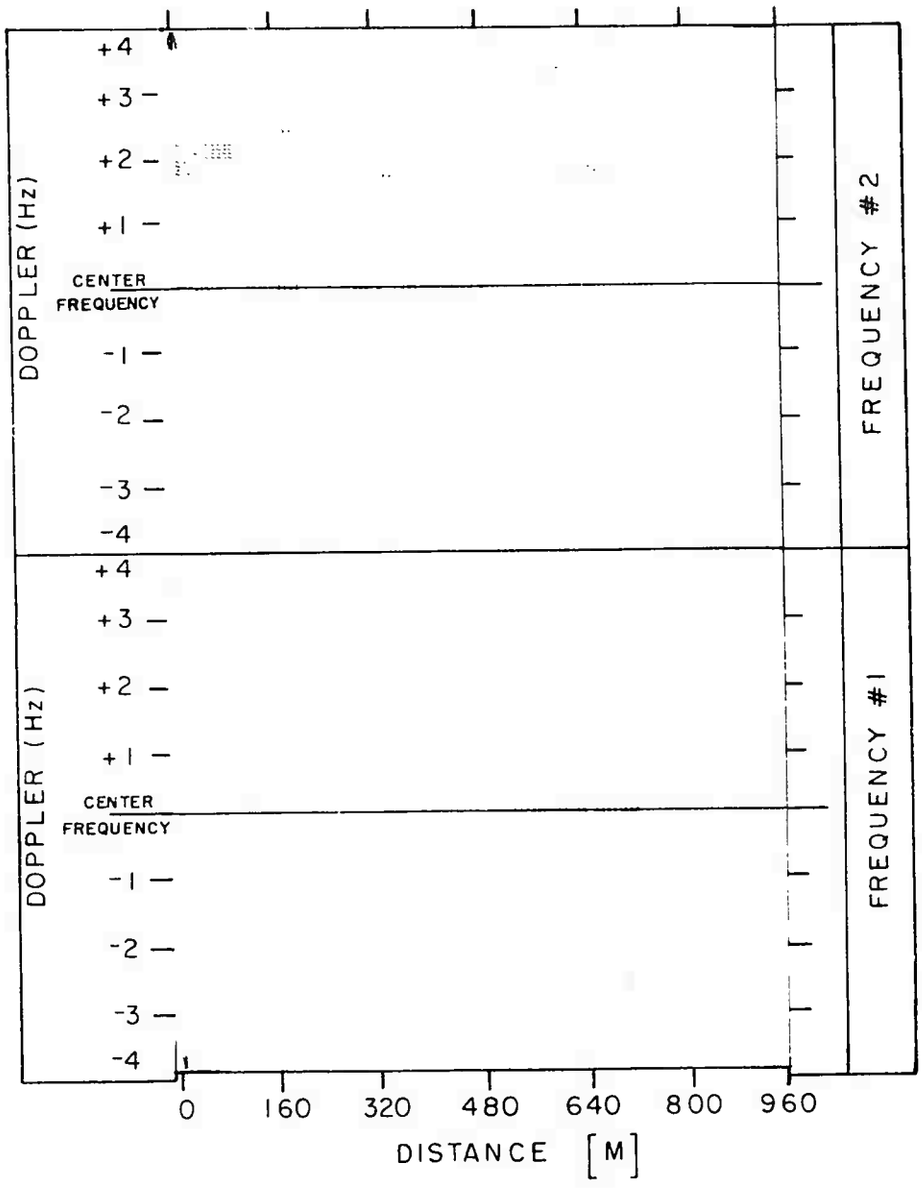

b. Coherence

Figure 12. Flight 4-142, 22 May 1974, UT 0251

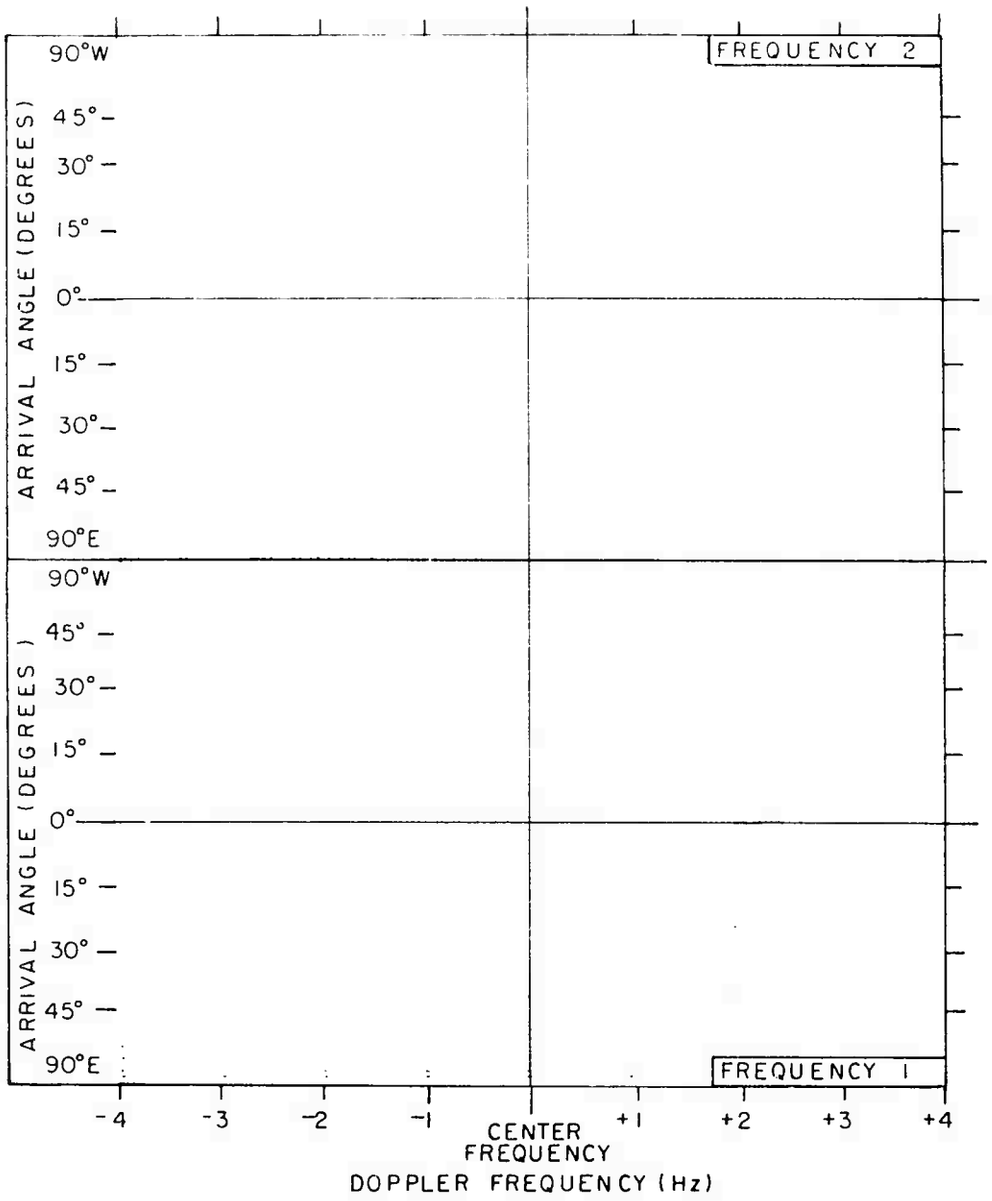

a. DAASM Map

DATE	5-22-74 (142)
TIME (UT)	0305
FREQ 1 (MHz)	8.22
FREQ 2 (MHz)	6.62
RANGE (Km)	1320
AZIMUTH (deg.)	349T
ANT. CONFIGURATION	7/6
CENTER FREQ (Hz)	+4

Figure 12. Flight 4-142, 22 May 1974, UT 0305

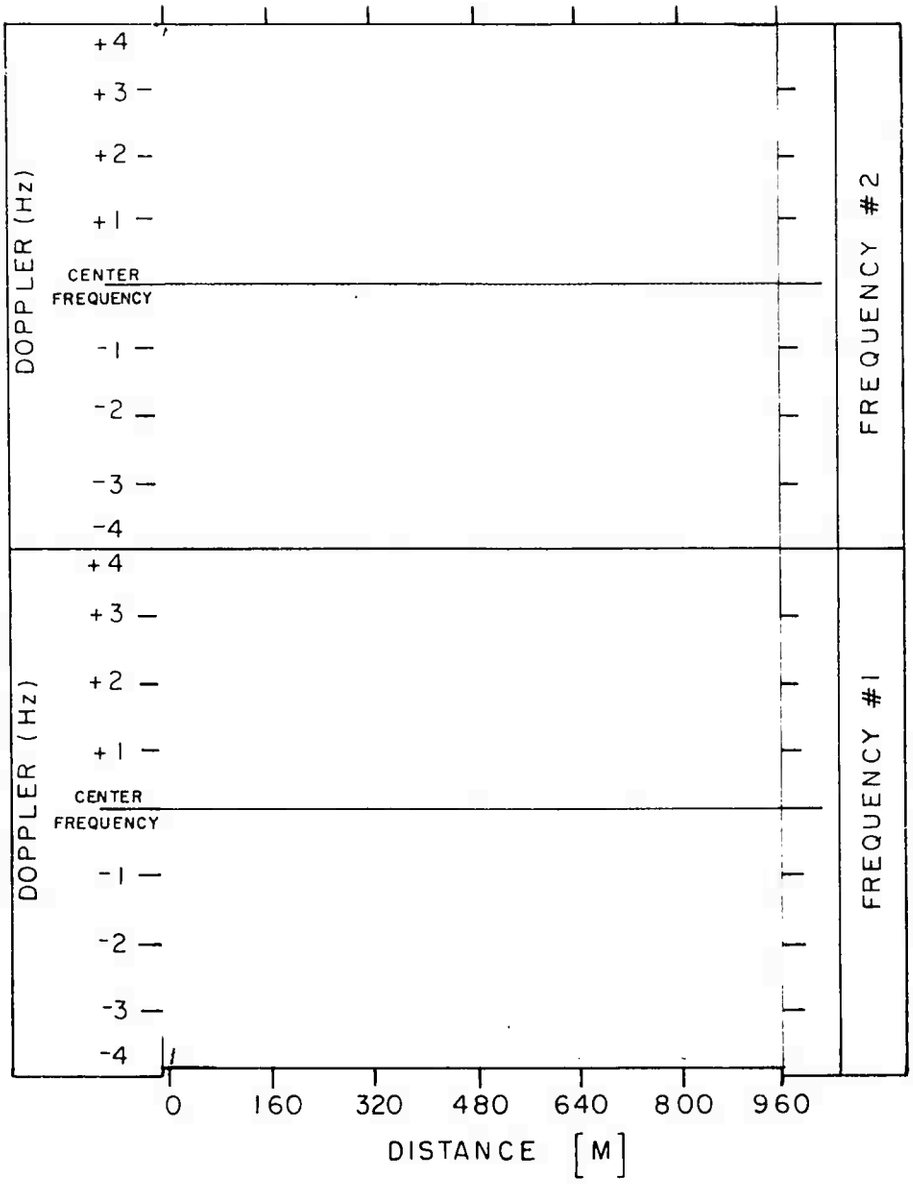

b. Coherence

Figure 12. Flight 4-142, 22 May 1974, UT 0305

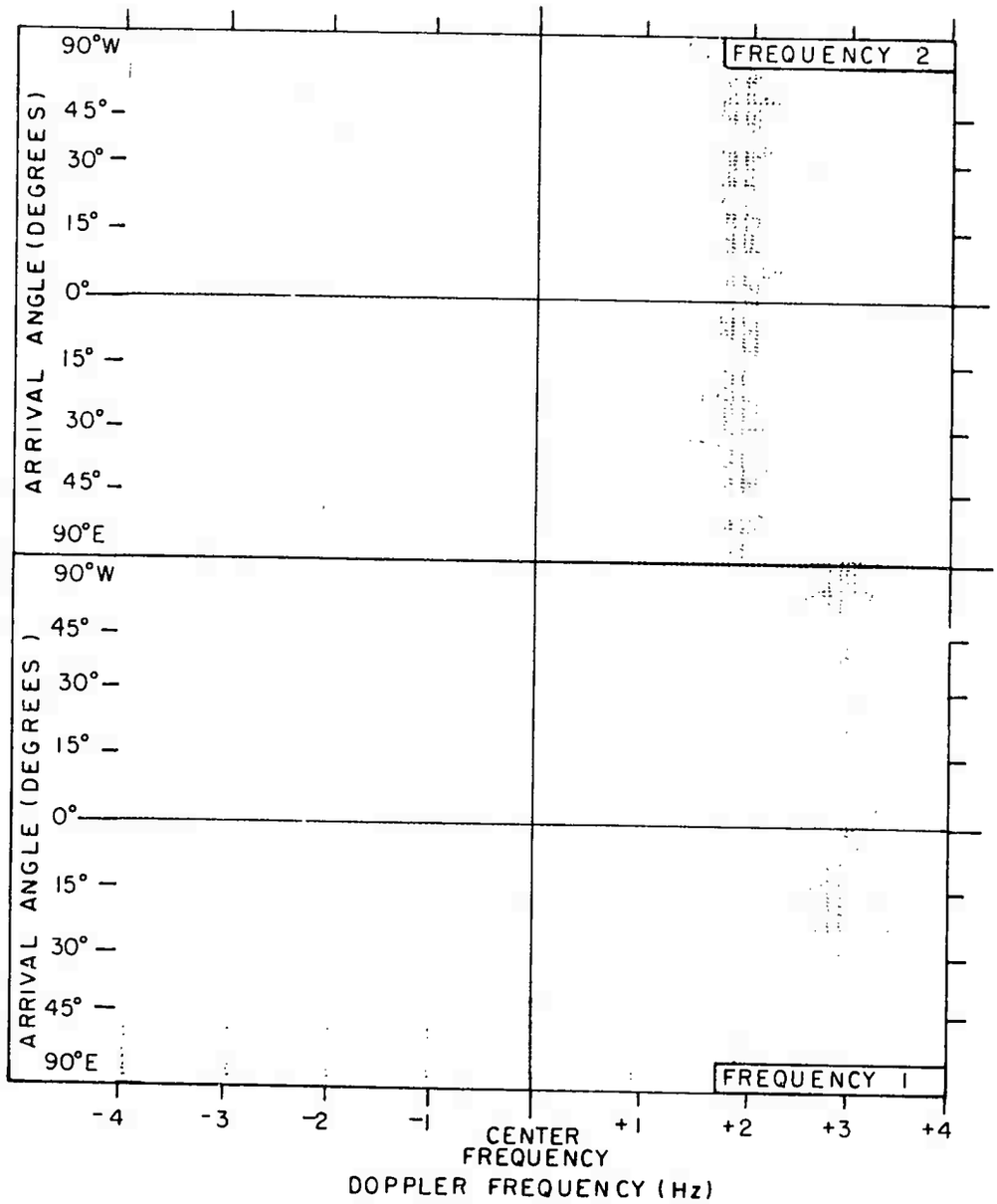

DATE ---------- 5-22-74 (142)
TIME (UT) ---------- 0336
FREQ 1 (MHz) ---------- 8.22
FREQ 2 (MHz) ---------- 6.62
RANGE (Km) ---------- 920
AZIMUTH (deg.) ------- 348T
ANT. CONFIGURATION - 7/6
CENTER FREQ (Hz) ------ +3

a. DAASM Map

Figure 12. Flight 4-142, 22 May 1974, UT 0336

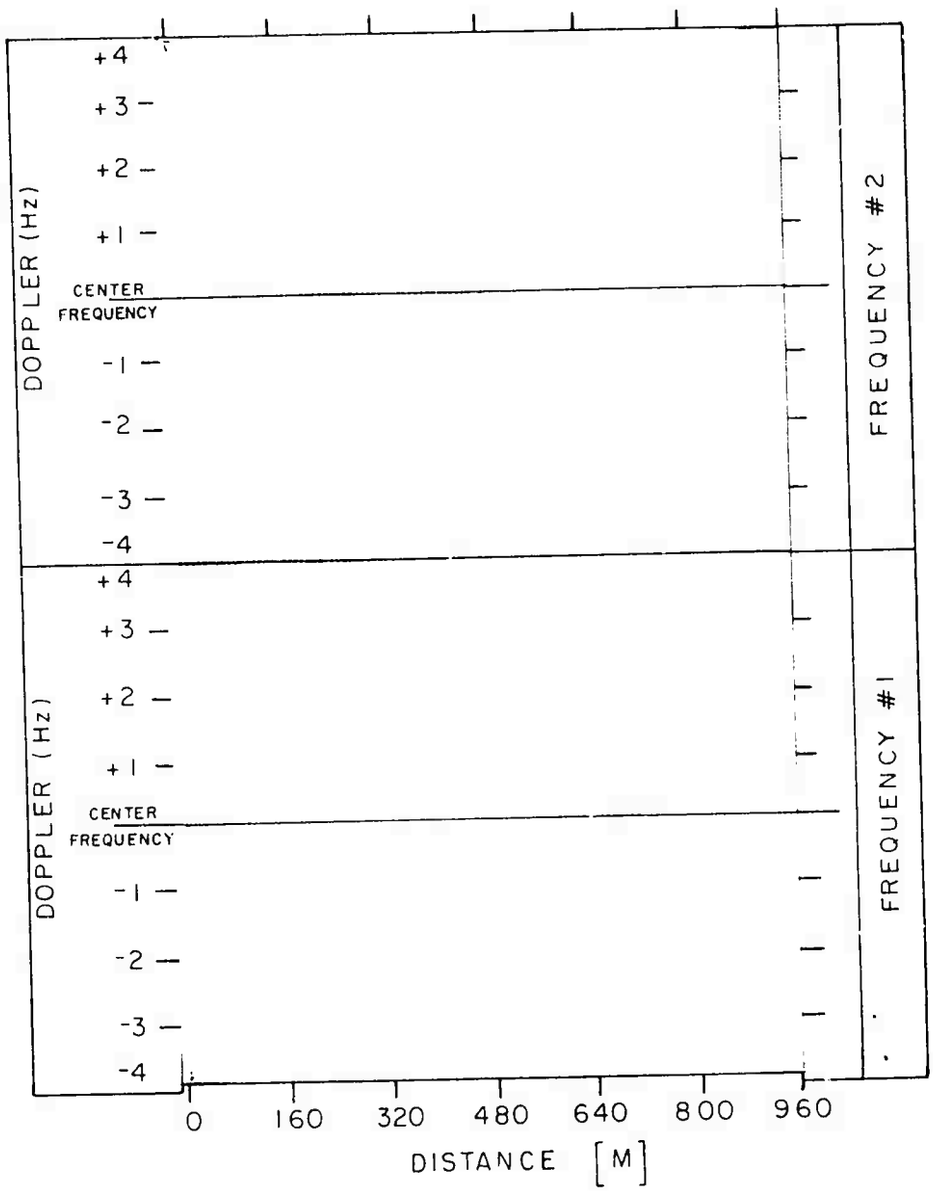

b. Coherence

Figure 12. Flight 4-142, 22 May 1974, UT 0336

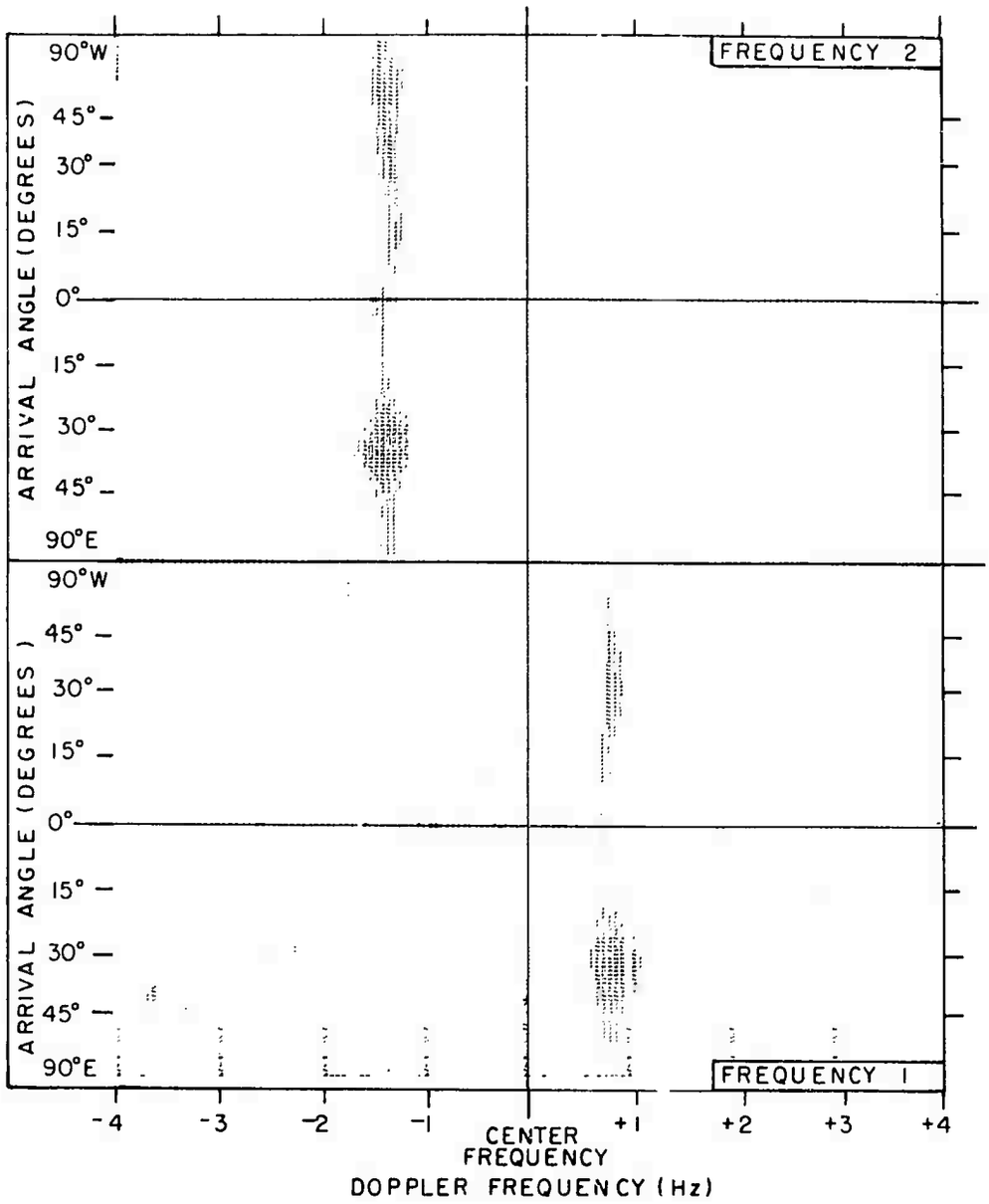

DATE ---------- 7-12-74 (193)
TIME (UT) ---------- 1655
FREQ 1 (MHz) ---------- 8.22
FREQ 2 (MHz) ---------- 11.22
RANGE (Km) ---------- 1380
AZIMUTH (deg.) ---------- 001T
ANT. CONFIGURATION - 7/0
CENTER FREQ (Hz) ---------- -7

a. DAASM Map

Figure 13. Flight 4-193, 12 Jul 1974, UT 1655

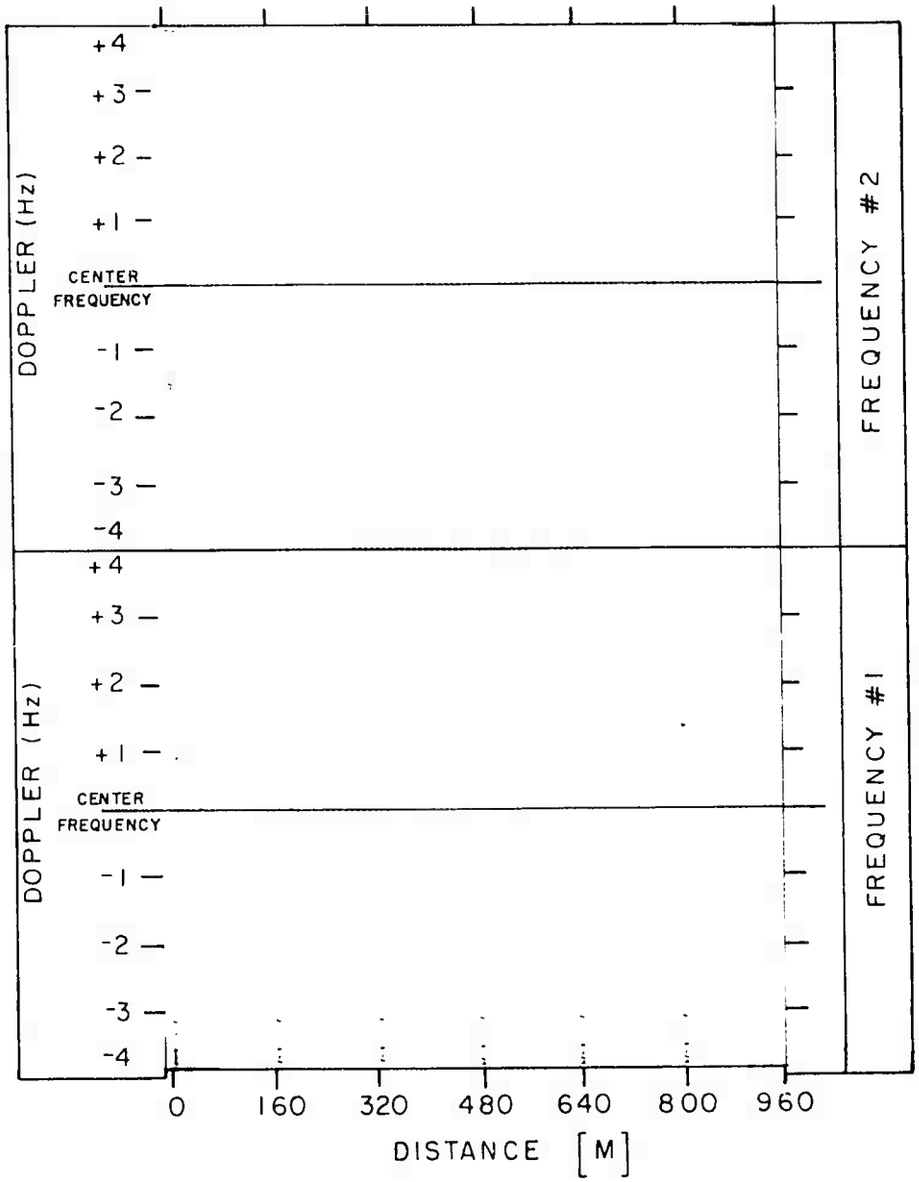

b. Coherence

Figure 13. Flight 4-193, 12 Jul 1974, UT 1655

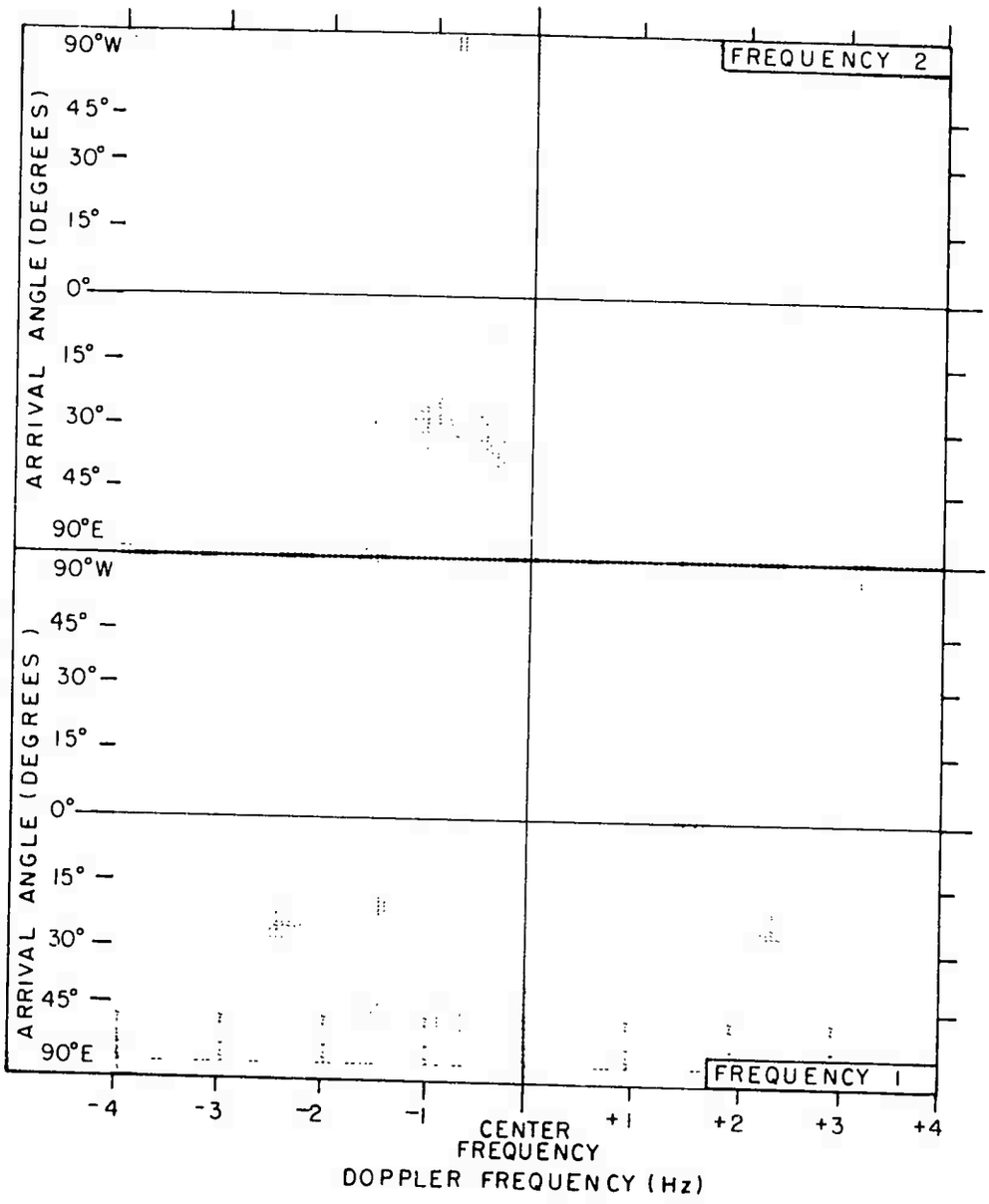

a. DAASM Map

DATE ---------- 7-12-74 (193)
TIME (UT) ---------- 1718
FREQ 1 (MHz) ---------- 13.22
FREQ 2 (MHz) ---------- 11.22
RANGE (Km) ---------- 1680
AZIMUTH (deg.) ------- 000T
ANT. CONFIGURATION - 7/0
CENTER FREQ (Hz) ------ -8

Figure 13. Flight 4-193, 12 Jul 1974, UT 1718

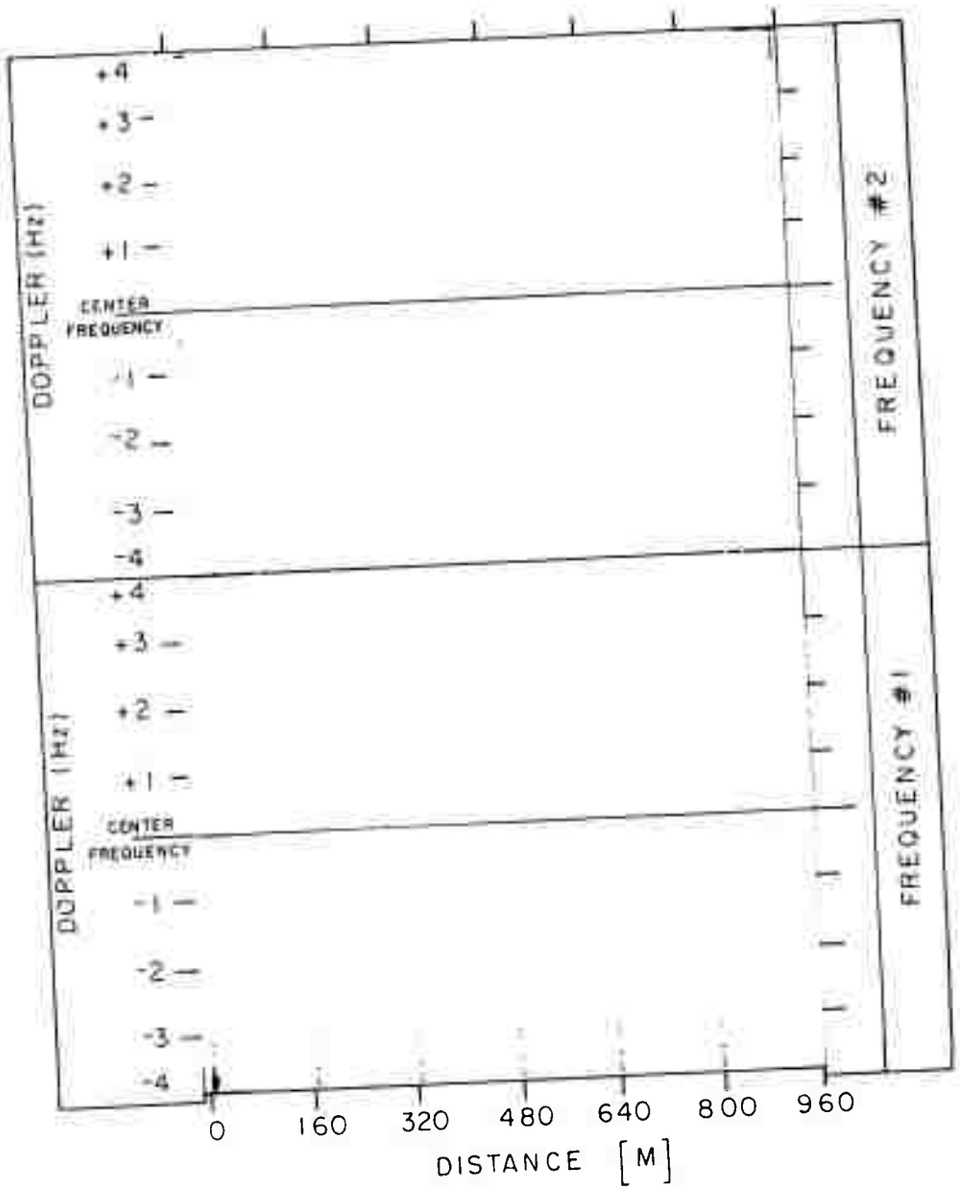

b.Coherence

Figure 13. Flight 4-193, 12 Jul 1974, UT 1718

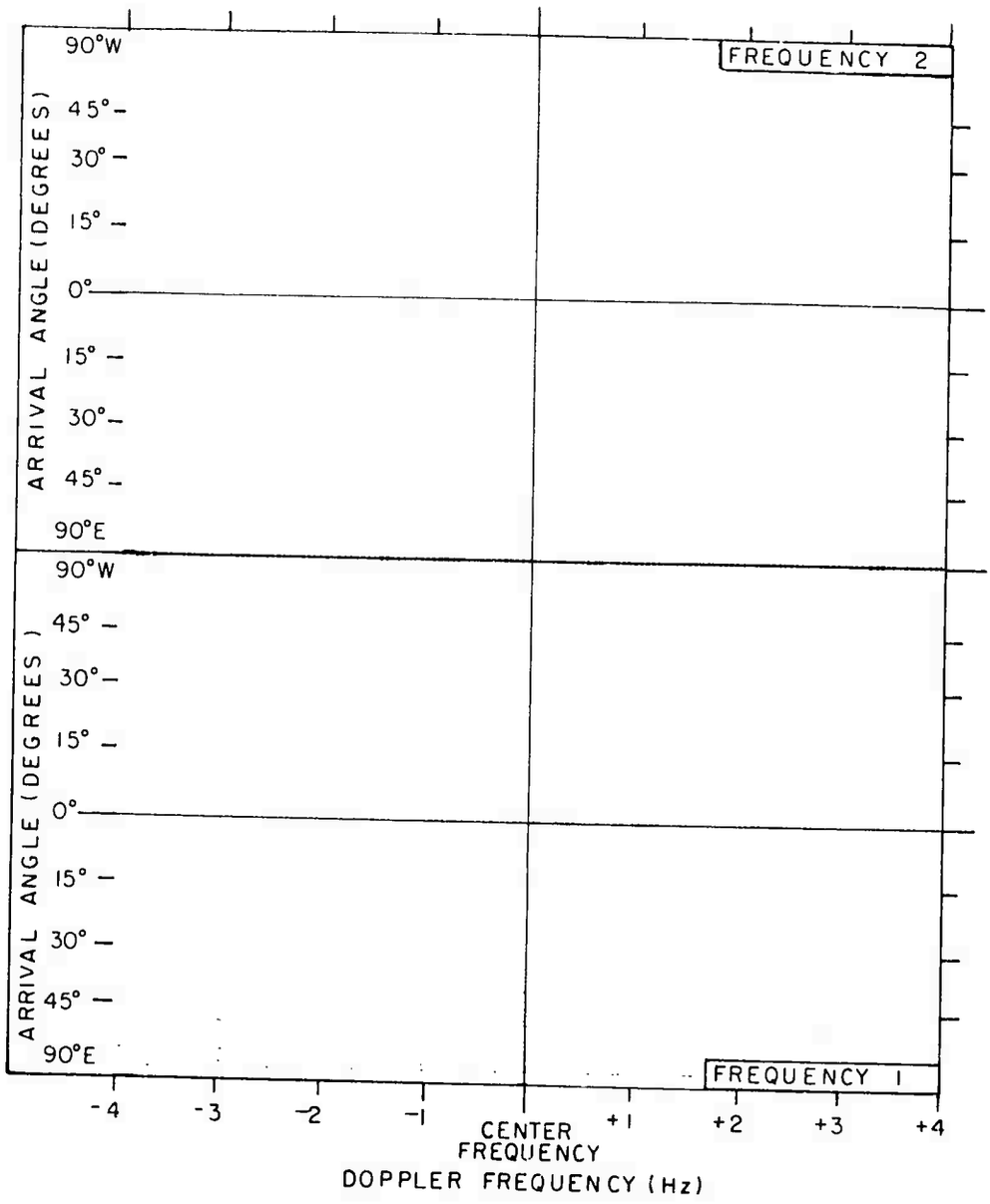

a. DAASM Map

DATE	7-12-74 (193)
TIME (UT)	1721
FREQ 1 (MHz)	13.22
FREQ 2 (MHz)	11.22
RANGE (Km)	1680
AZIMUTH (deg.)	000T
ANT. CONFIGURATION	7/0
CENTER FREQ (Hz)	-8

Figure 13. Flight 4-193, 12 Jul 1974, UT 1721

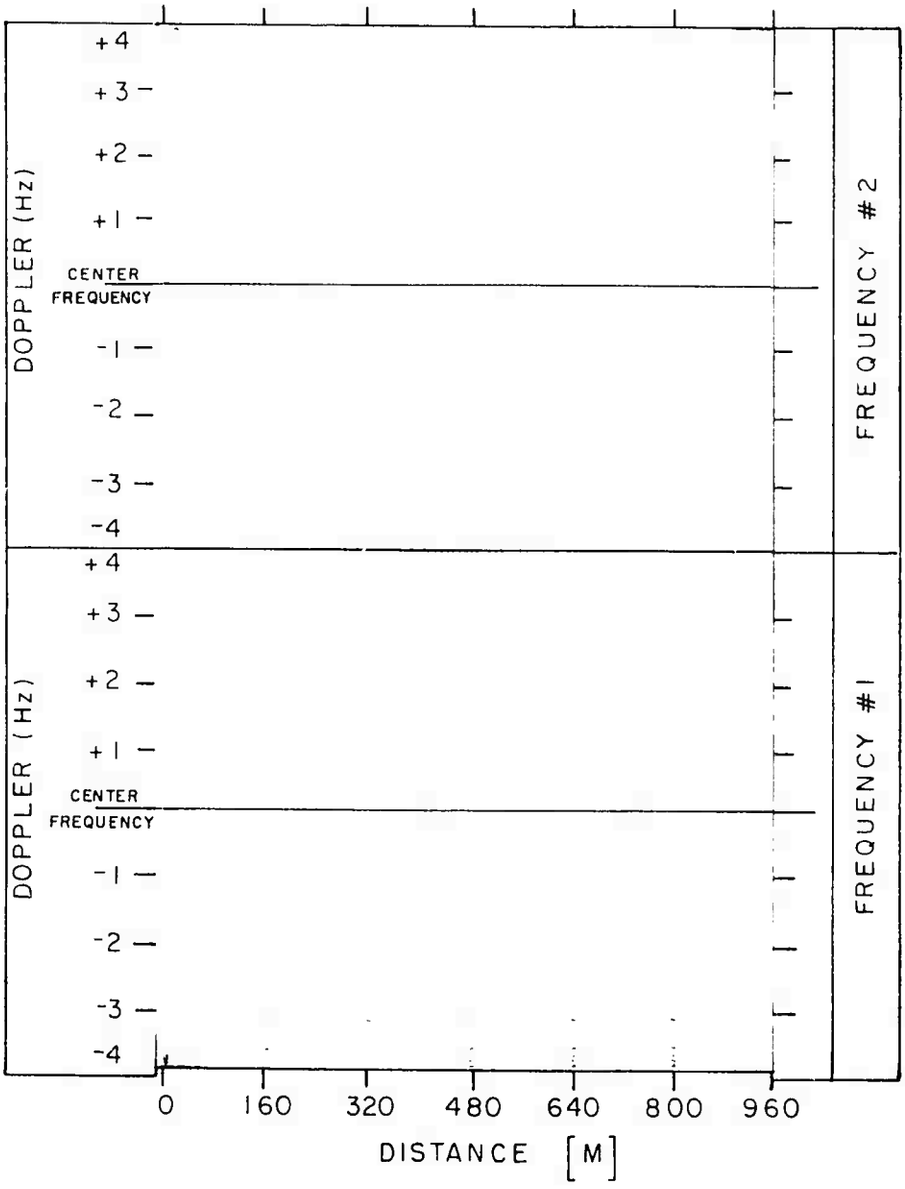

b. Coherence

Figure 13. Flight 4-193, 12 Jul 1974, UT 1721

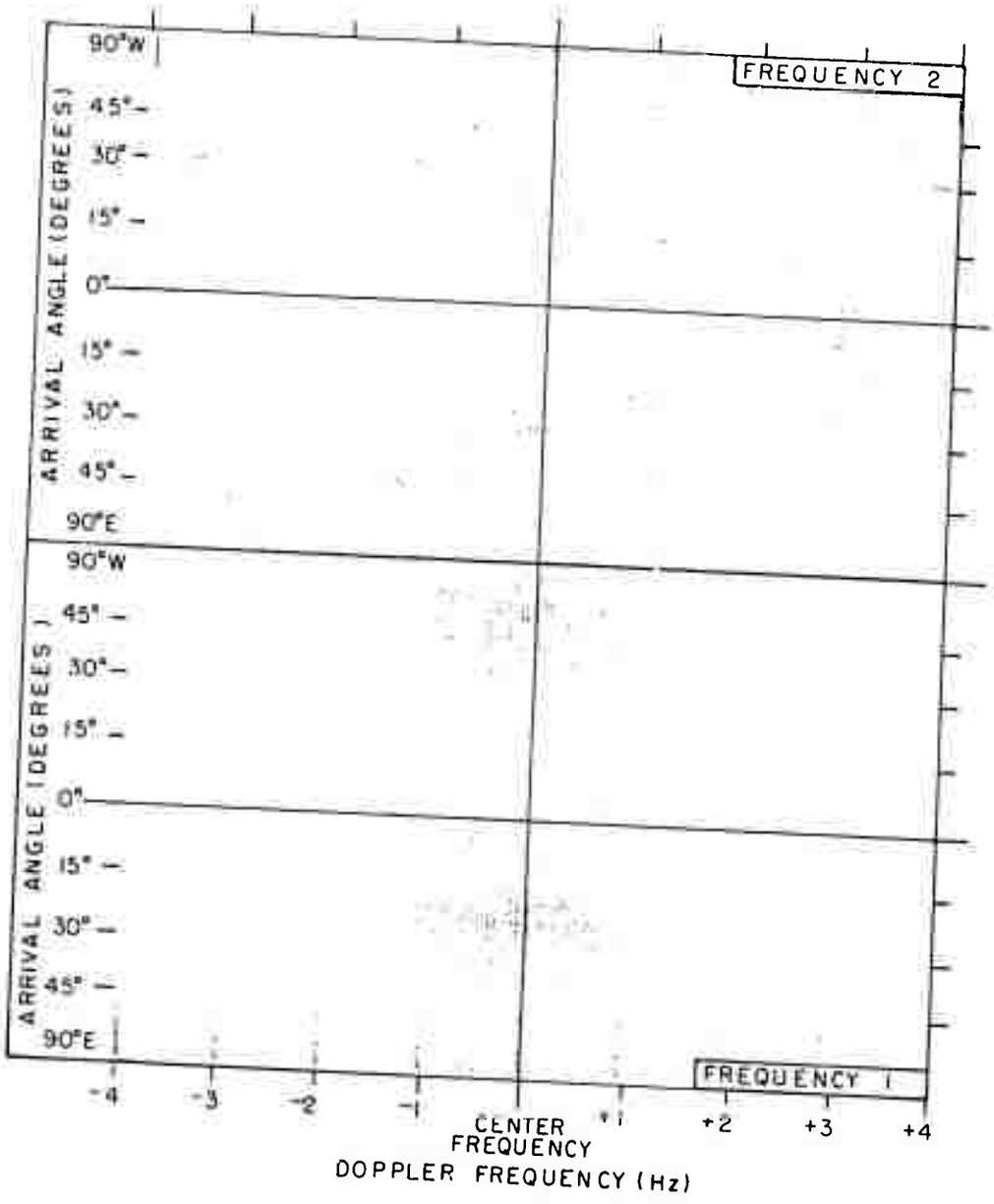

a. DAASM Map

DATE	7-12-74 (193)
TIME (UT)	1920
FREQ 1 (MHz)	8.22
FREQ 2 (MHz)	6.62
RANGE (Km)	1440
AZIMUTH (deg.)	000T
ANT. CONFIGURATION	7/6
CENTER FREQ (Hz)	+5

Figure 13. Flight 4-193, 12 Jul 1974, UT 1920

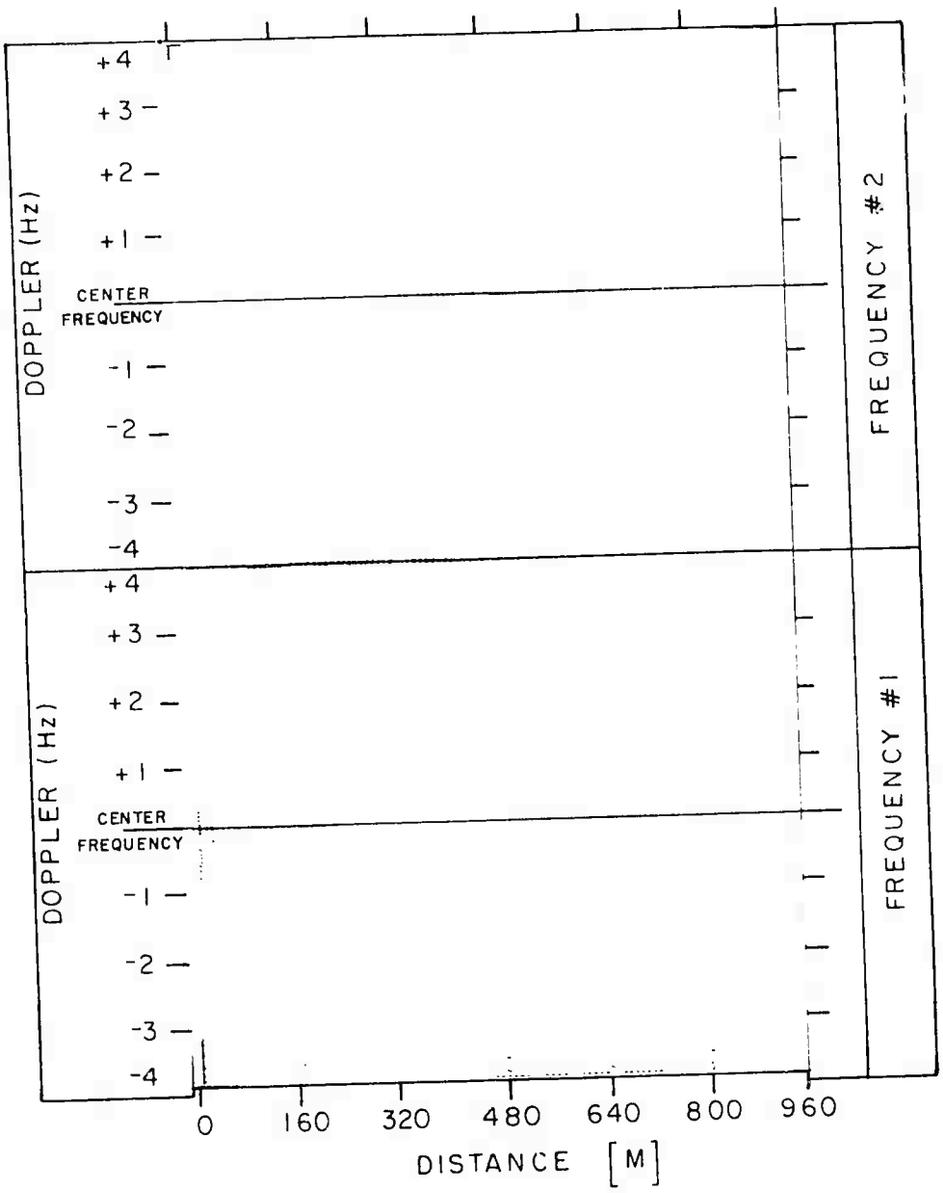

b.Coherence

Figure 13. Flight 4-193, 12 Jul 1974, UT 1920

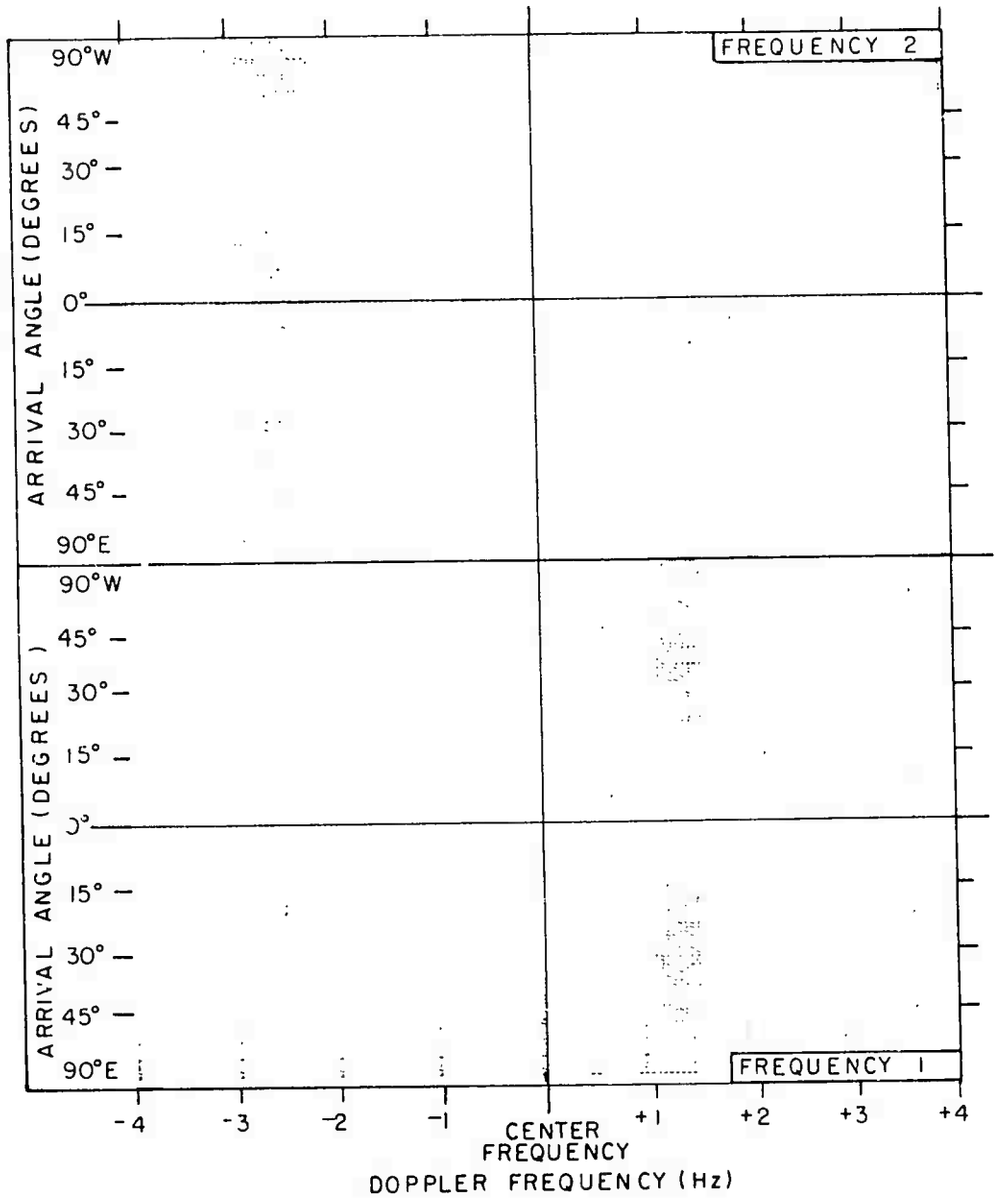

a. DAASM Map

DATE	7-12-74 (193)
TIME (UT)	1940
FREQ 1 (MHz)	8.22
FREQ 2 (MHz)	6.62
RANGE (Km)	1150
AZIMUTH (deg.)	001T
ANT. CONFIGURATION	7/6
CENTER FREQ (Hz)	+5

Figure 13. Flight 4-193, 12 Jul 1974, UT 1940

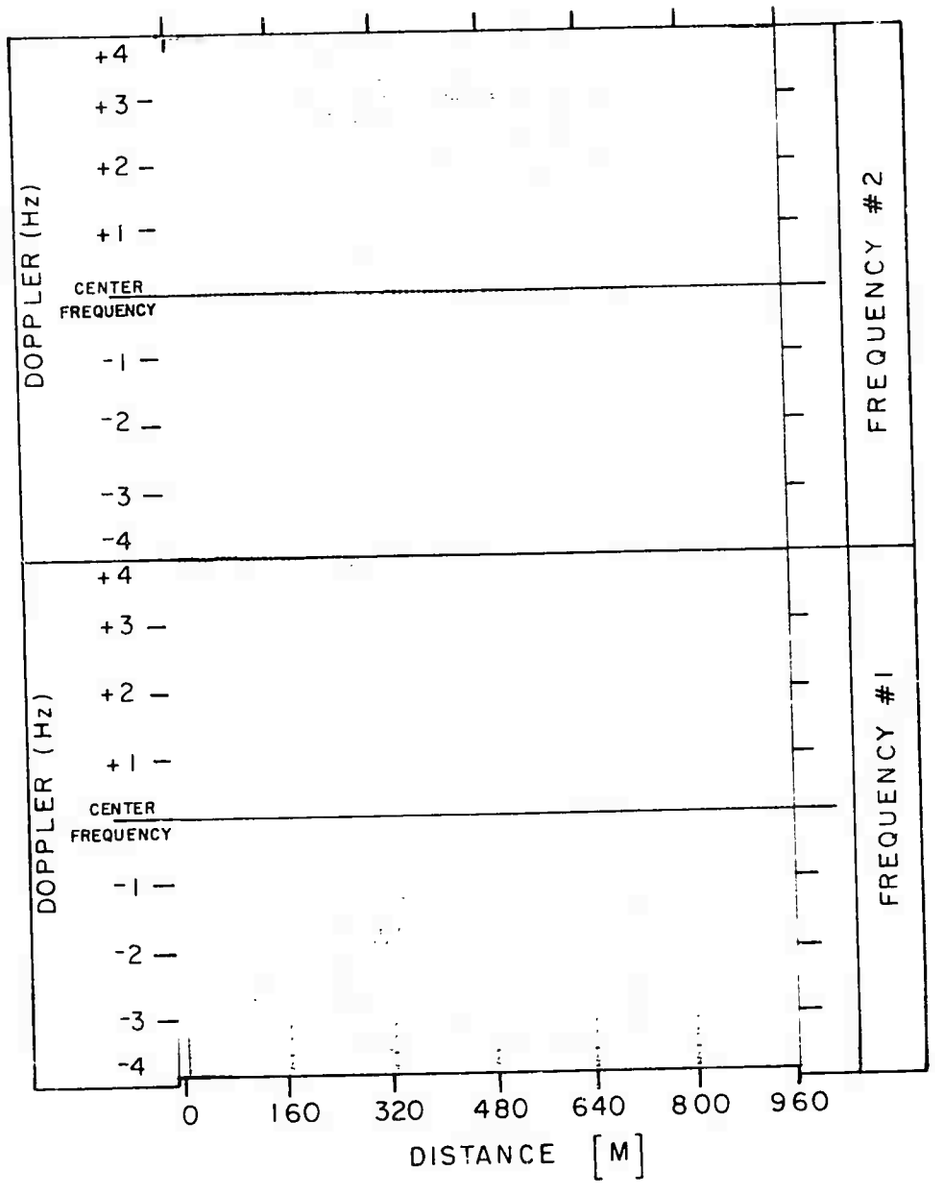

b. Coherence

Figure 13. Flight 4-193, 12 Jul 1974, UT 1940

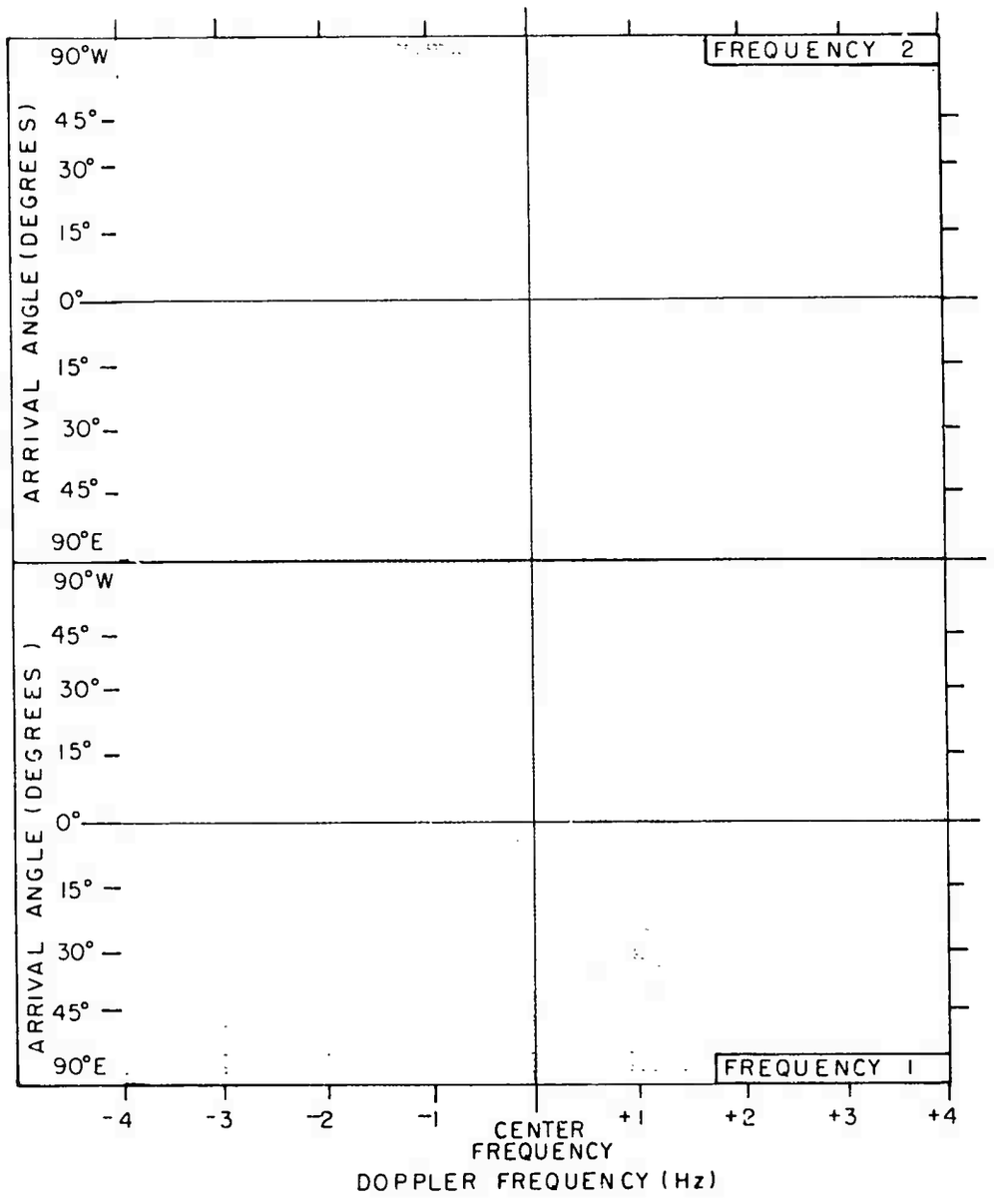

DATE ---------- 7-12-74 (193)
TIME (UT) ---------- 1941
FREQ 1 (MHz) ---------- 8.22
FREQ 2 (MHz) ---------- 6.62
RANGE (Km) ---------- 1150
AZIMUTH (deg.) ---------- 001T
ANT. CONFIGURATION - 7/6
CENTER FREQ (Hz) ------ +5

a. DAASM Map

Figure 13. Flight 4-193, 12 Jul 1974, UT 1941

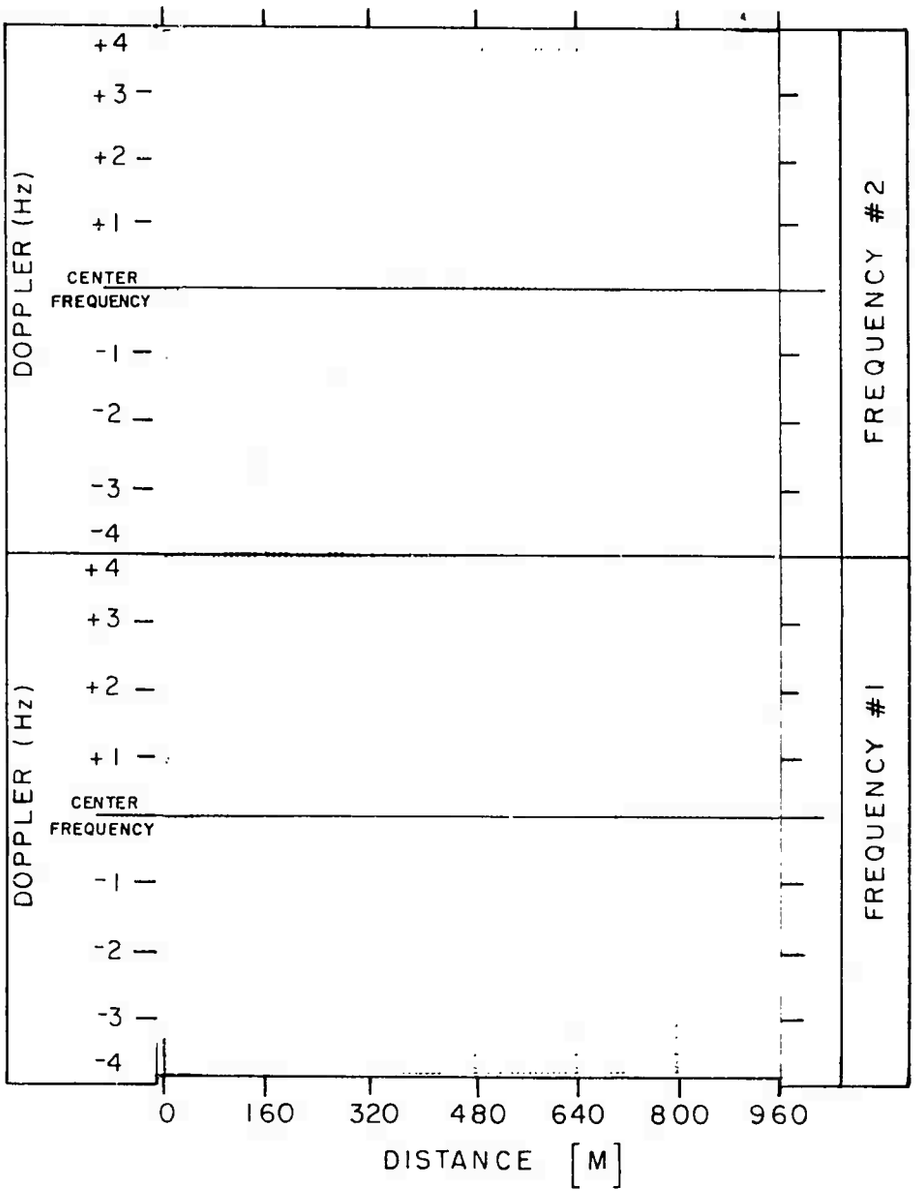

b. Coherence

Figure 13. Flight 4-193, 12 Jul 1974, UT 1941

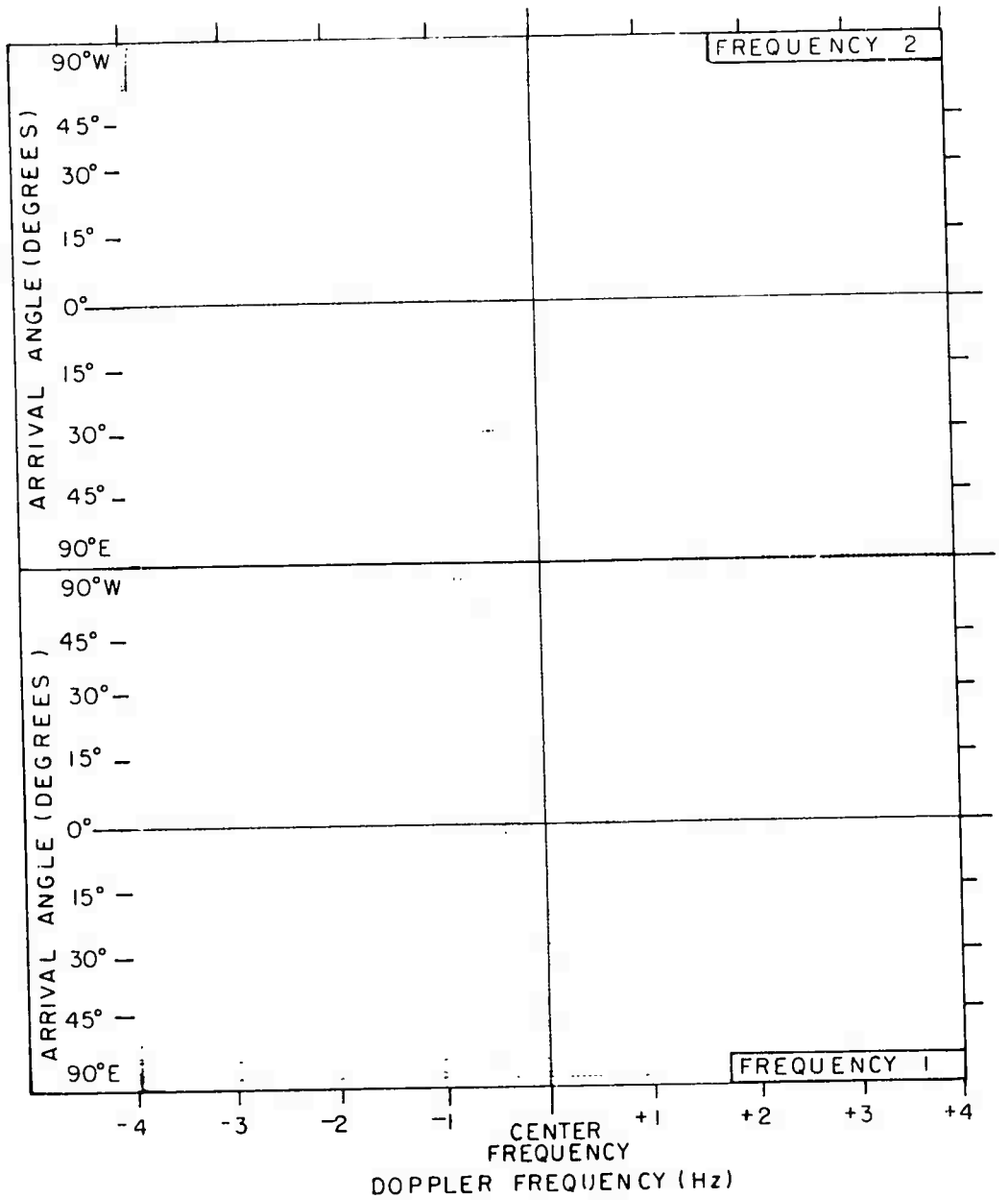

a. DAASM Map

DATE ---------- 7-12-74 (193)
TIME (UT) ---------- 1943
FREQ 1 (MHz) ---------- 8.22
FREQ 2 (MHz) ---------- 6.22
RANGE (Km) ---------- 1150
AZIMUTH (deg.) ---------- 001T
ANT. CONFIGURATION - 7/6
CENTER FREQ (Hz) ---------- +5

Figure 13. Flight 4-193, 12 Jul 1974, UT 1943

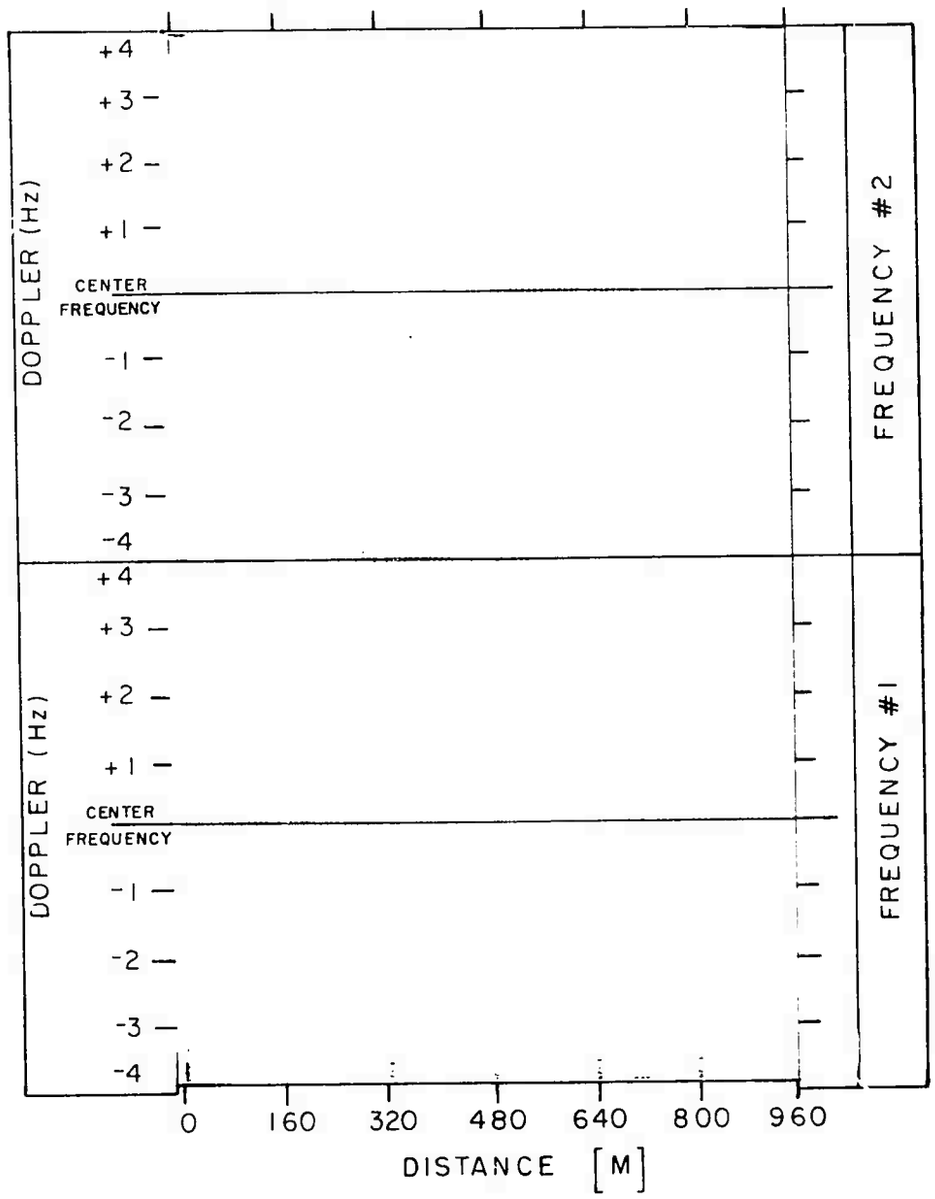

b.Coherence

Figure 13. Flight 4-193, 12 Jul 1974, UT 1943

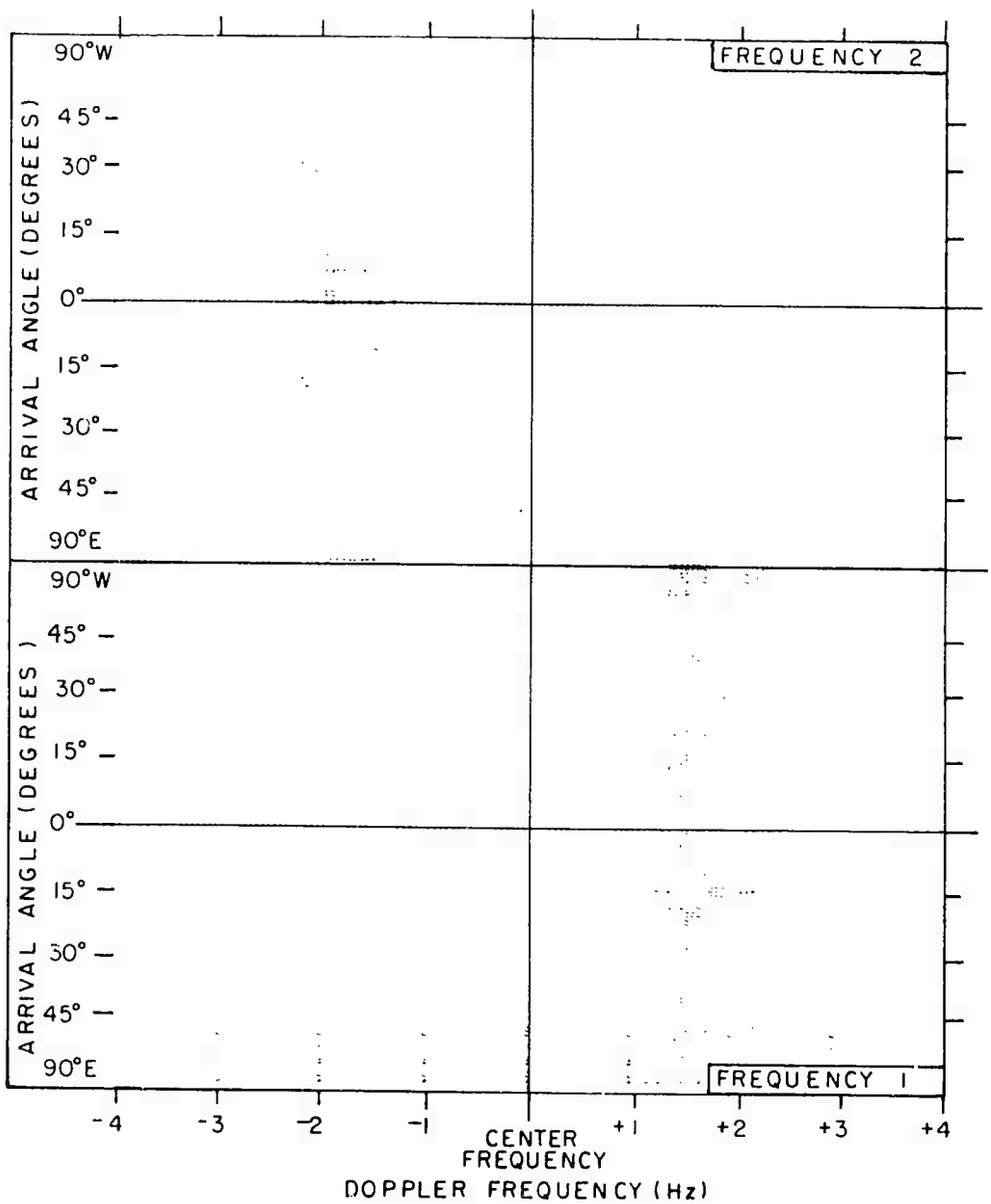

a. DAASM Map

DATE	7-15-74 (196)
TIME (UT)	1641
FREQ 1 (MHz)	8.22
FREQ 2 (MHz)	11.22
RANGE (Km)	1260
AZIMUTH (deg.)	347T
ANT. CONFIGURATION	7/6
CENTER FREQ (Hz)	-7

Figure 14. Flight 4-196, 15 Jul 1974, UT 1641

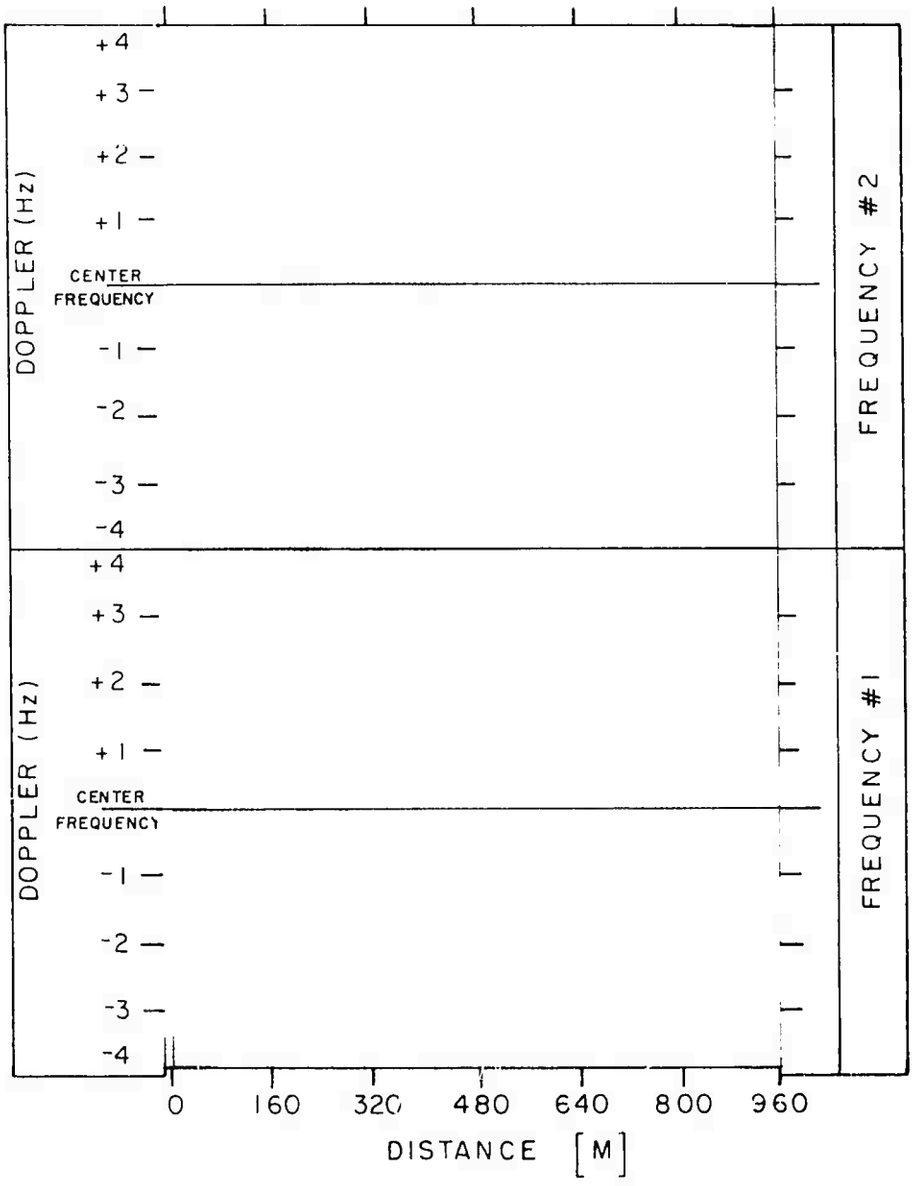

b. Coherence

Figure 14. Flight 4-196, 15 Jul 1974, UT 1641

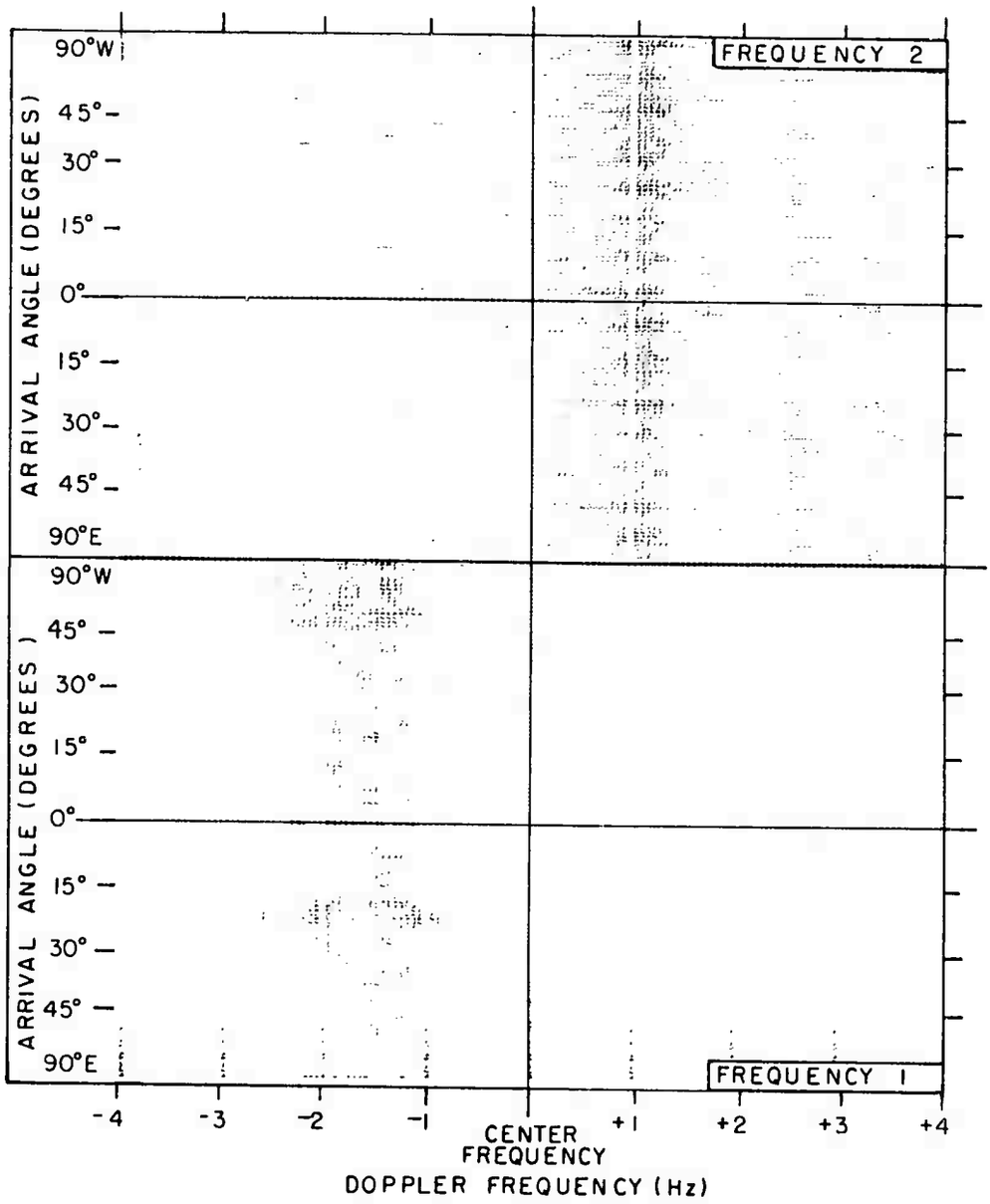

a. DAASM Map

DATE ---------- 7-15-74 (196)
TIME (UT) ---------- 1940
FREQ 1 (MHz) ---------- 8.22
FREQ 2 (MHz) ---------- 11.22
RANGE (Km) ---------- 1950
AZIMUTH (deg.) ---------- 353T
ANT. CONFIGURATION - 7/6
CENTER FREQ (Hz) ---------- +7

Figure 14. Flight 4-196, 15 Jul 1974, UT 1940

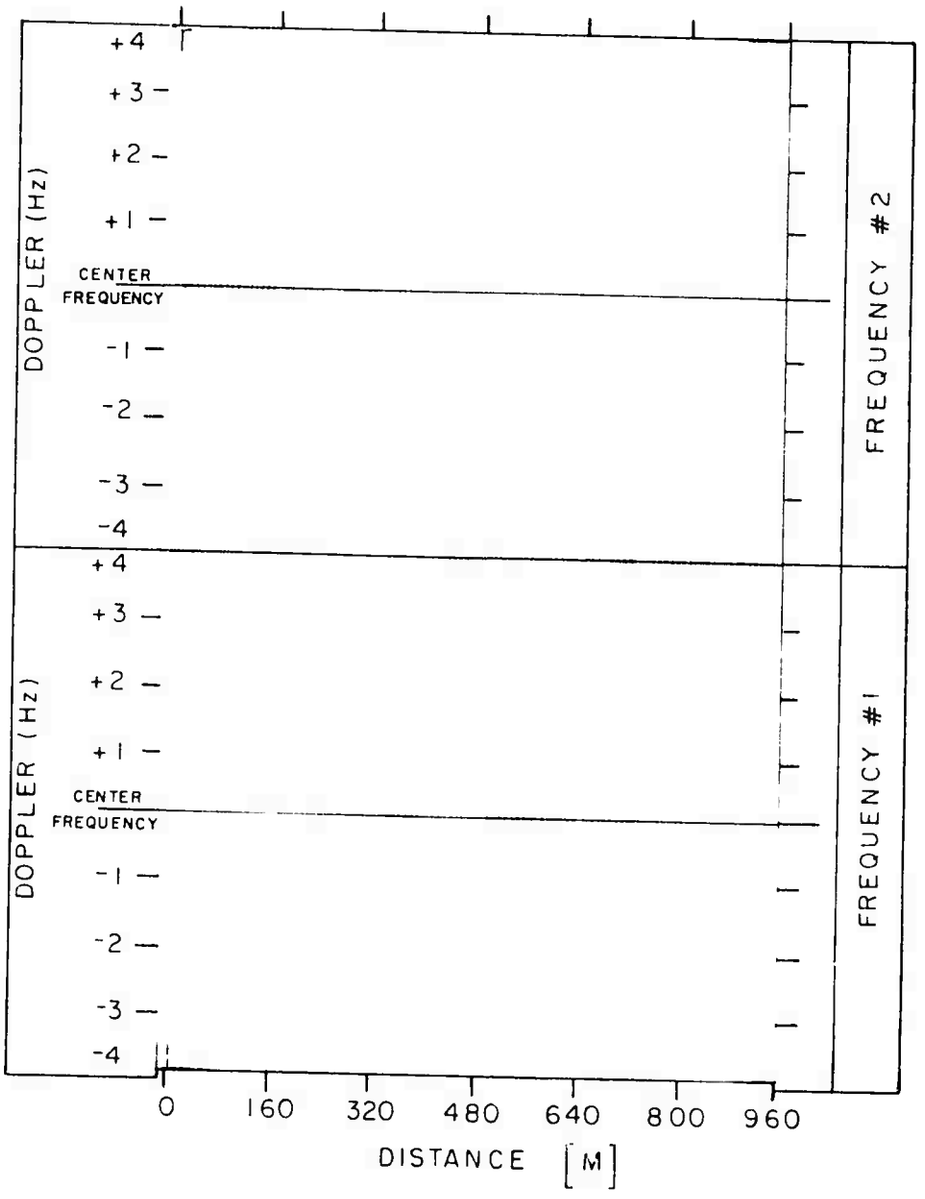

b. Coherence

Figure 14. Flight 4-196, 15 Jul 1974, GT 1940

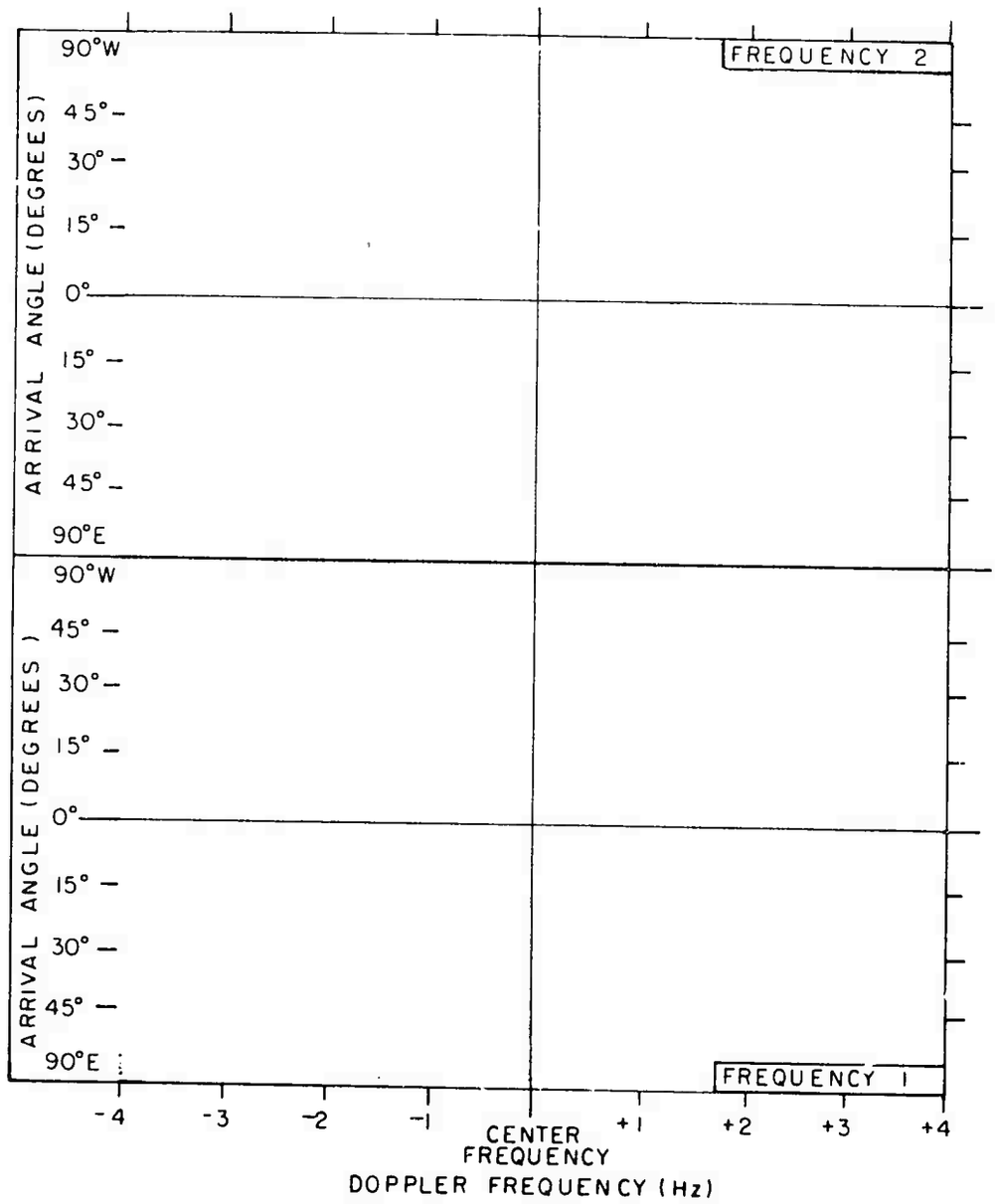

a. DAASM Mao

DATE ---------- 7-15-74 (196)
TIME (UT) ---------- 1940
FREQ 1 (MHz) ---------- 8.22
FREQ 2 (MHz) ---------- 11.22
RANGE (Km) ---------- 1950
AZIMUTH (deg.) ------- 353T
ANT. CONFIGURATION - 7/6
CENTER FREQ (Hz) ------ +7

Figure 14. Flight 4-196, 15 Jul 1974, UT 1940

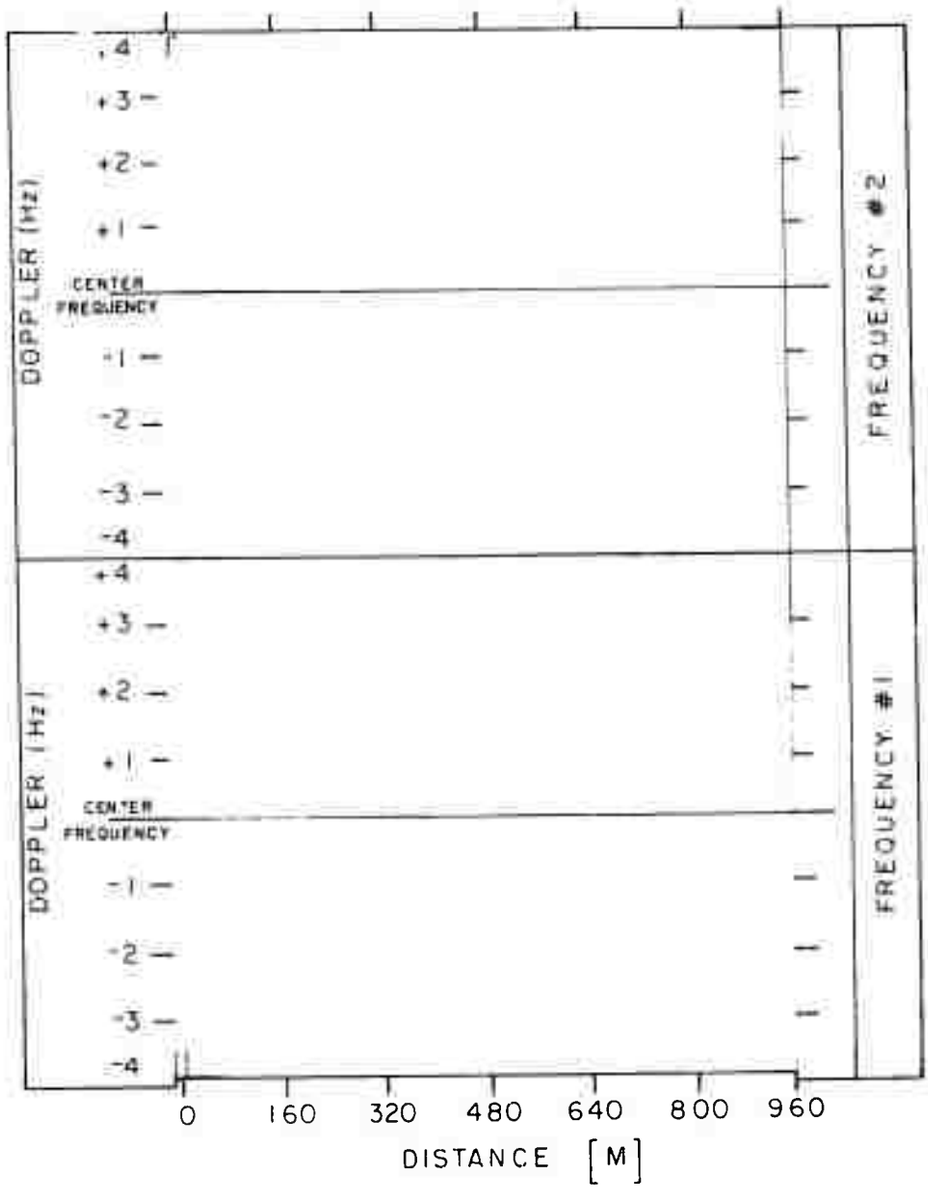

b. Coherence

Figure 14. Flight 4-196, 15 Jul 1974, UT 1940

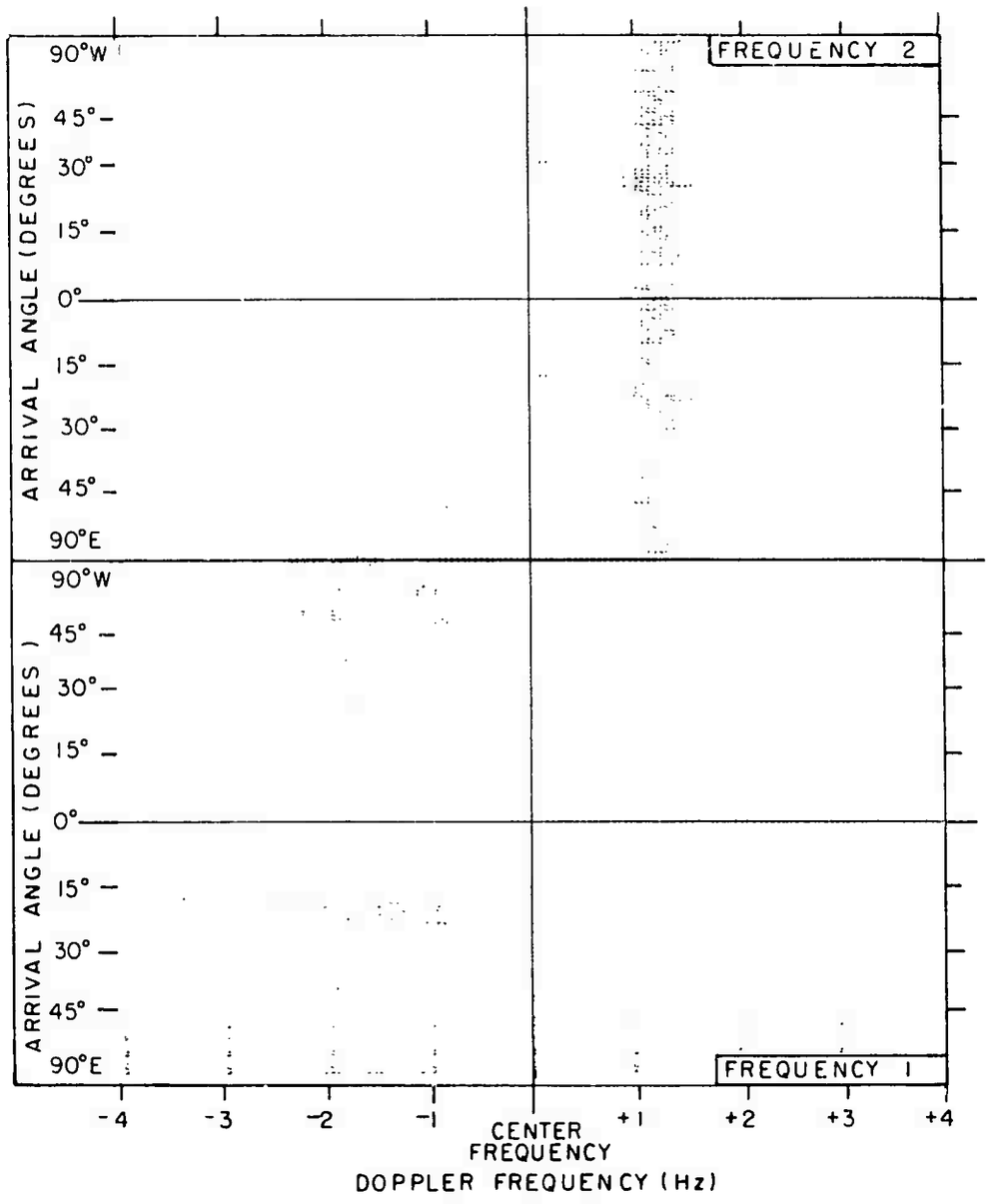

DATE ---------- 7-15-74 (196)
TIME (UT) ---------- 1941
FREQ 1 (MHz) ---------- 8.22
FREQ 2 (MHz) ---------- 11.22
RANGE (Km) ---------- 1951
AZIMUTH (deg.) ---------- 353T
ANT. CONFIGURATION - 7/6
CENTER FREQ (Hz) ------ +7

a. DAASM Map

Figure 14. Flight 4-196, 15 Jul 1974, UT 1941

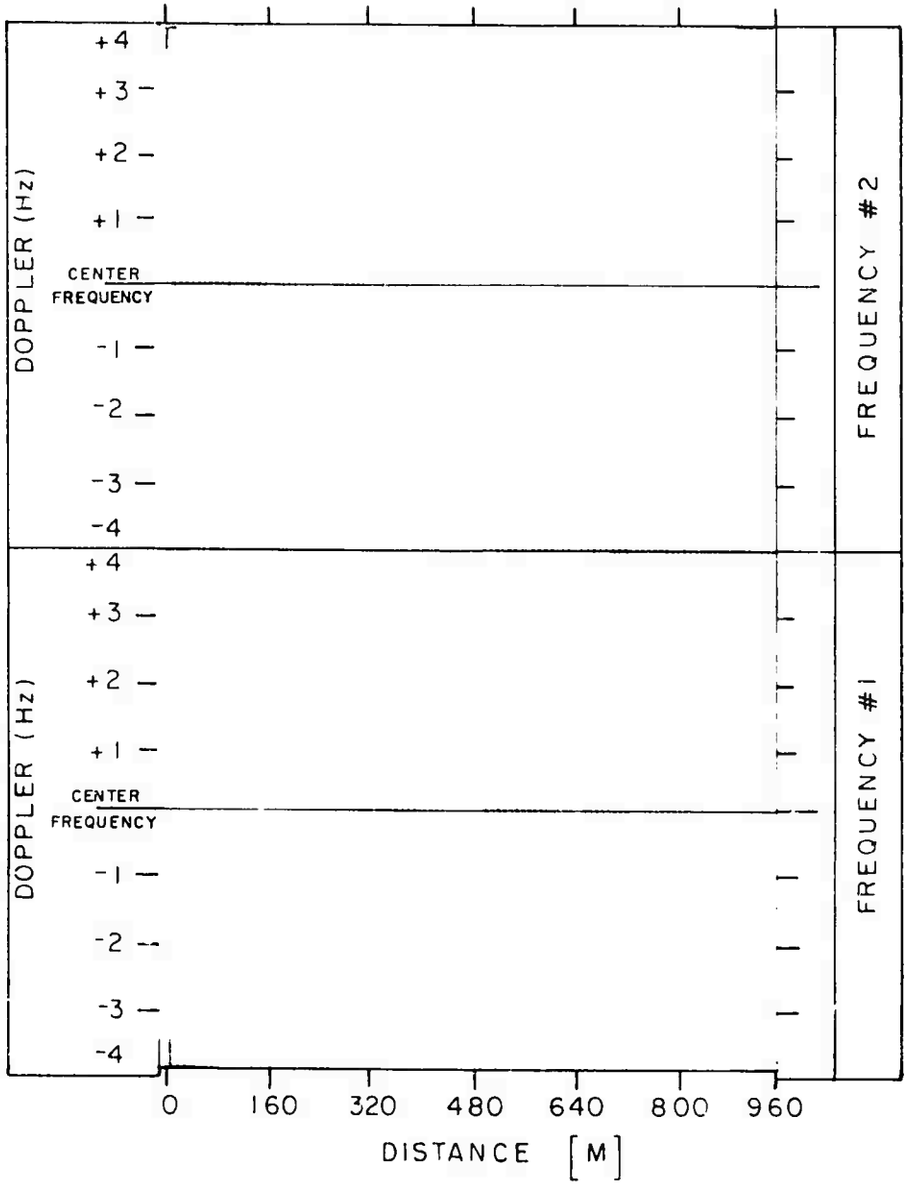

b. Coherence

Figure 14. Flight 4-196, 15 Jul 1974, UT 1941

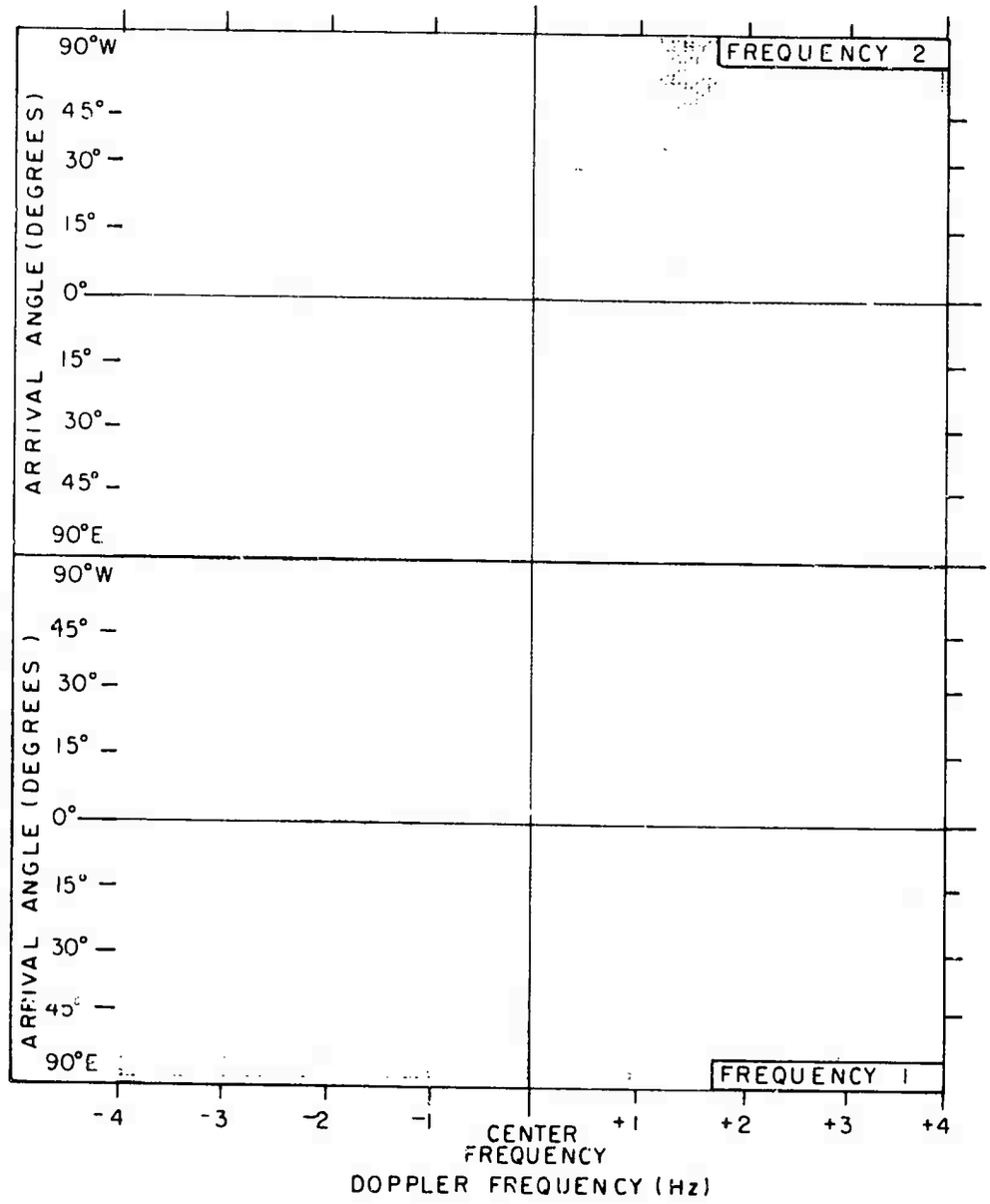

DATE ---------- 7-15-74 (196)
TIME (UT) ---------- 1942
FREQ 1 (MHz) ---------- 8.22
FREQ 2 (MHz) ---------- 6.02
RANGE (Km) ---------- 1950
AZIMUTH (deg.) ---------- 353T
ANT. CONFIGURATION - 7/6
CENTER FREQ (Hz) ------ +7

a. DAASM Map

Figure 14. Flight 4-196, 15 Jul 1974, UT 1942

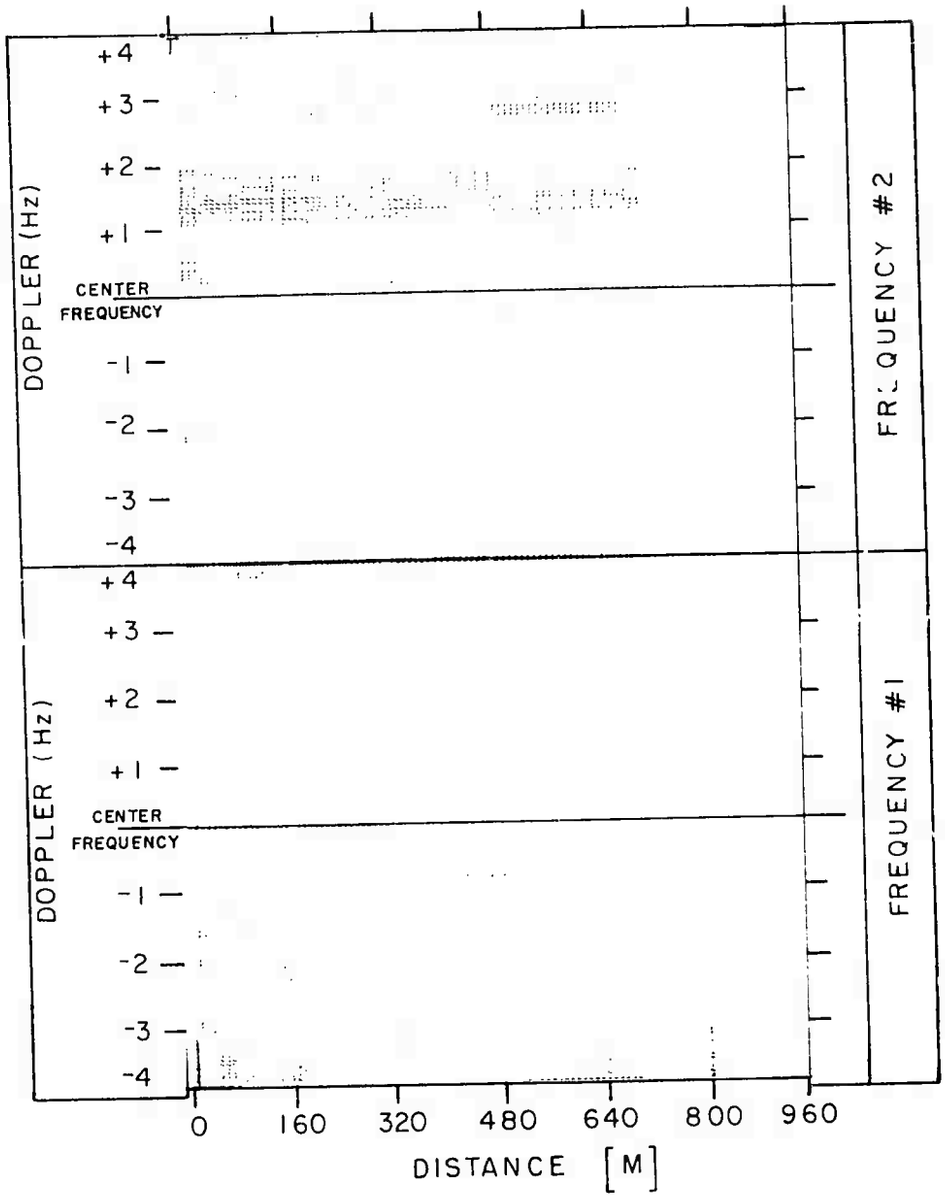

b. Coherence

Figure 14. Flight 4-196, 15 Jul 1974, UT 1942

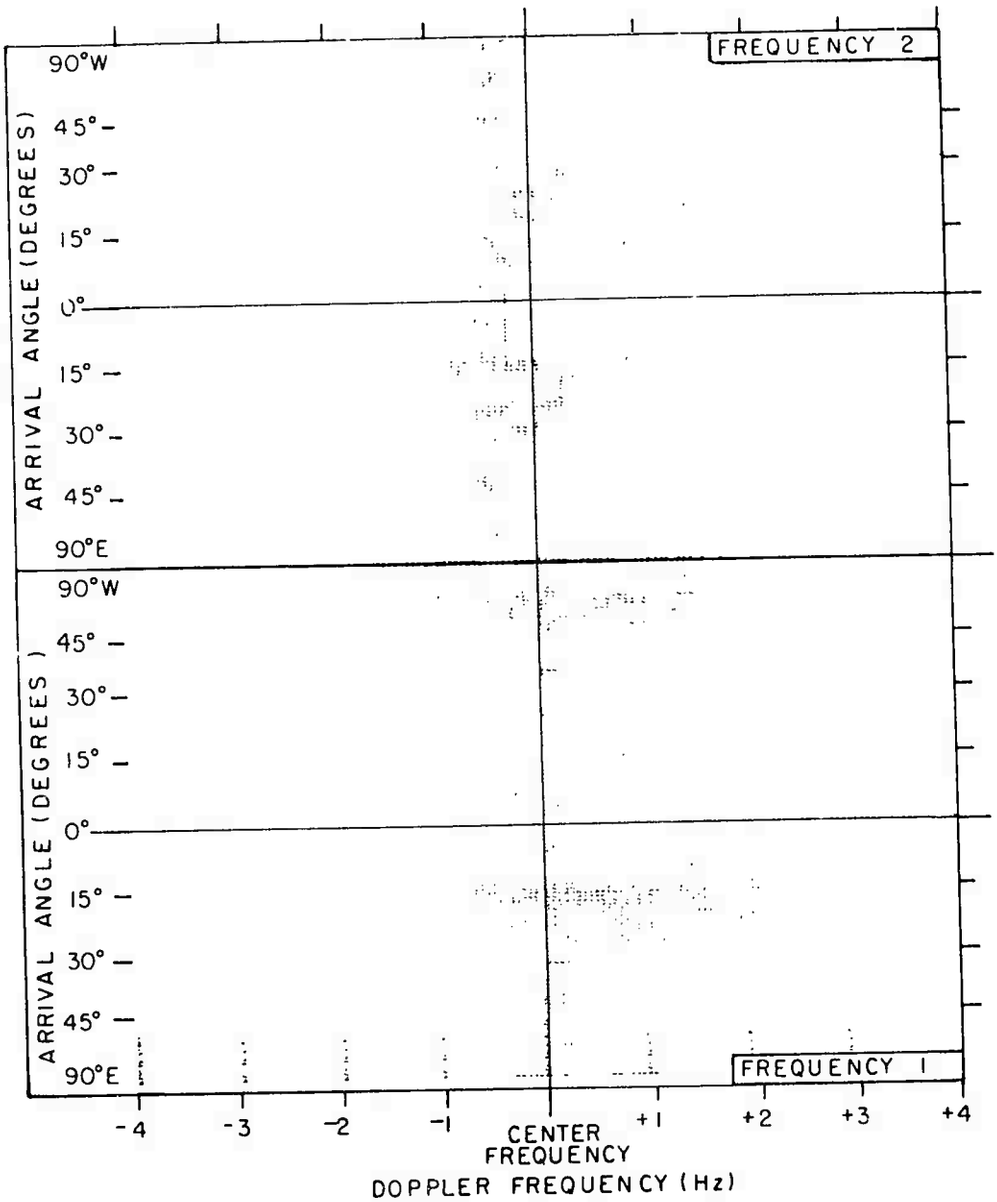

a. DAASM Map

DATE ---------- 7-15-74 (196)
TIME (UT) ---------- 2038
FREQ 1 (MHz) ---------- 8.22
FREQ 2 (MHz) ---------- 6.02
RANGE (Km) ---------- 1250
AZIMUTH (deg.) ------- 348T
ANT. CONFIGURATION - 7/6
CENTER FREQ (Hz) ------ +4

Figure 14. Flight 4-196, 15 Jul 1974, UT 2038

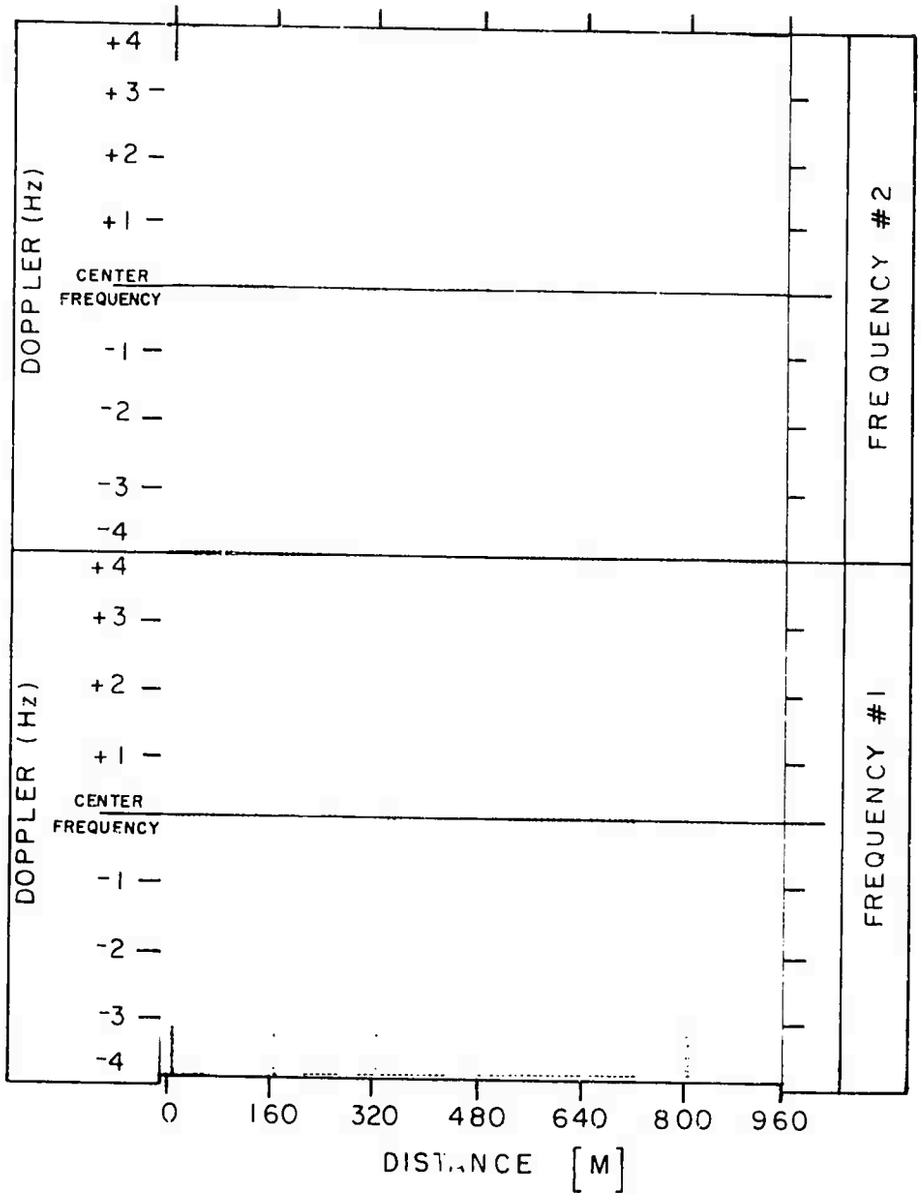

b. Coherence

Figure 14. Flight 4-196, 15 Jul 1974, UT 2038

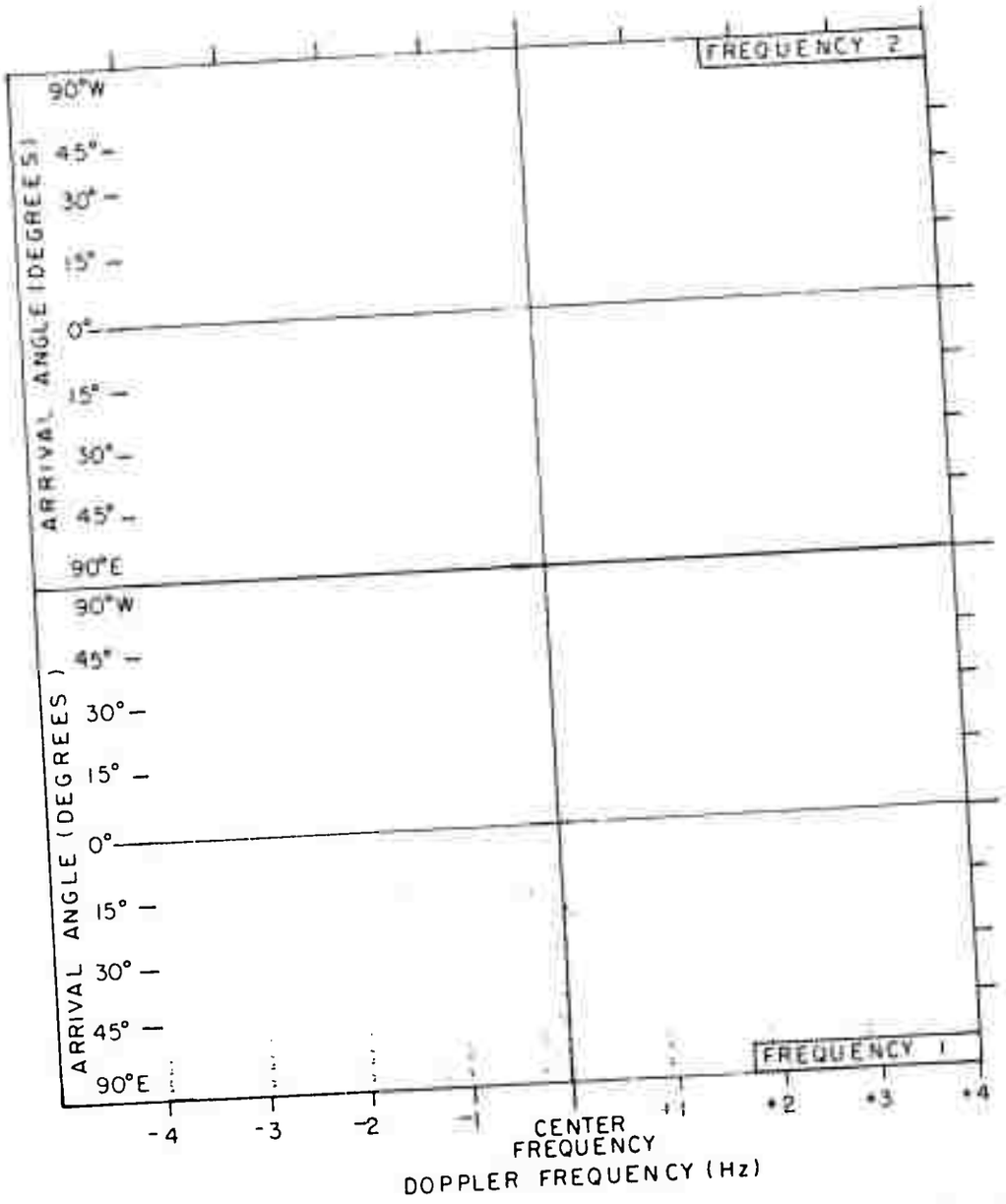

a. DAASM Map

DATE	7-15-75 (196)
TIME (UT)	2100
FREQ 1 (MHz)	8.22
FREQ 2 (MHz)	6.02
RANGE (Km)	960
AZIMUTH (deg.)	349T
ANT. CONFIGURATION	7/6
CENTER FREQ (Hz)	+6

Figure 14. Flight 4-196, 15 Jul 1974, UT 2100

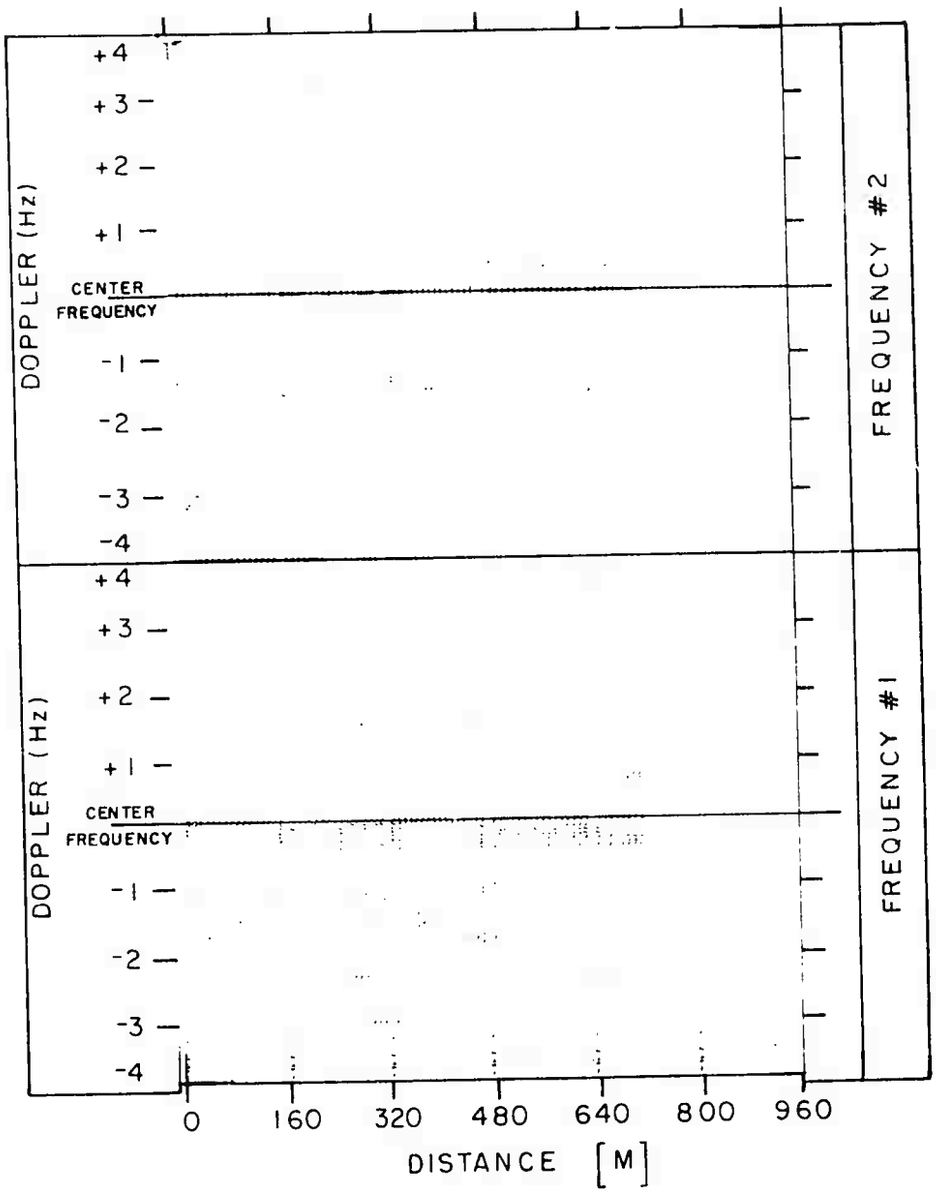

b. Coherence

Figure 14. Flight 4-196, 15 Jul 1974, UT 2100

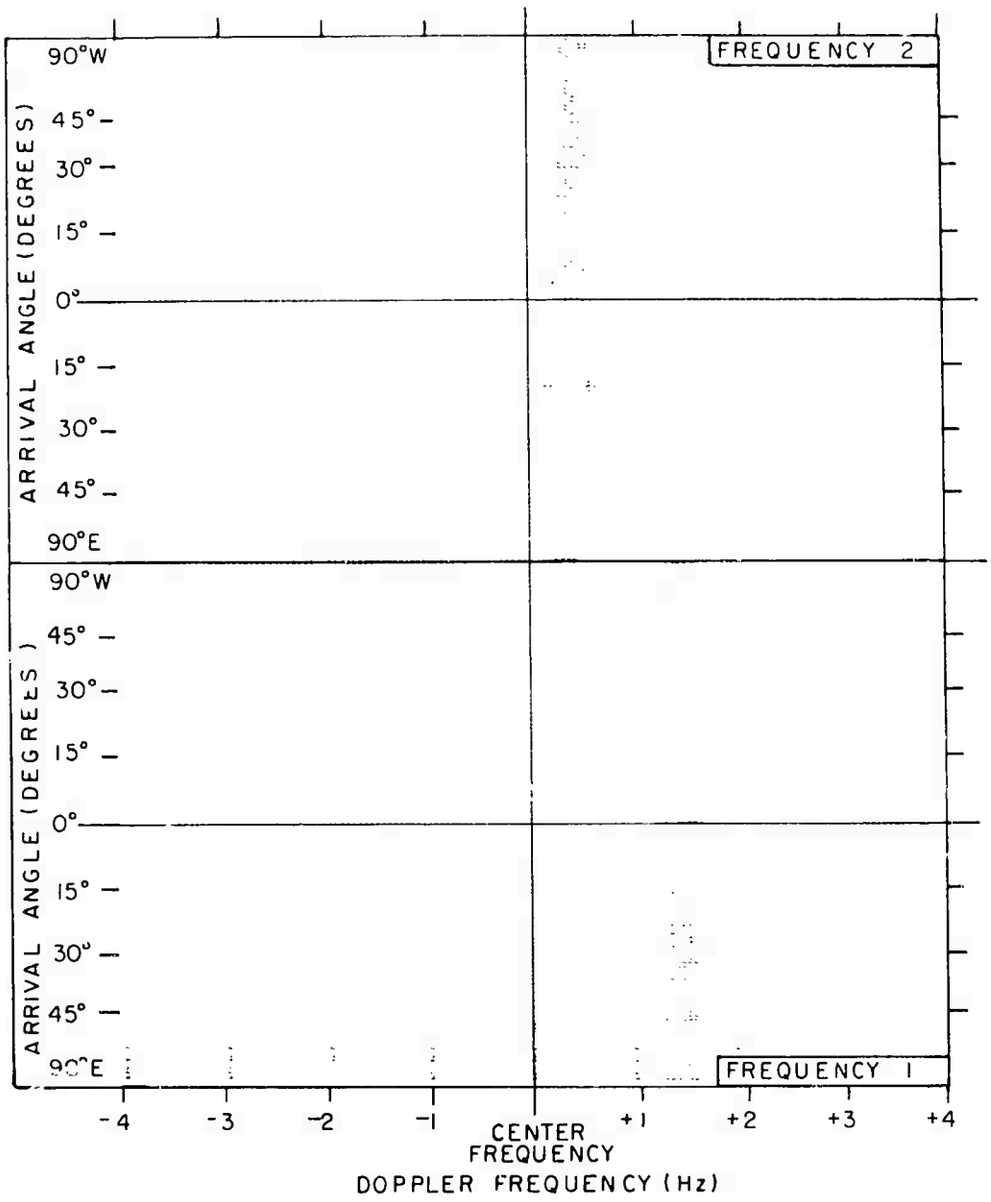

DATE ---------- 7-15-74 (196)
TIME (UT) ---------- 2130
FREQ 1 (MHz) ---------- 8.22
FREQ 2 (MHz) ---------- 6.02
RANGE (Km) ---------- 010
AZIMUTH (deg.) -------- 350T
ANT. CONFIGURATION - 7/6
CENTER FREQ (Hz) ------ +4

a. DAASM Map

Figure 14. Flight 4-196, 15 Jul 1974, UT 2130

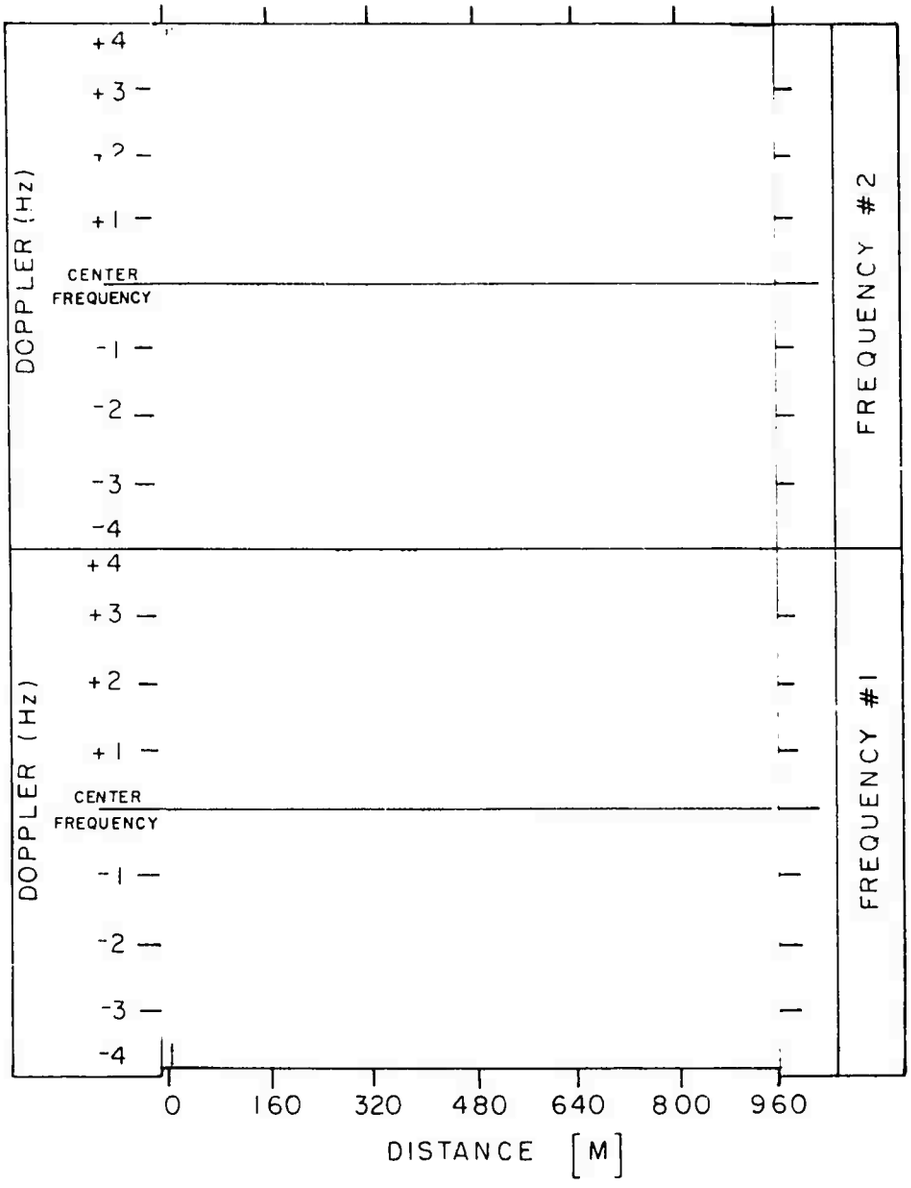

b. Coherence

Figure 14. Flight 4-196, 15 Jul 1974, UT 2130

References

1. Pfister, W., et al (1968-75) Pulse Sounding with Closely Spaced Receivers as as a Tool for Measuring Atmospheric Motions and Fine Structure in the Ionosphere,
   Vol. I, Environmental Research Paper No. 295, Dec 1968
   Vol. II, Environmental Research Paper No. 295, Dec 1968
   Vol. III, Environmental Research Paper No. 317, Mar 1970
   Vol. IV, Environmental Research Paper No. 329, Aug 1970
   Vol. V, Environmental Research Paper No. 468, Feb 1974
   Vol. VI, Environmental Research Paper No. 470, Mar 1974
   Vol. VII, Environmental Research Paper No. 506, Apr 1975
   Vol. VIII, Environmental Research Paper No. 507, Apr 1975
2. Richard, D.W. (1972) Twenty-Element Receive Array for the DAASM Experiment, Instrumentation Paper No. 178.
3. Bibl, K. (1973) Doppler/Angle of Arrival Spectral Measurement System, AFCRL-TR-73-0759.
4. Barghausen, A.F., et al (1969) Predicting Long Term Operational Parameters of High Frequency Sky-Wave Telecommunications Systems, ESSA Tech. Report ERL 110-ITS-78.
5. Bibl, K., et al (1970) Digital Interpreting Goniometric Ionospheric Sounder, AFCRL-71-0002.
6. Moffet, A.T. (1968) IEEE Transactions on Antennas and Propagation AP-16 (No. 2):172.
7. Elkins, T.J. (1973) An Empirical Model of the Polar Ionosphere, Survey in Geophysics, No. 267.
8. Jenkins, G.M., and Watts, D.G. (1968) Spectral Analysis and Its Applications, Holden-Day, pp 374-411.